Valorization of Sudanese biomass for the production of biocomposite and bioenergy.

Wadah Mohammed Mahdi Omer

▶ **To cite this version:**

Wadah Mohammed Mahdi Omer. Valorization of Sudanese biomass for the production of biocomposite and bioenergy.. Chemical and Process Engineering. Université de Pau et des Pays de l'Adour; University of Gezira (Wad Medani, Sudan), 2023. English. NNT : 2023PAUU3089 . tel-04718518

HAL Id: tel-04718518

https://theses.hal.science/tel-04718518v1

Submitted on 2 Oct 2024

HAL is a multi-disciplinary open access archive for the deposit and dissemination of scientific research documents, whether they are published or not. The documents may come from teaching and research institutions in France or abroad, or from public or private research centers.

L'archive ouverte pluridisciplinaire **HAL**, est destinée au dépôt et à la diffusion de documents scientifiques de niveau recherche, publiés ou non, émanant des établissements d'enseignement et de recherche français ou étrangers, des laboratoires publics ou privés.

DOCTORAL THESIS

ED 211 – Exact Sciences and their Applications

Presented and defended on: 21 December, 2023
By: Wadah MOHAMMED MAHDI OMER

Thesis to obtain the degree of
Doctorate from the University of Pau and the Adour Region
Specialty: Process Engineering

Valorization of Sudanese Biomass for the Production of Biocomposites and Bioenergy

JURY

Chairman of the jury

• Pr. Frederic MARIAS	University of Pau and the Adour Region

Reviewers

• Pr. Florent EYMA	University of Toulouse
• Pr. Stephane GRELIER	University of Bordeaux

Examiners

• Pr. Frederic MARIAS	University of Pau and the Adour Region
• Dr. Fatima CHARRIER - EL BOUHTOURY	University of Pau and the Adour Region
• Dr. Amine MOUBARIK	University of Sultan Moulay Slimane

Directors

• Pr. Bertrand CHARRIER	University of Pau and the Adour Region
• Pr. Zeinab OSMAN	National Center for Research, Sudan
• Pr. Salah ELARABI	University of Gezira, Sudan

ACKNOWLEDGMENT

I am immensely grateful to the Ministry of Higher Education and Scientific Research for granting me the scholarship that made this thesis possible. I would also like to express my sincere thanks to my thesis supervisor, Bertrand Charrier, for his unwavering support and guidance throughout the completion of this thesis work. My heartfelt gratitude goes to my thesis co-supervisor, Zeinab Osman, for her invaluable advice and supervision. Also, I am sincerely thankful to my co-supervisor, Salah Elarabi, for his support and encouragement.

I would like to extend my thanks to Florent Eyma from the University of Toulouse, Stephane Grelier from the University of Bordeaux, Frederic Marias from the University of Pau and the Adour Region, Fatima Charrier - El Bouhtoury from the University of Pau and the Adour Region, and Amine Moubarik from the University of Sultan Moulay Slimane for agreeing to be the jury members for my thesis.

I deeply thank my parents and family for their unwavering prayers and support. Without them, I wouldn't have come this far. In addition, I am grateful to my friends for their unwavering companionship and encouragement throughout my doctoral study.

Dedication

To the soul of my brother, who made the ultimate sacrifice for our country while helping and protecting others during the war, I am forever indebted.

To whom I shared my ambitions, hopes, and success - my parents and sisters, I am grateful for your unwavering support and prayers.

To those who have had a significant impact on my life - my soul mate and my best friends.

To all who have touched my heart, who have shaped my intellectual journey, who have shown kindness and support.

To all of them

I dedicate this work

with immense gratitude and love.

TABLE OF CONTENTS

LIST OF FIGURES

LIST OF TABLES

ABSTRACT

The general objective of this research work was to evaluate the properties of Sudanese bagasse, cotton stalks, and kenaf bast fibers for producing sustainable biocomposites and bioenergy. The chemical composition of these fibers was determined using the Technical Association of the Pulp and Paper Industry (TAPPI) methods and FTIR to assess the percentages of Cellulose, lignin, hemicellulose, and ash content. The Folin-Ciocalteu method was used to determine the total phenols. Thermogravimetric analysis (TGA), differential scanning calorimetry (DSC), and bomb calorimetry were used for the thermal analysis. The results showed that bagasse contained 50.6% cellulose and 21.6% lignin, cotton stalks had 40.3% cellulose and 21.3% lignin, and kenaf bast fibers recorded 58.5% cellulose and 10% lignin. The TGA showed degradation temperatures at 321°C for the bagasse, 289°C for the cotton stalks, and 354°C for the kenaf bast fibers. The DSC showed the glass transition temperatures of 81°C for the bagasse, 66.3°C for the cotton stalks, and 64.5°C for kenaf bast fibers. The higher heating values were 17.3 MJ/Kg for the bagasse, 17.1 MJ/Kg for the cotton stalks, and 16.6 MJ/Kg for the kenaf bast fibers. The results confirmed the suitability of these fibers for biocomposites and bioenergy production as they contained high percentages of cellulose, and their degradation temperature was above 300°C.

The study investigated the properties of panels made from the three studied fibers using casein and tannin adhesives with a 15% loading level (w/particles). A pressing cycle of maximum pressure of 2.5 MPa, different pressing time durations of 480s, 240s, 120s, and 60s, and a pressing temperature of 180°C were used. The target density was 0.6 $g.cm^{-3}$. The panels were tested for their mechanical, physical, and thermal properties according to European standards EN (310), EN (317), and EN (12664). The results showed that casein panels had higher mechanical properties and lower physical properties compared to tannin panels. Kenaf bast fibers panel exhibited the lowest mechanical and physical properties and did not meet the standard values. The mechanical properties of the tannin panels did not achieve the standard requirements. To investigate the sustainability of the panel production, the fibers were blended with ratios of 50:50 (w/w) for the binary panels and 40:30:30 for the tripartite panels for bagasse, cotton stalks, and kenaf bast fibers, respectively. The same manufacturing method for the individual fiber panels was used with the same adhesive loads. The results revealed that the individual fibers had better properties than blended fibers. The thermal conductivity of both was below EN standard. Casein panels made from individual bagasse and cotton stalk fibers were suitable for furniture and thermal insulation and conformed with EN standards (P2). Also, this part of the study explored the potential of producing

bio-based foam using different types of tannins as a second option for producing green insulation based on bioadhesives.

In order to investigate the bioenergy production performance, the fibers were subjected to pyrolysis using a macro thermogravimetric reactor. The pyrolysis process was conducted at 500°C with a heating rate of 10°C/min and a holding time of 60 minutes. The bio-oils were analyzed using FTIR and GC-MS to identify their composition. Cotton stalks exhibited the highest biochar and pyrolysis liquid, followed by bagasse and kenaf bast fibers. The biochars exhibited favorable thermal properties, with low volatile and ash content, high fixed carbon and carbon content, and high heating value. The TG and DTG indicated improved thermal stability, with a significant increase in degradation temperature for bagasse (65.9%), cotton stalks (87.5%), and kenaf bast fibers (76.1%) compared to raw materials. Biochars release significantly more energy and thermal stability than raw materials. The bio-oil analysis revealed similar compounds among the three fibers. The findings of biochars provide a clear understanding of their immense potential for energy applications.

RESUME

L’objectif général de ce programme de recherche était d’évaluer les propriétés de trois biomasses produites au Soudan et d’en étudier l’aptitude pour la production de biocomposites et de bioénergie. Ces trois biomasses (bagasse, tiges du cotonnier et fibres libériennes de kénaf) ont été sélectionnées en fonction de leur importance économique pour le Soudan. La composition chimique de ces fibres a été déterminée à l’aide de méthodes de l’Association technique de l’industrie des pâtes et papiers (TAPPI), de techniques classiques d’analyses physico-chimiques ainsi que par spectroscopie infrarouge à transformée de Fourier (FTIR).

La méthode de Folin-Ciocalteu a été utilisée pour déterminer le pourcentage en phénols totaux. L'analyse thermogravimétrique (TGA), la calorimétrie différentielle à balayage (DSC) et l’étude calorimétrique ont été employées pour analyser les comportements à la chaleur de chacune des biomasses. Les analyses chimiques ont montré que la bagasse possédait environ 50,6 % de cellulose et 21,6 % de lignine, alors que les tiges de cotonnier avaient 40,3 % de cellulose et 21,3 % de lignine, et les fibres de kénaf enregistraient 58,5 % de cellulose et 10 % de lignine. Les études physico chimiques (TGA et DSC) ont montré des températures de dégradation de 321 °C pour la bagasse, 289 °C pour les tiges de coton et 354 °C pour les fibres de kénaf. La DSC a révélé des températures de transition vitreuse de 81 °C pour la bagasse, 66,3 °C pour les tiges de coton et 64,5 °C pour les fibres de kénaf. Les moyennes des valeurs calorifiques supérieures étaient de 17,3 MJ/kg pour la bagasse, 17,1 MJ/kg pour les tiges de coton et 16,6 MJ/kg pour les fibres de kénaf. Les résultats ont montré que ces fibres étaient adaptées à la production de biocomposites et de bioénergie car elles contenaient des pourcentages élevés de cellulose et que leur température de dégradation était supérieure à 300 °C.

Durant ces recherches, ont été examinées les propriétés des panneaux fabriqués à partir des trois catégories de fibres en utilisant des adhésifs à base de caséine et de tanins avec un taux de colle de 15 % (poids/particules). Un cycle de pressage avec une pression maximale de 2,5 MPa a été utilisé, avec différentes durées de temp de pressage de 480s, 240s, 120s et 60s. La température de pressage était de 180 °C pour une densité cible de 0,6 g/cm³. Les panneaux ont été caractérisées pour leurs propriétés mécaniques, physiques et thermiques conformément aux normes européennes EN (310), EN (317) et EN (12664). Les résultats ont montré que les panneaux à base de caséine avaient des propriétés mécaniques plus élevées que les valeurs des normes de référence, mais des propriétés physiques plus faibles par rapport aux panneaux à base de tanins. Les panneaux à base de fibres de kénaf ont présenté des propriétés mécaniques et physiques plus faibles. Les propriétés

mécaniques des panneaux à base de tanins ne répondaient pas non plus aux exigences des valeurs standards. Afin d'étudier la soutenabilité de la production de panneaux au Soudan, des fibres de nature différente ont été mélangées selon des rapports de 50:50 (poids/poids) pour les panneaux mixtes et de 40:30:30 pour les panneaux tripartites (mélange de bagasse, de tiges de cotonnier et de fibres de kénaf respectivement). La même méthode de fabrication que pour les panneaux de fibres a été employée. Les résultats ont montré que les panneaux non mélangés présentaient de meilleures propriétés que ceux produits avec des fibres mélangées. La conductivité thermique des deux types de panneaux était inférieure à la norme européenne. Les panneaux à base de caséine fabriqués à partir de la bagasse et des tiges de cotonnier possèdent des propriétés adaptées pour le mobilier et l'isolation thermique et répondent à la norme EN (P2). Cette partie de l'étude explore également le potentiel de production de mousse biosourcée en utilisant différents types de tanins dans un premier temps, ouvrant ainsi la voie à l'utilisation de tanins provenant de tiges de coton dans des travaux futurs.

Les fibres ont été soumises à des essais de pyrolyse à l'aide d'un réacteur thermogravimétrique macro. Les tiges de cotonnier ont présenté la plus grande production de biochar et de liquide de pyrolyse, suivies de la bagasse et des fibres de kénaf. Les biochars présentaient des propriétés thermiques favorables, avec une faible teneur en composés volatils et en cendres, une teneur élevée en carbone, ainsi qu'une valeur calorifique élevée. La TG et la DTG ont permis d'identifier la stabilité thermique des biomasses, avec une augmentation significative de la température de dégradation pour la bagasse (65,9 %), les tiges de cotonnier (87,5 %) et les fibres de kénaf (76,1 %). Les biochars ont libéré significativement plus d'énergie et ont présenté une meilleure stabilité thermique que les biomasses. L'analyse des bio-huiles a révélé des composés similaires parmi les trois types de fibres. Les résultats des biochars issus des trois biomasses nous ont permis d'avoir une meilleure compréhension de leur potentiel très important pour de futures applications énergétiques.

1. GENERAL INTRODUCTION

Agricultural biomass, derived from various plant-based sources such as crop residues, agricultural byproducts, and dedicated energy crops, presents a promising avenue for sustainable and renewable resource of utilization (Saeed et al., 2017). It is a valuable feedstock for diverse applications, such as biocomposites and bioenergy production (Monteiro et al., 2012). Its utilization is critical in reducing waste and promoting the transition towards greener alternatives that mitigate environmental concerns while reducing dependence on fossil fuels and providing valuable sources of bioenergy. The chemical composition and thermal properties of natural fibers are critical factors that determine their overall properties. They also influence their processing and use in various applications. The content of cellulose, hemicellulose, lignin, and other fiber extractives can be evaluated to estimate their thermal and mechanical properties (H. Chen et al., 2006; Liu, N. A. and Fan, 1999). These components are present in almost all-natural fibers, but the difference in their composition, which depends on the geographic location, makes the fibers behave differently. Due to their inherent advantages, there is growing interest in using agricultural biomass to create biocomposite materials. Biocomposites from natural fibers provide a sustainable alternative to traditional synthetic composites. Incorporating agricultural fibers into biocomposites enhances their mechanical properties while reducing environmental impact (Gumowska et al., 2021; Holt et al., 2014). Additionally, using agricultural biomass in these materials can lower their carbon footprint, promoting a circular and eco-friendly approach. Furthermore, using bio-based adhesives such as tannin and casein to bond biocomposites is an eco-friendly alternative to synthetic adhesives (Ndiwe et al., 2019).

Residual biomass can be converted into energy in the form of heat, electricity, and biofuels through biomass conversion (A. I. Osman et al., 2021). Biomass is a renewable feedstock for bioenergy production. Technologies like combustion, gasification, and pyrolysis can be used. Depending on factors such as the type of biomass feedstock, desired energy output, and specific application, each method has unique advantages and disadvantages (Dziike et al., 2022). Using agricultural biomass for bioenergy production reduces greenhouse gas emissions significantly compared to fossil fuels. Pyrolysis is a highly effective process that utilizes heat in an oxygen-free environment to break down the components of lignocellulosic biomass, including cellulose, hemicellulose, and lignin. This process forms solid, liquid, and gas fractions, making it an indispensable technique for biomass conversion (Boer et al., 2020). The quantity of the most desired products can be controlled by adjusting pyrolysis process parameters, such as temperature,

heating rate, and residence time. (Glushkov et al., 2021). Slow pyrolysis is a thermal decomposition process in which biomass is heated to temperatures between 300°C and 500°C and exposed to longer residence times. This process yields more solid biochar but generates less liquid and gas due to slower reaction kinetics (F. Lin et al., 2015).

This research utilized sugarcane bagasse, kenaf bast fibers, and cotton stalks. Sugarcane bagasse was obtained from the Al-Gunied sugar factory in Sudan. Kenaf stems were taken from the University of Khartoum demonstration farm, specifically from Shambbat area in Khartoum-North, Sudan. Cotton stalks used were collected from Gezira state in Sudan. The study investigates the potential of producing biocomposites and bioenergy from Sudanese agricultural biomass materials such as sugarcane bagasse, cotton stalks, and kenaf bast fibers. Utilizing agricultural residues sheds light on these applications' feasibility and benefits, addressing waste management challenges and aligning with sustainable development and environmental stewardship principles. Agricultural biomass is valuable in the journey toward a more sustainable future. These fibers were selected based on their availability and production quantities in Sudan.

2. General Objectives

The general objective of this research work was to evaluate the properties of Sudanese bagasse, cotton stalks, and kenaf bast fibers for producing sustainable biocomposites suitable for use in furniture and thermal applications. It also aimed to investigate the possibilities of producing bioenergy from the three fibers.

2.1. Specific Objectives

- To assess the chemical composition, of the bagasse, cotton stalks, and kenaf bast fibers by using appropriate methods of chemical analysis such as TAPPI and FTIR spectroscopy.
- To determine the thermal properties of these fibers using TGA, DSC, and Bomb Calorimetry.
- To produce eco-friendly particleboards from individual and blended fibers using casein and tannin adhesives.
- To test the mechanical, physical, and thermal properties of the particleboards according to the relevant European standards.
- To evaluate the panels' suitability for furniture and thermal insulation applications following the relevant EN standards.
- To explore the potential for producing bio-insulations based on the tannins foams.
- To produce the biochar from the three fibers by using a slow pyrolysis process.
- To analyze and characterize the chemical composition and thermal properties of the biochar by using TGA and Bomb calorimetry to determine its suitability for bioenergy applications.

- To identify the composition of bio-oil obtained as a by-product from the pyrolysis process.

The thesis is structured into five distinct parts. The first part is dedicated to the literature review on lignocellulosic materials, biomass valorization and utilization for biocomposite materials, and biomass conversion processes. The second, third, and fourth parts cover the findings of the experimental works conducted in this research study. The second part provides a detailed analysis of bagasse, cotton stalks, and kenaf bast fibers' chemical composition and thermal properties, exploring their potential for sustainable applications such as biocomposite materials and bioenergy production. The third part explores the potential for manufacturing eco-friendly particleboards that can be used for general uses, including furniture and thermal insulation. It also compares the physical, mechanical, and thermal characteristics of blended and individual fiber particleboards made from bagasse, cotton stalk, and kenaf bast fibers using tannins and casein adhesives. In addition, this part examines the potential of producing bio-based foam from different types of tannins to be used as bio-insulation materials. The fourth part investigates using studied fibers for bioenergy applications via slow pyrolysis. It evaluates the resulting yield of biochar and its thermal properties for potential energy applications. Additionally, it analyzes the bio-oil obtained from the process using FT-IR and GC-MS to explore its composition and possible uses. The final part provides a general conclusion on the work, findings, and future work.

Part I. Literature review

CHAPTER 1

BIOMASS VALORIZATION

1. Biomass valorization

1.1. Overview of lignocellulosic biomass

The word "biomass" is derived from two Greek words: "bio," meaning life, and "maza," meaning to gather or assemble. Biomass refers to nonfossilized biological material derived from living/recently living organisms and biodegradable organic or carbon-based material originating from plants, animals, vegetable-derived materials, and microorganisms (de Galiza Barbosa et al., 2022; Jawaid et al., 2017). Lignocellulosic biomass is a complex structural material found in the cell walls of woody plants and consists of cellulose and hemicellulose polysaccharides and lignin (Jensen et al., 2017). Lignocellulosic biomass is a promising renewable resource that has the potential to be used as a feedstock to produce various types of biofuels, such as bioethanol, biodiesel, and biogas, as well as a wide range of value-added compounds, including platform chemicals, biopolymers, and other bio-based products. (Ning et al., 2021). Fig. 1 illustrates the different resources of biomass.

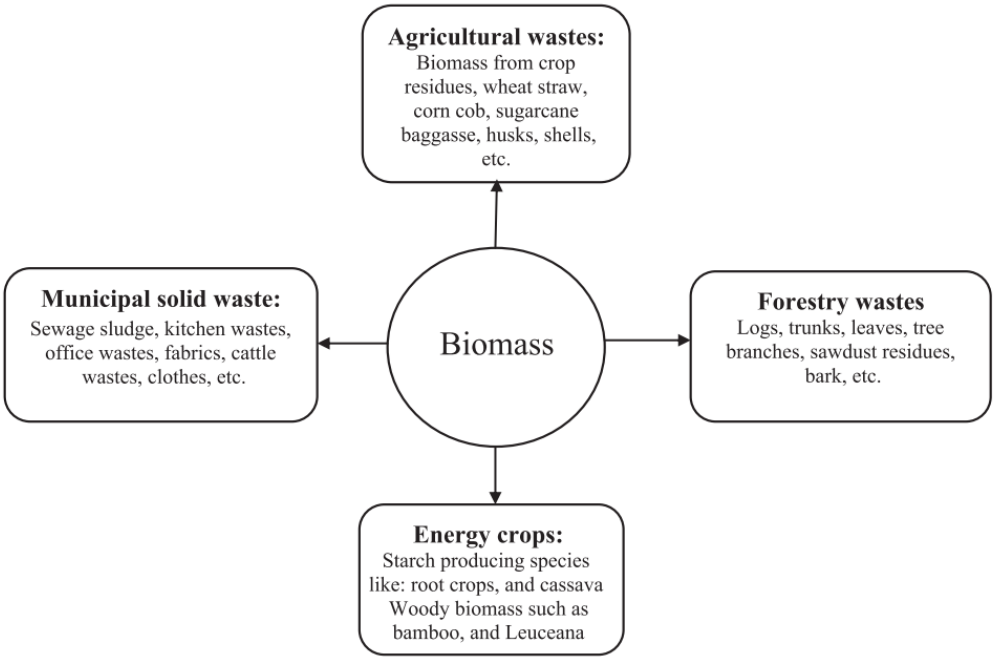

Figure 1: Biomass resources (G. K. Gupta & Mondal, 2019)

1.1.1. Chemical composition of lignocellulosic biomass

Lignocellulosic biomass comprises three fundamental compounds: cellulose, hemicellulose, and lignin (Popp et al., 2021). According to (Mustafa et al., 2022), the lignocellulosic biomass is composed of (30-60) % cellulose, (14-40) % hemicellulose, and (7-25) % lignin. Cellulose is packed with hemicellulose and lignin, constituting the plant cell wall (Fig. 2) (Nargotra et al., 2023). Pectin and proteins are also in smaller amounts and play essential roles in cell adhesion and growth. The depolymerization of cellulose and hemicellulose into sugars is critical in producing biofuels and other bioproducts. Microorganisms can ferment these sugars to produce bioethanol and biobutanol, which can be used as alternative fuels. They can also be converted into valuable chemicals, such as itaconic acid, which has synthetic fibers and resins (Ning et al., 2021). Lignin works like an embedding material for structural rigidity, protecting the cell wall from microbial degradation. Lignin is a complex aromatic polymer composed of phenylpropane units linked together by various chemical bonds. These aromatic units can be depolymerized or broken down into smaller fragments, which can then be extracted and used to produce valuable aromatic chemicals (Davis & Moon, 2020). The composition of cell walls varies widely among species and may vary within an individual, depending on the cell type or in response to environmental conditions (Popper et al., 2011).

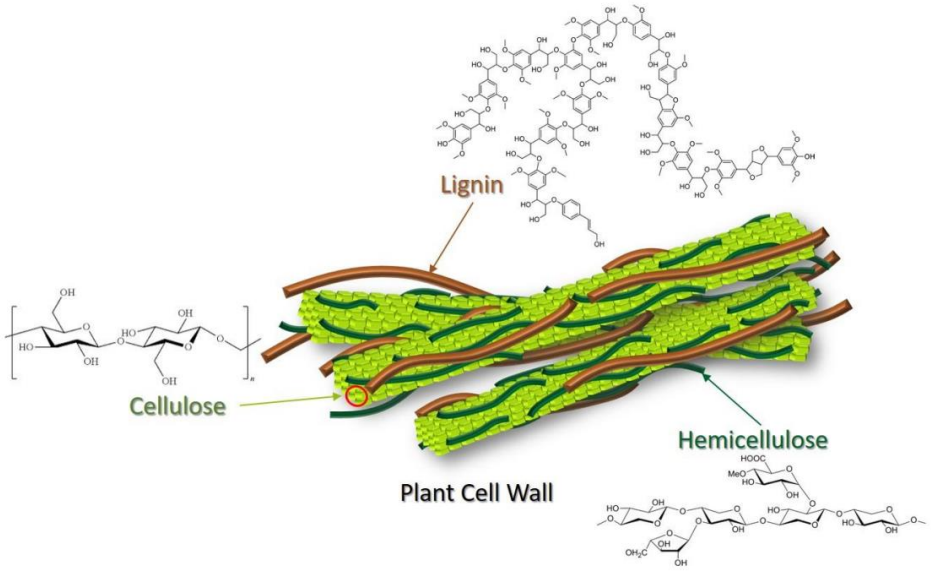

Figure 2: Structure of lignocellulosic biomass (Jensen et al., 2017)

1.1.1.1. Cellulose

Cellulose is the primary load-bearing component of plant cell walls and is considered the most abundant biopolymer on Earth (Sorek et al., 2014). Cellulose is a kind of polysaccharide

$(C_6H_{12}O_5)_n$ that is formed through the link of D-glucopyranose units with β-(1-4)-glycoside linkages, where *n* is the degree of polymerization (DP). It usually is polymerized with a degree of around 10,000 (X. Li et al., 2007) and possibly as high as 15,000 (S. Wang et al., 2017). The polymer consists of two glucose molecules. Each glucose unit has three hydroxyl groups, as shown in Fig. 3, which can interact, forming intra- and intermolecular hydrogen bonds, giving cellulose a crystalline structure and its unique properties of mechanical strength and chemical stability (Dhyani & Bhaskar, 2018). The crystallinity of cellulose varies widely in various biomasses. The cellulose molecular arrangement in the crystalline region is uniform and ordered with intra-molecular and inter-molecular hydrogen bonds. In contrast, the hydrogen bonding network is loose and disordered in the amorphous area, with fewer H-bonds (Leng et al., 2018).

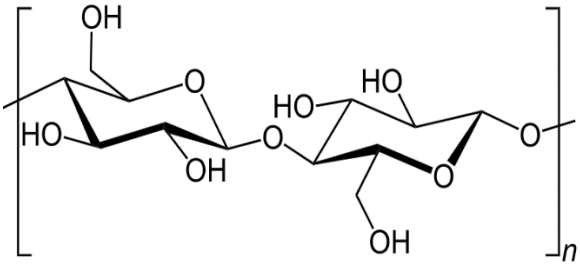

Figure 3: Basic monomer structure of cellulose (de Galiza Barbosa et al., 2022; Ning et al., 2021)

1.1.1.2. Hemicellulose

Hemicellulose is a polysaccharide in plant cell walls chemically bonded to cellulose and lignin (Pan et al., 2023). Hemicelluloses comprise various sugar units, including xylose, arabinose, mannose, galactose, and glucuronic acid, arranged in different proportions and with different substituents (Gabrielii et al., 2000). The components and the units of hemicellulose are illustrated in Fig. 4. The degree of polymerization (DP) of hemicellulose is lower than cellulose, with an average range of 80–200 (Peng et al., 2012). Hemicellulose in hardwood consists of xyloglucan, glucomannan, and glucuronoxylan, while softwood is primarily composed of arabinoglucuronoxylan, xyloglucan, and galactoglucomannan (S. Wang et al., 2017; X. Zhou et al., 2017).

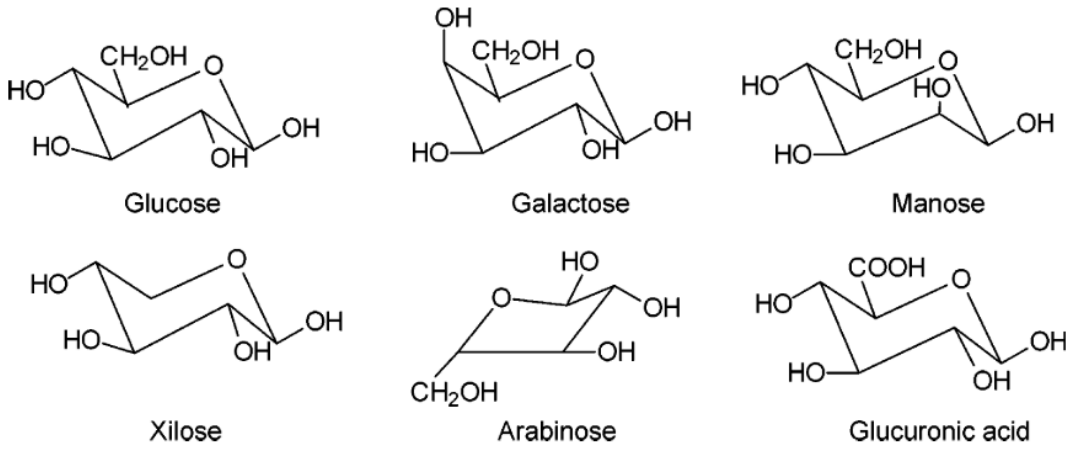

Figure 4: Components of hemicellulose (Mohan et al., 2006)

1.1.1.3. Lignin

Lignin is a complex and heterogeneous aromatic polymer composed of three primary phenylpropane precursors: p-coumaryl alcohol, coniferyl alcohol, and sinapyl alcohol (Fig. 5). These precursors are linked together through various chemical bonds to form a highly cross-linked and branched polymer structure (Lourenço & Gominho, 2023). These precursors are abbreviated as S, G, and H, which have different numbers of methoxy groups (none, one, and two, respectively) connected to the aromatic ring (Ning et al., 2021). Hardwood and softwood lignin have different structures. Softwood lignin has a content of guaiacyl units resulting from the polymerization of a higher fraction of coniferyl phenylpropane units. In contrast, a mixture of guaiacyl and syringyl units is typically found in many hardwoods (Mohan et al., 2006). Lignin is a very complex phenolic polymer whose content and composition vary depending on many factors, such as species, specimen age, environment, growth conditions, and harvesting time (Bonawitz & Chapple, 2010; S. Wang et al., 2017).

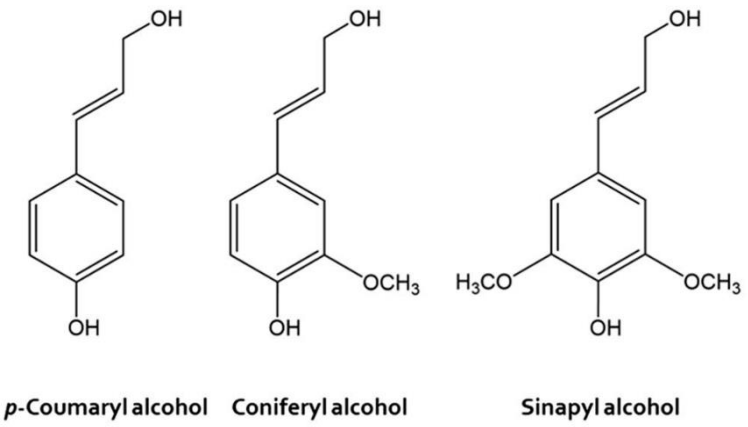

Figure 5: The structural characteristics of three typical units in lignin (Ning et al., 2021)

1.1.1.4. Extractives and inorganic components

Besides the three major components in biomass, small amounts of extractives do not constitute cell walls or cell layers but are nonstructural components (S. Wang et al., 2017). Organic extractives can be extracted with polar solvents (such as methylene chloride, alcohol, and water) or nonpolar solvents (such as toluene or hexane). These extractives include fats, waxes, alkaloids, resins, proteins, phenolics, simple sugars, saponins, pectins, mucilages, gums, starches, glycosides, and essential oils (Dhyani & Bhaskar, 2018; Mohan et al., 2006). Tannins are the most common group of phenolic compounds and can be divided into hydrolyzable tannins and condensed tannins (Nunes et al., 2018). Inorganic compounds, especially potassium, sodium, silicon, calcium, phosphorus, and chlorines, are the main constituents of the ash in biomass feedstocks (Dahou et al., 2021). The ash concentrations in softwoods start from less than 1% and reach 15% in herbaceous biomass and agricultural residues (Agblevor & Besler, 1996).

1.1.2. Biomass properties

The main biomass properties related to the production of biocomposites and bioenergy conversion are:

1.1.2.1. Moisture content

Moisture content plays a crucial role in the storage and handling of biomass. It can be present in two forms: (a) Intrinsic and (b) Extrinsic moisture. Intrinsic moisture refers to the naturally present water within the biomass material's structure. It can be measured by determining the equilibrium moisture content of the material under specific temperature and humidity conditions (Cai et al., 2017; M. yi Chen et al., 2018). (b) Extrinsic moisture refers to the moisture content acquired from the environment surrounding the biomass material. This type of moisture content can be influenced by various factors such as temperature, relative humidity, precipitation, and other weather

conditions. Moisture content affects the high heating value. The higher heating value of biomass decreases with increasing moisture content (Demirbas, 2007). In addition, moisture content affects the pressing process of the particleboards (Chiang et al., 2014) and can cause their failure.

1.1.2.2. Ash content

Ash content represents the quantity of solid residue left after the biomass is completely burned (Cai et al., 2017; Makavana et al., 2020). The residue left behind comprises a mix of inorganic and organic compounds that are complex, diverse, and have varying compositions. The primary ingredients of biomass ash are the oxide form of silica, aluminum, calcium, potassium, iron, magnesium, titanium, and sodium (Vassilev et al., 2013).

1.1.2.3. Proximate and ultimate analysis

Proximate analysis is used to determine the percentages of moisture content, volatile matter (VM), fixed carbon (FC), and ash of biomass (Park et al., 2023), while the ultimate analysis determines the percentage of carbon (C), hydrogen (H), nitrogen (N), sulfur (S), and oxygen (O) in the material. The ratio of elements obtained from the ultimate analysis provides a better comparison among the feedstock (Dhyani & Bhaskar, 2018).

1.1.2.4. Fixed carbon and volatile matter

Fixed carbon (FC) and volatile matter (VM) are critical parameters that characterize biomass. FC refers to the solid residue left after the volatile matter and moisture are removed from the biomass. The carbon content of biomass remains after combustion and is considered the source of energy in biomass (Posom & Sirisomboon, 2017). The volatile matter content of biomass is an essential factor that affects its ignition and combustion behavior. The light volatiles, small molecules formed during thermal degradation, are responsible for the initial stages of biomass ignition (Caillat & Vakkilainen, 2013).

1.1.2.5. Calorific values

Calorific, or heating value, is the energy released when a substance is burned. It is the most essential of biomass as it determines the energy value and the potential applications of biomass as a fuel source. Calorific value is typically measured in units of energy per unit of mass (Petráš et al., 2019; M. Singh et al., 2020). There are two types of heating values: (a) The lower heating value (LHV), which is the amount of heat stored in the biomass excluding the latent heat of vaporization of water, and (b) The high heating value (HHV), which include the latent heat of water vapor (G. K. Gupta & Mondal, 2019). The heating or calorific value of biomass fuel can be determined experimentally using a bomb calorimeter. This device measures the enthalpy change of reactants and products that result from the combustion of the biomass sample in a controlled oxygen environment (Flores et al., 2006; Posom & Sirisomboon, 2017; Z. T. Yu et al., 2011). Fig. 6

illustrates the bomb calorimeter device and its cutaway diagram. In addition, the calorific value can be estimated by correlating the heating value of biomass with the data of proximate analysis by using various empirical equations (Boumanchar et al., 2017; Demirbas, 2007; Sheng & Azevedo, 2005).

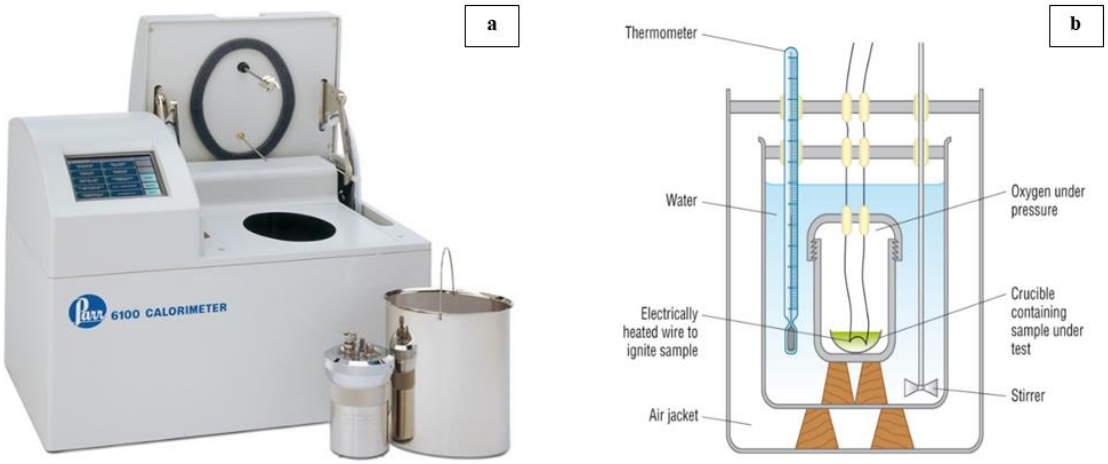

Figure 6: a) A typical bomb calorimeter, and b) A cutaway diagram (Melville, 2014; Parr Instrument Company, 2013)

1.1.3. Sudanese biomass

Sudan has abundant biomass resources, including agricultural residues such as sugarcane bagasse, and cotton stalks, and forestry residues like wood chips and sawdust. These biomass resources are potential feedstocks for various applications, including energy production, biofuels, and value-added products (Omer and Fadalla, 2003). Sudan's varied environments, ranging from desert to tropical rainforest, contribute to its ecological richness and make it home to many plant species. The country's natural resources play a vital role in its economy and provide opportunities for sustainable development and conservation efforts. Research on Sudanese biomass is relatively limited, but several studies have explored its potential applications and challenges. Khristova et al., (2002) evaluated the suitability of Sudanese kenaf varieties for papermaking, explicitly focusing on the soda and alkaline sulfite methods. The work aimed to examine different components of the Kenaf plant, including the bark, core, and whole stalk to produce particleboard from Kenaf using urea formaldehyde adhesive.

Omer and Fadalla, (2003) studied biogas energy technology from biomass in Sudan, considering its ecological, social, cultural, and economic impacts. Their research emphasized the importance of biogas technology, particularly for remote rural areas.

The study conducted by Z. Osman et al., (2009), focused on manufacturing particleboard using various agro fibers, namely bagasse, cotton stalks, maize straws, hemp, and eucalyptus. The study aimed to develop new bonding materials that are both high-performance and cost-effective, as the lighter weight of these agro fibers may require higher resin loadings. Additionally, the research aimed to identify the optimal conditions and process technology for utilizing these fibers without further treatment, such as chemical or mechanical processes, to reduce the overall manufacturing cost. Considering their unique properties and characteristics, the goal was to explore sustainable and efficient ways of utilizing these agro fibers in particleboard production.

Ellatif Ahmed Habib, (2014), explored the possibility of obtaining carbon-free and amorphous ash through additional sugarcane bagasse ash combustion processes. The aim was to unlock the valuable properties of sugarcane bagasse ash and explore its potential applications. The research conducted by Elbadawi et al., 2015, investigated how adding tannins to urea-formaldehyde resin could improve the mechanical and physical qualities of particleboard made from Acacia seyal wood. Acacia seyal is a tree native to Sudan commonly found in Kordofan and Blue Nile states.

The previous study by Bledzki et al., 2015, introduced biocomposites that utilized natural fibers, including Sudanese kenaf, for technical purposes. They contained equal fiber-to-matrix weight ratios and compatibilizer content and were manufactured and processed similarly. This approach gave a better insight into how fibers' physical properties influence their composites' mechanical properties. This gives a far more accurate estimation than most provided collations of data from different overview articles and handbooks. The researchers aimed to enhance the performance and features of the particleboard by incorporating tannins into the resin.

Saeed et al., (2017) focused on the suitability of Sudanese sorghum straw and bagasse for pulp and papermaking applications. They investigated the characteristics of these biomass materials and their potential use in the papermaking process. The challenges of implementing biomass gasifier-based projects for decentralized power supply in Sudan were examined by Mohamed and Fawzi, (2020).

1.1.3.1. Sugarcane bagasse

Sugar cane bagasse (Saccharum officinarum) is the fibrous residue that remains after juice extraction from sugarcane (Fig. 7), and it is widely available in many countries where sugarcane is grown (Ajala et al., 2021). Bagasse is a promising bioenergy production feedstock due to its high availability and energy content. As a byproduct of sugarcane processing, bagasse is a readily available and low-cost feedstock for bioenergy production (Edreis et al., 2014). The composition of sugarcane bagasse can vary depending on the variety of sugarcane, growing conditions, and other factors, but in general, cellulose and hemicellulose are the two main components, followed

by lignin. The composition of cellulose is between 36 to 46.8 %, hemicellulose is between 15.9 and 28.7 %, and lignin is between 9.8 and 26.2% (Nasution et al., 2022).

Sudan has six sugar plants (Kenana, Asalaia, Al-Gunied, Halfa, Sennar, and White Nile). The six sugar factories are classified into two groups: The Kenana and White Nile are privately limited companies, while the Al-Guneid, Halfa, Sennar, and Asalaia, are publicly owned. The quantity of sugar cane pressed yearly in Sudan is more than 8 million tons (Ibrahim, 2020). This quantity produces a significant amount of sugarcane bagasse waste residue, up to 27 thousand tons (Saeed et al., 2017). The bagasse can be a pollutant to the environment if it is disposed of without treatment. Nevertheless, the utilization of sugarcane bagasse is still limited and mainly used as a fuel to power sugar mills (Hua et al., 2022).

Figure 7: a) Sugar cane plant and b) sugarcane bagasse (Batstone, 2021)

1.1.3.2. Cotton stalks

Cotton stalks (*Gossypium herbaceum L.*) are the residual parts of the cotton plant that remain after the cotton bolls, which contain the cotton fibers, are harvested (Fig. 8). Cotton stalks can be a valuable source of energy and can be used as feedstock for various thermochemical and biochemical conversion processes (Sidhu and Sandhya, 2015). According to G. Li et al., (2022), the cotton stalks contain 45% cellulose, 20% hemicellulose, and 21% lignin.

Cotton cultivation in Sudan dates back to the 19th century when it was first grown in the Tokar area of Eastern Sudan. Commercial production began in 1905, but establishing the Sennar dam in 1925 marked a significant milestone in irrigated agricultural production in Sudan. Essential quantities of cotton stalks are burned annually in Sudan because of the lack of suitable and available processing facilities (Saeed et al., 2017).

Figure 8: a) Cotton plant and b) cotton stalks

1.1.3.3. Kenaf bast fibers

Kenaf (Hibiscus cannabinus L.) is a warm-season annual fiber crop widely grown for its fibrous stems used for various industrial and commercial applications. Kenaf is a member of the Malvaceae family, which also includes other essential fiber crops like cotton, okra, and jute (Ishak et al., 2010; Keshk et al., 2006). Kenaf has been cultivated for thousands of years and is believed to have originated in ancient Africa, specifically in the western Sudan region. It was then introduced to Egypt, where it was cultivated as early as 4000 BC for its fiber (Keshk et al., 2006).

Kenaf has been grown extensively in Sudan as a rope fiber in high Savanna areas with heavy rains, such as the Abu-Namaa area and Gezira state Central part of Sudan (Khristova et al., 2002). The kenaf plant has an inner woody core and an outer fibrous bark surrounding the core (Ishak et al., 2010). Fig. 9 shows the kenaf plant and its parts. The woody core makes up about (60-65)% of the stem, while the outer fibrous bark makes up the remaining (35-40)% of the stem (Bledzki et al., 2015; Khristova et al., 2002). The retting or degumming process separates bast fibers from the woody core and outer bark of kenaf plant stems. The process involves soaking the harvested stems in water to allow for the natural degradation of the pectin and lignin that hold the fibers in place. Then, they can be cleaned, dried, and processed into various products (Tsubota & Ichiryu, 2005). Kenaf bast fiber has been used to produce particleboard, fuel, textiles, and as a reinforcement material for composites (Amel et al., 2013). The kenaf bast fibers comprise 35-57% cellulose, 21.5% hemicellulose, and 15-19% lignin (Al Faruque et al., 2022).

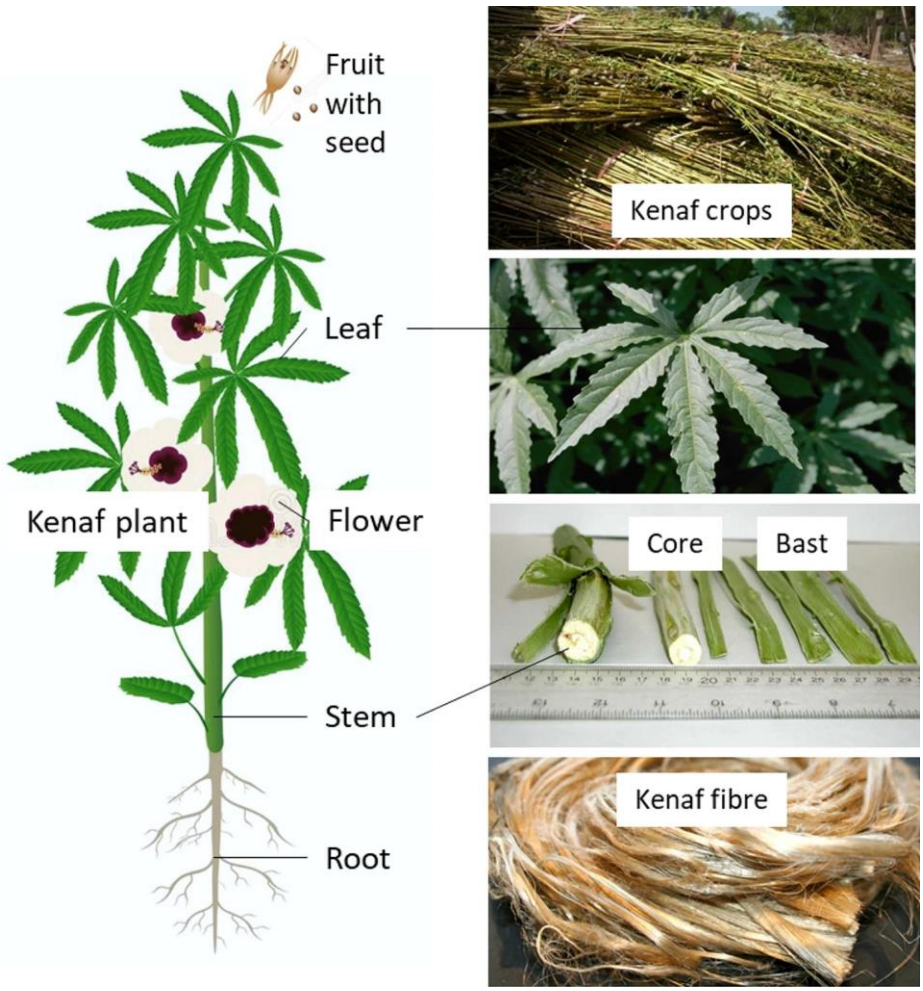

Figure 9: Kenaf plant and its parts (Harussani & Sapuan, 2022)

CHAPTER 2

BIOMASS UTILIZATION FOR BIOCOMPOSITES

2. Biomass utilization for biocomposites

2.1. Biocomposites materials

Biocomposite materials utilize natural or renewable resources as at least one of their constituents (Odetoye & Adeoye, 2022; Yaghoobi & Fereidoon, 2019). They are considered eco-friendly materials and have gained significant attention recently due to their sustainability and potential to reduce the environmental impact of traditional composite materials that rely on non-renewable resources (Guillou et al., 2018). Fig. 10 displays the global percentage distribution of different manufactured products in 2019.

Biocomposites can be obtained by blending natural fibers with other matrices, such as bio-derived thermoset resins, biodegradable plastics, and bio-based polymers (Righetti et al., 2019). Biocomposites have shown potential in the construction industry as renewable and sustainable building materials (Dziike et al., 2022). Biocomposites can be divided into two categories: non-wood fibers and wood fibers. The use of hardwood species in the manufacture of wood-based panels is gaining popularity due to their environmental benefits. Hardwood species can increase biodiversity and promote sustainable forest management practices. However, it's worth noting that hardwood species are typically more expensive than softwood species, so the cost factor must also be taken into consideration (Pędzik et al., 2021).

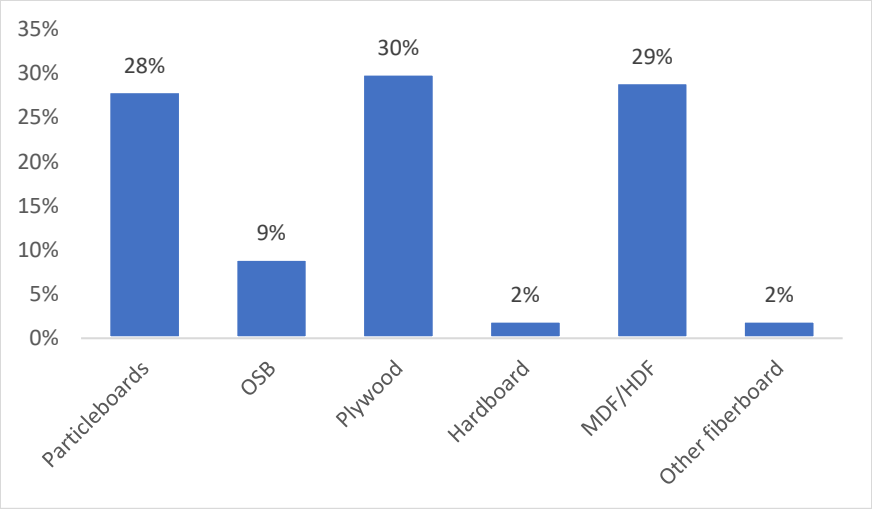

Figure 10: The percentage distribution of various types of products manufactured worldwide in 2019

Particleboard is a composite panel made from wood particles or other lignocellulosic materials, such as agricultural fibers, bonded with resin or binder under heat and pressure. The resulting board is uniform in texture and density and can be used for various applications, including furniture, cabinetry, flooring, and wall paneling (Jimenez et al., 2022; Papadopoulou & Chrissafis, 2017).

Lignocellulosic agricultural waste has been extensively researched as a potential raw material for particleboard production (S. H. Lee et al., 2022; D. L. Nguyen et al., 2023). The use of agricultural wastes in particleboard production has the potential to reduce greenhouse gas emissions and mitigate the environmental impact of agricultural waste disposal (Aisien et al., 2015). Asia is the largest producer of particleboard, with China being the highest producer, followed by Europe, America, Africa, and Oceania. Germany, Poland, Italy, Austria, and France are some of the leading producers of particleboard in Europe (Fig. 11). The production of particleboard has been steadily increasing over the years, with an estimated production quantity of 96.01 million m^3 worldwide in 2020 (Hua et al., 2022).

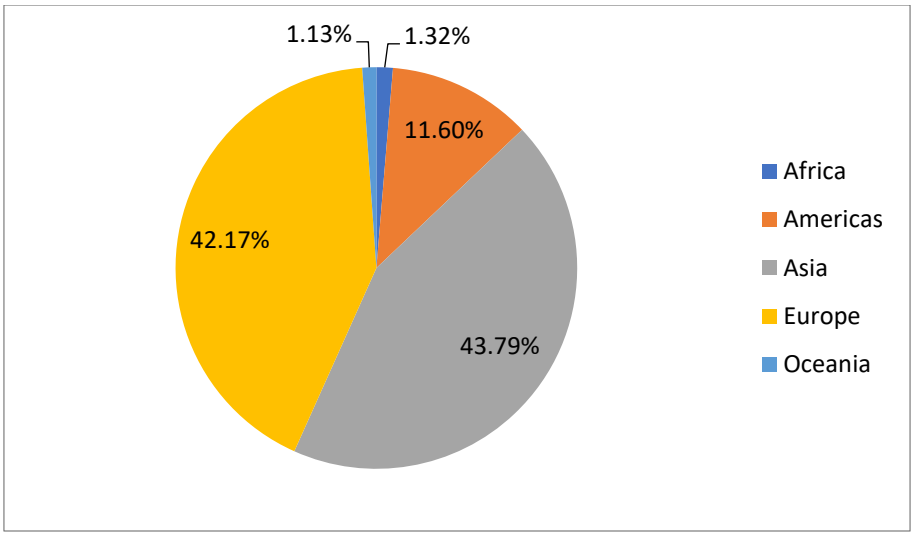

Figure 11: Global particleboards production quantity (m^3) in 2020 (Hua et al., 2022)

2.2. Particleboards adhesives

A variety of adhesives could be natural or synthetic derived from petrol and fossil. The use of adhesives dates back to ancient times, the Egyptians' first recorded use of animal-based adhesives was in the 18th century BCE. These adhesives produced wooden artifacts (Raydan et al., 2021). Over time, the development of synthetic and chemical adhesives has expanded their use in engineering and artistic purposes. Adhesives are widely used in various industries today, including construction, aerospace, automotive, electronics, etc. Some natural adhesives, such as blood, gums, pitch, and rubber latex, could be used with little processing. In contrast, others, like soy protein, milk casein, and collagen adhesives, require more processing before they can be used as adhesives.

2.2.1. Synthetic adhesives

Synthetic adhesives as urea-formaldehyde (UF), phenol-formaldehyde (PF), melamine urea formaldehyde (MUF), and polyurethane (PU) are widely used in the manufacturing of wood composites due to their excellent binding strength and other desirable properties such as water resistance, durability, and high-temperature resistance (Boussetta et al., 2022; Ferdosian et al., 2017). Urea-formaldehyde (UF) adhesives are the wood industry's most widely used type of amino resin adhesive (Elbadawi et al., 2015; Ferdosian et al., 2017). Formaldehyde is a colorless, strong-smelling gas commonly used to manufacture many household products and building materials, including particleboard, plywood, and adhesives (Engozogho Anris et al., 2021). Formaldehyde emissions can harm human health, including eye and throat irritation, respiratory issues, and cancer (Bacigalupe & Escobar, 2021). Formaldehyde has been classified as a Group 1 carcinogen

(carcinogenic to humans) by the International Agency for Research on Cancer (IARC), which is part of the World Health Organization (WHO) (Boussetta et al., 2023).

2.2.2. Bio-based adhesives

Bio-based adhesives are made from natural, renewable materials such as plant and animal sources and are seen as a more sustainable alternative to mimic the performance of synthetic adhesives (Mahieu et al., 2021). The term "bio-based adhesive" has a narrow definition, which refers to materials exclusive of natural, non-mineral origin and can be used as they are or with minimal modifications. The most commonly used materials in bio-based adhesives are tannins, lignins, carbohydrates, unsaturated oils, and protein hydrolysates (Owodunni et al., 2020). These materials are derived from renewable resources and offer an eco-friendly alternative (Pizzi, 2013).

The use of bio-based adhesives in the manufacturing of particleboard and other wood-based composites is a promising development that can help reduce the environmental impact of the construction industry while also providing high-performance materials that meet industry standards (Abd El-Sayed et al., 2019; Zhao & Umemura, 2014). Protein-based adhesives are made from proteins derived from various sources, such as animals, plants, and microorganisms (Papadopoulou & Chrissafis, 2017). They also have gained attention as an alternative to conventional synthetic adhesives due to their biodegradability, renewability, and low toxicity (Nikvash et al., 2012). Proteins can form adhesive solid bonds due to their ability to crosslink, which is the process of forming chemical bonds between protein molecules to create a three-dimensional network (Bacigalupe & Escobar, 2021). Some examples of protein-based adhesives include soy protein adhesives (Pothula, 2016), casein adhesives (derived from milk proteins) (Herzog et al., 2021), and collagen-based adhesives which are derived from animal sources (Raydan et al., 2021).

2.2.2.1. Tannin

Tannins are a type of polyphenolic compound found in various plant species, and they can be broadly classified into two categories based on their chemical structure: hydrolyzable tannins and condensed tannins (Aristri et al., 2022). Condensed tannins are polymeric and are composed of their flavan-3-ol units linked together by carbon-carbon bonds, forming a complex network of intermolecular and intramolecular hydrogen bonds (Jahanshahi et al., 2016). Condensed tannins are widely found in nature and various trees such as Acacia, Schinopsis, Tsuga, Rhus, and Pinus species. These tannins are mainly concentrated in the wood and bark of these trees, making them an abundant source of tannin extracts (Pizzi, 2013). Commercial tannin extracts can be manufactured from these sources and used in various applications, including adhesives, coatings, and tanning agents (Naima et al., 2015). In contrast, hydrolyzable tannins are typically more extensive and complex molecules composed of a central core of glucose or other polyol units

attached to multiple gallic acids or ellagic acid units (Ghahri & Pizzi, 2018). When hydrolyzed, these units are released from the central core as individual molecules.

2.2.2.2. Casein

Casein has been used as an adhesive for thousands of years. The ancient Egyptians used casein-based glues for a variety of applications of construction and furniture (Ebnesajjad & Landrock, 2015; M. Guo & Wang, 2016b). Casein is one of the main proteins found in milk, and it can be obtained by precipitating it out of the milk using acid (Mahieu et al., 2021). This process results in the formation of curds, which are then washed and dried to obtain a powder that can be used in various applications, including as an adhesive (El Hajj et al., 2012). Casein glues are water-soluble adhesives that dissolve casein protein in water (M. Guo & Wang, 2016b; Schwarzenbrunner et al., 2020). Lime and sodium hydroxide are usually used with casein as the hardener. Changing the proportions of lime or sodium hydroxide with casein can alter the properties of the resulting adhesive (Raydan et al., 2021). The glue is applied in a liquid state and dries by evaporation of water, leaving behind a solid adhesive layer. As the casein dries, the protein molecules undergo a chemical transformation, becoming more insoluble and forming a solid bond between the joined surfaces (Ebnesajjad & Landrock, 2015). Casein adhesives typically require longer pressing times than other types of adhesives (Herzog et al., 2021).

2.3. Particleboards Manufacturing

Particleboard is a versatile and cost-effective material widely used in construction and manufacturing industries. It is made by breaking down wood particles or fibers into small pieces, mixing them with a resin adhesive, and forming them into boards under heat and pressure (Hua et al., 2022). The particleboard manufacturing process can be summarized in the following steps: (a) Drying, in which the particles are subjected to a drying process to eliminate excess moisture and enhance the bonding strength of the resin; (b) Adhesion, in which the particles are blended with a resin binder in a rotating drum; (c) Mat-forming, in which the dried particles are placed in the mold and distributed and compressed to form a mat; (d) Pre-pressing, in which the mat is pre-pressed to eliminate any remaining air and ensure the uniform distribution of the particles; and (e) Hot pressing, in which the mold is subjected to high temperature and pressure in a hot press (Cesprini et al., 2022; Halvarsson et al., 2009).

The resulting boards are uniform in density and strength, making them ideal for various applications (Popescu, 2017). The type of binder used can significantly impact the physical and mechanical properties of the resulting particleboard. The choice of adhesive depends on various factors, including the desired properties of the particleboard, the cost of the adhesive, and any environmental or health considerations (Nadhari et al., 2020).

2.3.1. Particleboards properties

There has been a lot of research and development in the field of particleboards to improve their properties and performance of the particleboards. The focus has been on enhancing particleboards' mechanical, physical, and thermal properties, making them more competitive with conventional materials (Ndazi et al., 2006). The mechanical, physical, and thermal properties are essential indicators of particleboard quality (Dahmardeh Ghalehno et al., 2011). The important mechanical properties of particleboard include modulus of elasticity (MOE), modulus of rupture (MOR), internal bond strength (IB), and screw-holding strength (SHS) (Pędzik et al., 2021). The physical properties of particleboard include thickness swelling (TS), water absorption (WA), and density (Şahin, 2020). Thermal properties include thermal conductivity (Srichan & Raongjant, 2020). These properties determine particleboard's strength, durability, and resistance to various external factors, such as moisture, heat, and impact.

2.3.1.1. Modulus of rupture (MOR)

MOR measures a material's strength and the maximum stress a material can withstand before breaking or rupturing (Zuber et al., 2020). It can be calculated using Eq. (1) (Yunusa et al., 2022):

$$\text{MOR} = \frac{3 \times F_{max} \times L}{2 \times b \times h^2} \quad (1)$$

where F is the maximum load at rupture in Newtons (N), L is the span length in millimeters (mm), b is the width of the specimen in millimeters (mm), and h is the thickness of the specimen in millimeters (mm).

2.3.1.2. Modulus of elasticity (MOE)

MOE measures a material's stiffness and resistance to bending or deformation under load (Ojo & Olugbade, 2022). MOE can be calculated using Eq. (2) (Tawasil et al., 2021):

$$\text{MOE} = \frac{L^3 \times (F_2 - F_1)}{4 \times b \times t^3 \times (a_2 - a_1)} \quad (2)$$

where L is the span length in meters (m), b is the width of the test specimen in meters (m), t is the thickness of the test specimen in meters (m), $(F_2 - F_1)$ is the incremental load increase between two deflection points on the straight-line portion of the load-deflection curve, and $(a_2 - a_1)$ is the increase in the deflection at mid-length of the specimen (corresponding to $F_2 - F_1$).

2.3.1.3. The internal bond (IB)

The internal bond strength (IB) test measures the bonding strength between the particles in the particleboard. The test involves gluing square test specimens to metal loading blocks using a hot melt adhesive and subjecting them to a tensile force perpendicular to the particleboard surface until rupture occurs. The IB value is then calculated based on the maximum force required to rupture

the specimen and its cross-sectional area (Nourbakhsh, 2010). The internal bond (IB) of a particleboard can be calculated using Eq. (3) (Adefris Legesse et al., 2022):

$$IB = \frac{F_{max}}{A} \tag{3}$$

where F_{max} is the maximum force required to break the test specimen, and A is the cross-sectional area of the specimen.

2.3.1.4. Screw holding strength (SHS)

Screw-holding strength refers to the ability of particleboard to hold screws in place without the screws pulling out or causing damage to the board. It is an essential property of particleboard, especially for applications where the board will be used as a substrate for screws and fasteners, such as furniture and cabinetry construction. According to (He et al., 2020), many different types of screws can be used with particleboards: (1) Cross groove countersunk head self-tapping screw: This type of screw has a tapered head with a cross-shaped groove in the top. (2) Cross groove round head self-tapping screw: This type of screw has a rounded head with a cross-shaped groove on the top. (3) Cross groove large flat head self-tapping screw: This type of screw has a large flat head with a cross-shaped groove on the top.

2.3.1.5. Water absorption (WA) and thickness swelling (TS)

Water absorption (WA) and thickness swelling (TS) are important properties to consider when evaluating the performance of particleboard. Water absorption refers to the amount of water a particleboard panel can absorb over time (Farag et al., 2020). This property is crucial because it can affect the dimensional stability and durability of the boards. Thickness swelling refers to the percentage of increase in thickness that occurs in a particleboard panel after it has been exposed to water for a certain amount of time (Ojo & Olugbade, 2022). The WA and TS are illustrated by Eqs (4) and (5), respectively (Mitchual et al., 2020).

$$Water\ absorption = \frac{W_f - W_0}{W_0} \times 100\ \% \tag{4}$$

Where W_0 is the initial weight of the test sample before soaking in water, and W_f is the final weight after soaking in water.

$$Thickness\ swelling = \frac{T_f - T_0}{T_0} \times 100\ \% \tag{5}$$

where, T_0 is the initial thickness of the test sample before soaking in water, and T_f is the ultimate thickness of the specimen following immersion in water.

2.3.1.6. Thermal conductivity (k)

Thermal conductivity is the term used to describe a material's capacity to conduct heat. It is typically measured in watts per meter-kelvin (W/m. K) (S. Wang et al., 2020). Thermal conductivity can be measured using a Hot Disk device (He, 2005). The Hot Disk device works by sandwiching a thin, flat sensor between two samples of the material being tested (Nagai et al., 2000; Zheng et al., 2020). A small amount of heat is applied to one side of the sensor, and the temperature increase on the opposite side is measured. Thermal conductivity can be determined by analyzing the rate at which heat flows through the material (Mihiretie et al., 2017).

2.4. Bio-based foams

Over the past few years, tannins-based foams have emerged as an alternative to synthetic phenolic foams due to their high performance, particularly as insulation material, characterized by low thermal conductivity, self-extinguishing properties, and high fire resistance (Lacoste, Pizzi, Basso, et al., 2014). Additionally, they possess high chemical resistance and outstanding fireproofing properties, making them valuable in applications where fire safety and insulation are crucial (Issaoui et al., 2021). Tannin-based foams can be created using various foaming methods. The most commonly employed approach is the physical foaming method. In the physical method, a solvent with a low boiling point, such as pentane or diethyl ether, induces resin expansion through solvent evaporation. The increase in temperature, resulting from the exothermic self-condensation of furfuryl alcohol, reaches the boiling point of the solvent (Santiago-Medina et al., 2018). Additional foaming techniques employed in the production of tannin-based foams include chemical foaming (Basso et al., 2014) and mechanical foaming (Szczurek et al., 2014).

CHAPTER 3

VALORIZATION AND CONVERSION OF BIOMASS FOR BIOENERGY

3. Valorization and Conversion of Biomass for Bioenergy production

3.1. Biomass Conversion

Conversion of biomass refers to the process of converting organic matter such as agricultural waste, forest residues, municipal solid waste, and energy crops into valuable products such as fuels, chemicals, and energy (A. I. Osman et al., 2021). While biomass is used for feed and food, it is mainly used for energy production, heating, and electricity generation (Danso-Boateng & Achaw, 2022) and fuels and chemical feedstock production. Biomass as a renewable energy source has been increasing in developed countries to reduce carbon dioxide emissions from fossil fuels (Popp et al., 2021). It accounts for 10-14 % of the world's energy supply (McKendry, 2002). Solid, liquid, and gaseous biofuels are different forms of converting biomass. Wood pellets, biodiesel, bioethanol, biogas, and syngas are the types of biofuels that exist in solid, liquid, and gaseous forms (Özbay et al., 2001). The general overview of biomass conversion technology is stated in this part. Also, the pyrolysis process and its products are presented.

3.1.1. Direct combustion

Direct combustion is a thermochemical technique in which the biomass is burned in the presence of air or oxygen; this process is carried out inside a furnace, steam turbine, or boiler. The flue gases produced during combustion contain carbon dioxide, water vapor, nitrogen, and other trace gases released into the atmosphere (Lam et al., 2019). The major challenge for the direct combustion of biomass for energy production is that these resources must be far from industrial areas. Still, it can also be advantageous in reducing air pollution and minimizing the potential for negative impacts on human health (Q. Yu et al., 2021).

3.1.2. Biochemical conversion

Biochemical conversion of biomass involves using microorganisms or enzymes to transform biopolymers into gaseous or liquid biofuels (S. Y. Lee et al., 2019). The most common biological conversions in the biochemical process for biomass conversion are fermentation and anaerobic digestion (Ferreira, 2017). This process is slower than thermochemical conversion but does not require as much external energy and is more environmentally friendly (Fertilizers, 2021). Tab. 1 illustrates the main differences between thermochemical and biochemical conversion.

Table 1: Comparison between the thermochemical and biochemical conversion of biomass

Thermochemical conversion	Biochemical conversion
▪ Using heat and catalyst	▪ Using enzymes and microorganisms
▪ Process occurs fast (a few seconds to hours)	▪ Process takes time (in the range of days)
▪ Utilize the whole feedstock to produce value-added hydrocarbons (not feedstock specific)	▪ Convert carbohydrates into sugar. Produce lignin as a by-product.

3.1.3. Thermochemical conversion

Thermochemical conversion processes, such as combustion (complete oxidation), pyrolysis (oxygen-free), and gasification (partial oxidation), are commonly used to convert plant biomass into proper energy forms, such as heat, electricity, and biofuels. These processes involve heating biomass under controlled conditions to produce various energy products, such as gases, liquids, and solids. Each method has its unique advantages and disadvantages, and the choice of process depends on factors such as the type of biomass feedstock, the desired energy output, and the specific application (Dziike et al., 2022). Compared to combustion, gasification has several advantages, such as higher efficiency, lower emissions, and the ability to use a broader range of feedstocks, including low-quality biomass and waste materials (Kumar et al., 2009). Fig. 12 illustrates the main products of biochemical and thermochemical conversion of biomass. Tab. 2 shows the differences between the types of Thermochemical Conversion regarding their temperature, heating rate, reaction time, medium, pressure, and solid, liquid, and gas yield.

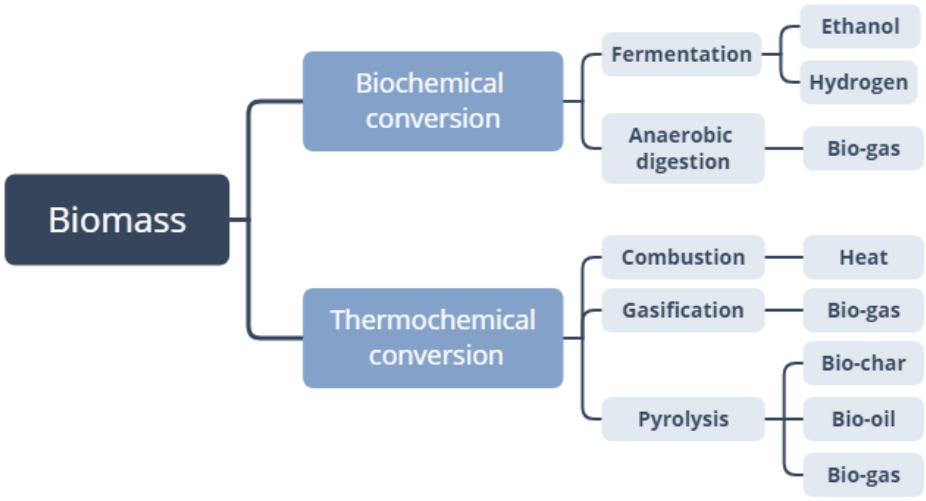

Figure 12: Biochemical and thermochemical conversion of biomass with the main products (Ferreira, 2017)

Table 2: Thermochemical Conversion Processes type (Ronsse et al., 2015)

	Torrefaction	**Slow pyrolysis**	**Fast pyrolysis**	**Gasification**
Temperature	<300°C	> 400°C	~500°C	600 – 800°C
Heating rate	-	< 80 °C/min	Fast, Up to 1000 °C/min	-
Reaction time	< 2 hours	Hours ˷ days	Few seconds	-
Medium	Oxygen-free	Oxygen-free or limited	Oxygen-free	Oxygen-limited (air or steam/oxygen)
Pressure	Atmospheric	Atmospheric (or elevated up to 1 MPa)	Atmospheric	Atmospheric, pressurized up to 8 MPa
Solid yield	80%	35%	12%	10%
Liquid yield	5%	30%	75%	5%
Gas yield	15%	35%	13%	85%

Torrefaction is the distinct process used for the thermal treatment of biomass. Torrefaction involves subjecting biomass to mild pyrolysis conditions, typically at temperatures ranging from 200 to 300°C and for shorter residence times. It is considered a form of slow pyrolysis. The main objective of torrefaction is to pretreat biomass to enhance its fuel properties compared to the original biomass. The process aims to improve properties such as energy density, grind ability, hydrophobicity, and stability. Torrefied biomass can be used as a feedstock in various applications, including pyrolysis, gasification, and combustion. It can be used alone or with fossil coal as a fuel source (Nunes et al., 2018; Ronsse et al., 2015).

The gasification process typically involves three main steps: (a) Drying and pyrolysis, in which biomass feedstock is heated in a limited amount of oxygen. (b) Tar cracking, in this step, the gases are heated to a high temperature, causing the tars to break down into simpler molecules that are easier to handle. (c) Char gasification: In this step, the char residue from the first step is reacted with a controlled amount of oxygen or steam, producing a gas mixture composed primarily of carbon monoxide and hydrogen, known as syngas (Ab Karim et al., 2010).

Pyrolysis is a process that involves heating organic materials in the absence of oxygen or with limited oxygen to produce char, liquid bio-oil, and combustible gas (X. Wang et al., 2022). The end products depend on the type of feedstock used and the operating conditions (Mohan et al., 2006). The main difference between gasification and pyrolysis is that gasification produces a fuel gas (syngas) that can be used for heat, power generation, or chemical feedstock. In contrast, pyrolysis, besides the char, produces a liquid fuel known as pyrolysis oil or bio-oil, which can be used as a substitute for fuel oil or as a feedstock for the production of chemicals (S. Y. Lee et al., 2019; Pinheiro Pires et al., 2019).

The pyrolysis process is commonly categorized into three groups: "slow pyrolysis," "fast pyrolysis," and "flash pyrolysis" (Bridgwater et al., 2007; Güleç et al., 2022; S. Y. Lee et al., 2019). These categories are based on the process conditions' heating rate, temperature, and residence time (Makavana et al., 2020). Slow pyrolysis: In this mode, biomass is heated at a lower temperature (around 300-500°C) and a longer residence time (several minutes to hours). This results in a higher yield of solid biochar and a lower yield of liquid bio-oil and gas (F. Lin et al., 2015). Fast pyrolysis is a process in which biomass is heated rapidly to high temperatures (typically 400-600°C) in the absence of oxygen with a short residence time (up to 3 seconds) and high heating rates (greater than 103 °C/s) (A. I. Osman et al., 2021). This process produces a high yield of liquid bio-oil, a small amount of non-condensable gases, and solid biochar. Flash pyrolysis is a rapid thermal degradation process involving biomass heating at very high temperatures (typically 700-1000 °C) without oxygen and for a very short residence time (typically less than 2 seconds). This results in the rapid production of liquid bio-oil and char and gas products. This process's fast heating rate

and short residence time are critical, as they help minimize secondary reactions and increase bio-oil yield (Priharto et al., 2020).

The mode and conditions of pyrolysis can be controlled to optimize the yield and properties of the products obtained for a particular application. For example, fast pyrolysis may be preferred for producing liquid bio-oil as a fuel. In contrast, slow pyrolysis may be selected for biochar production as a soil amendment or for carbon sequestration (Güleç et al., 2022). In addition, the yield of biomass pyrolysis products can be increased according to the following conditions: (1) char yield, low heating rate, and temperatures; (2) liquid yield, high heating rates with average temperature, and short gas residence time; and (3) gas yield, low heating rate, high temperature, and long gas residence time (Glushkov et al., 2021).

3.1.4. Biomass pyrolysis and its mechanisms

Pyrolysis and gasification are the two primary thermochemical conversion processes studied for converting biomass into usable forms of energy. Pyrolysis is a thermal decomposition process without oxygen and typically involves biomass heating. The optimal temperature range for pyrolysis depends on the type of biomass being processed and the desired products (S. Y. Lee et al., 2019). Biomass pyrolysis is considered a preliminary stage in biomass gasification, as the pyrolysis process produces a mixture of gases and liquids known as pyrolysis gas or pyrolysis oil, which can be further processed and refined into synthetic gases or liquid fuels through gasification (H. Li et al., 2019). The pyrolysis mechanism is complicated because it involves the thermal decomposition of significant biomass components, including cellulose, hemicellulose, and lignin (D. Chen et al., 2022). Fig. 13 shows the Pyrolysis mechanism of biomass. The three main steps involved in biomass pyrolysis are (a) Drying and devolatilization, which consists of removing free moisture and volatile components from the biomass. (b) Primary pyrolysis: This is the main mechanism of pyrolysis, which involves the thermal degradation of solid components, such as cellulose, hemicellulose, and lignin. (c) Secondary pyrolysis comprises the cracking and condensation of the liquid bio-oil produced during primary pyrolysis (Kan et al., 2016; Prakash Bamboriya et al., 2019).

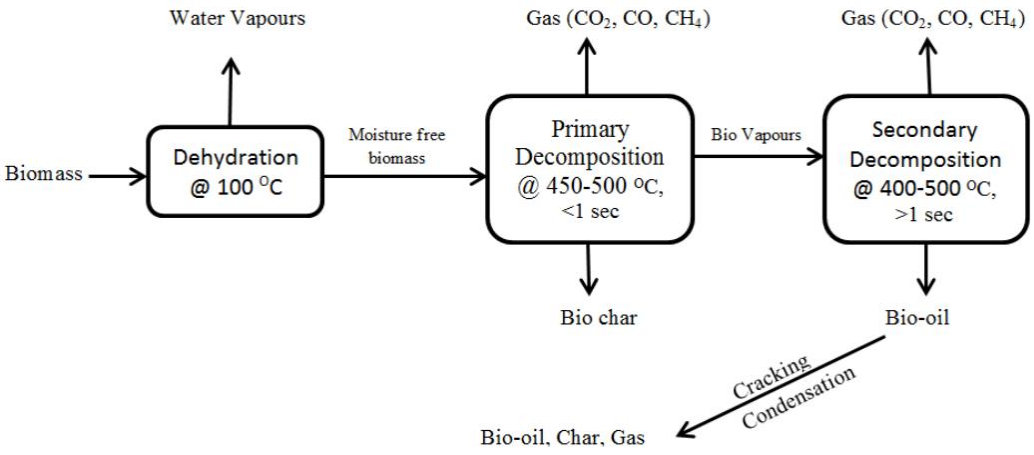

Figure 13: Pyrolysis mechanism of biomass (R. K. Mishra et al., 2022; Prakash Bamboriya et al., 2019)

Thermogravimetric analysis (TGA) and differential scanning calorimetry (DSC) are commonly used techniques to study the thermal decomposition behavior of biomass during pyrolysis (Wielage et al., 1999). TGA measures the weight change of the sample as it is heated at a constant rate under a controlled atmosphere, while DSC measures the heat flow into or out of the sample as it is heated or cooled at a constant rate. These techniques provide essential information on the thermal degradation behavior of biomass, including the temperature and rate of weight loss, the reaction kinetics, and the energy required for the pyrolysis process. Fig. 14 shows the thermal behavior of cellulose, hemicellulose, and lignin.

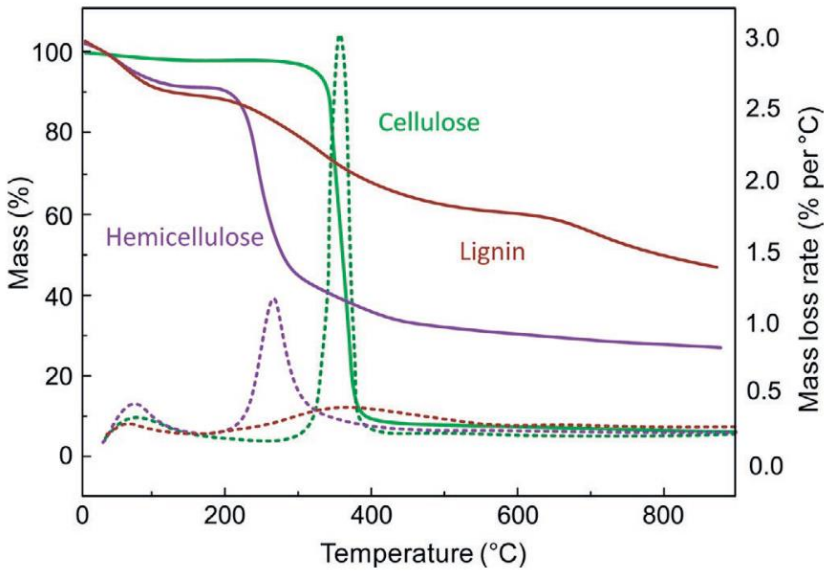

Figure 14: TG and DTG curves for cellulose, hemicellulose, and lignin (Ronsse et al., 2015)

The three main components of biomass, cellulose, hemicellulose, and lignin, have different pyrolysis behaviors. Hemicellulose starts decomposing quickly, with the maximum weight loss rate occurring at a lower temperature range of 220-315°C. Cellulose pyrolysis is focused at a higher temperature range of 315-400°C, with a maximum weight loss rate at 355°C. Lignin is the most challenging component to decompose, and its decomposition occurs slowly over the entire temperature range from ambient to 900°C with a very low mass loss rate (H. Yang et al., 2007).

Several conditions, such as heating rate, temperature, residence time, feedstock type and composition, catalysts, reactor type, and atmosphere, can influence biomass pyrolysis (Kan et al., 2016). According to (Glushkov et al., 2021), The yield of biomass pyrolysis products can be increased according to the following conditions:

a) Char yield: low heating rate and temperatures
b) Liquid yield: high heating rates with average temperature and short gas residence time
c) Gas yield: low heating rate, high temperature, and long gas residence time

3.1.5. Pyrolysis products

3.1.5.1. Biochar

Biochar is a type of solid char produced from biomass through pyrolysis, has much carbon, and is porous. It has been shown to have a range of potential uses, including as a soil amendment, carbon sequestration tool, and feedstock for energy production (Dobariya et al., 2022; Meyer et al., 2011). The biochar yield can vary depending on the type of biomass being used, as well as the specific

pyrolysis conditions. Some types of biomass may produce more biochar than others due to their chemical composition and structure (Ighalo & Adeniyi, 2021).

Biochar typically has a higher heating value than raw biomass feedstock (15 to 30 MJ/kg), making it a potentially attractive substitute for coal in specific fuel applications, particularly in industries traditionally used as feedstock. Biochar has a lower carbon content than coal, making it a more environmentally friendly alternative (Kan et al., 2016). The bulk density for biochar is low. However, the bulk density depends on factors such as the type of feedstock, pyrolysis conditions, and post-treatment processes (Pecha & Garcia-Perez, 2020). Biochar can improve soil fertility by increasing water retention, reducing nutrient leaching, and providing a habitat for beneficial microorganisms. Biochar can also sequester carbon in the soil for long periods, helping mitigate climate change (Kharel et al., 2019; Pecha & Garcia-Perez, 2020).

3.1.5.2. Pyrolysis liquid

Generally, pyrolysis liquid is dark in color, has a high acidity (pH between 2 and 4), and is typically a single-phase liquid with relatively low viscosity (Pinheiro Pires et al., 2019). Various factors, including the feedstock type and pyrolysis conditions like temperature, heating rate, and residence time, determine the properties of pyrolysis liquid. Pyrolysis liquid is a complex mixture of organic compounds that typically contains a significant amount of water and a wide range of organic compounds, including acids, alcohols, ketones, aldehydes, phenols, ethers, esters, sugars, furans, alkenes, nitrogen compounds, miscellaneous oxygenates, and solid particles (Rezaei et al., 2014). The water content of pyrolysis liquid can range from ~25 to 50% depending on the feedstock and pyrolysis conditions, which is difficult to separate from the organic components (Mohan et al., 2006). Tab. 3 shows the physical properties of wood pyrolysis liquid.

In the pyrolysis liquid, the yield of bio-oil is determined after separating the aqueous phase from the pyrolysis liquid fraction by a simple decantation process where the aqueous phase is separated from the organic phase based on the difference in their densities (Barros et al., 2018a). Some of the common synonyms for pyrolysis liquid, which is a liquid product obtained from the pyrolysis of biomass, are bio-oil, pyrolysis oils, bio-crude oil, wood liquids, pyroligneous acid, and liquid smoke (Mohan et al., 2017). Gas chromatography coupled with mass spectrometry (GC/MS) is commonly used to characterize bio-oil. This technique allows for separating and identifying the various volatile and semi-volatile compounds in the bio-oil, which can then be analyzed at the molecular level through their mass spectrum (Torri et al., 2016). Other techniques, such as Fourier-transform infrared (FTIR) spectroscopy and nuclear magnetic resonance (NMR) spectroscopy, can also be used for the characterization (Ingram et al., 2008). Bio-oil can be used

as a fuel for transportation and heat generation (Varma & Mondal, 2016). However, it has some limitations due to its high acidity, low stability, and high water content.

Table 3: Typical properties of wood pyrolysis liquid

Physical property	**Reference 1**	**Reference 2**
	(Mohan et al., 2017)	(Rezaei et al., 2014)
Moisture content (wt %)	15 - 30	15-30
pH	2.5	2.8-3.8
Specific gravity	1.2	1.05-1.25
Elemental composition (wt %)		
C (%)	55-58	55-56
H (%)	5.5-7	5-7
O (%)	35-40	28-40
N (%)	0-0.2	<0.4
Ash (wt %)	0-0.2	<0.2
HHV (MJ/kg)	16-19	16-19
Viscosity (Cp)	(40-100) at 40 °C	(40-100) at 50 °C

3.1.5.3. Gaseous product

Pyrolysis gas, also known as pyrolysis syngas or bio-syngas, is a mixture of gases produced during biomass pyrolysis. It typically comprises carbon monoxide, carbon dioxide, hydrogen, methane, and small amounts of other gases such as nitrogen, oxygen, and water vapor (H. Li et al., 2019; Policella et al., 2019). During pyrolysis, the carbonyl (C=O) and carboxyl (COOH) groups break down, releasing CO and CO_2 (Strezov et al., 2008). The ratio of CO to CO_2 in the pyrolysis gas depends on the pyrolysis conditions, such as temperature, heating rate, and residence time. Light hydrocarbons, including methane (CH_4), are typically produced during biomass pyrolysis as a result of the decomposition of weakly bonded methoxyl (-O-CH_3) and methylene (-CH_2-) groups, as well as the secondary decomposition of oxygenated compounds (Q. Liu et al., 2008; Uddin et al., 2014). H_2 gas is primarily produced through secondary decomposition and reforming reactions involving aromatic compounds' C=C and C-H bonds, such as phenols and lignin (Q. Liu et al., 2008). In addition to direct use for heat or electricity production, pyrolysis gas can also be used as a fuel gas for boilers or furnaces or as a chemical feedstock for the production of various chemicals and materials (Becidan et al., 2007; Kan et al., 2016).

4. Conclusion

This part presented the literature review on lignocellulosic materials, their properties, the significance of utilizing biomass for biocomposites, and their potential for conversion into valuable materials and energy. In the upcoming part, a detailed analysis of the chemical composition and thermal properties of bagasse, cotton stalks, and kenaf bast fibers will be conducted to explore their potential for sustainable applications, including biocomposite materials and bioenergy production.

Part II. Thermo-chemical characterization of the Sudanese biomass

CHAPTER 1

INTRODUCTION

1. Introduction

Natural fibers' chemical composition and thermal properties play a crucial role in determining their overall properties and suitability for various applications, including bioenergy production and the development of biocomposite materials. Key components such as cellulose, hemicellulose, lignin, and other extractives present in natural fibers influence their thermal and mechanical properties. These components vary in composition among different fiber types, leading to variations in behavior and performance (Popp et al., 2021). Evaluating the content of these components can provide insights into the thermal and mechanical characteristics of natural fibers, enabling their appropriate selection and utilization in specific applications. While these fibers are commonly used as an energy source in rural and economically limited areas, efficient biomass production and utilization are crucial to meet growing energy demands (Monteiro et al., 2012). Understanding the thermal decomposition process of natural fibers is essential for predicting their behavior during composite processing and energy conversion and for designing efficient systems (Kaygusuz & Bilgen, 2009). Numerous studies have explored the thermal decomposition characteristics of natural fibers, focusing on the behaviors of cellulose, lignin, and hemicelluloses (H. Chen et al., 2006; Liu, N. A. and Fan, 1999).

This part aimed to comprehensively analyze the chemical composition and thermal properties of bagasse, cotton stalks, and kenaf bast fibers for biocomposite materials and bioenergy applications. The chemical analysis involved various essential properties such as moisture content, ash content, solubility in water, extraction with NaOH and organic solvent, total phenols, cellulose, and lignin. The chemical composition analysis followed the Technical Association of the Pulp and Paper Industry Standards (TAPPI) methods. The total phenol content was quantified using the Folin-Ciocalteu method. Furthermore, Fourier transforms infrared spectroscopy (FTIR) was used to gain insights into the types of chemical bonds in the fibers. The thermal behavior and stability of the fibers were investigated through thermogravimetric analysis (TGA) and differential scanning calorimetry (DSC), while their high heating values were measured using bomb calorimetry. These characterizations provide valuable insights into the potential sustainable applications of the studied fibers.

CHAPTER 2

MATERIALS AND METHODS

2. Materials and Methods

2.1. Biomass preparation

Bagasse and cotton stalks were utilized without any further processing. Kenaf bast fibers were obtained after peeling the outer part of the kenaf fresh stalks and immersed in the water for one week, then washed thoroughly with water and dried at room temperature. The fibers under investigation were stabilized in a controlled environment chamber with a maintained temperature of 20°C ± 2 and a relative humidity of 64 ± 2%.

2.1.1. Chemical characterization

Representative samples of the three studied fibers (One kilogram of chips) were milled in a laboratory mill (Retsch SK 100). The obtained powder was further fractionated using sieves. The chemical analysis portion was retained on a 60-mesh sieve according to the Technical Association of the Pulp and Paper Industry standard (TAPPI 11M-59). The air-dried powder was stored in a plastic jar overnight to homogenize moisture content. The Chemical analysis of raw materials was carried out using the Technical Association of Pulp and Paper Industry (TAPPI) Standard methods, as shown in Tab. 4:

Table 4: Standard methods used in the chemical characterization

No	Test (%)	Method
1	Moisture content	TAPPI T 208 om-94
2	Ash	TAPPI T 211 om-93
3	Solubility in hot/cold water	TAPPI T 207 om-93
4	Extraction by NaOH (1%)	TAPPI T 212 om-98
5	Extraction by organic solvent	TAPPI T 204 cm-97
6	Cellulose	TAPPI T 203 om-93
7	Lignin	TAPPI T 222 om-98

Ash content was determined by placing 2 g of each sample in porcelain crucibles and heated in an oven at 575°C for 3 hours. The ash percentage was then calculated using Eq. (6). The organic matter content and organic carbon content were calculated and given by Eqs (7) and (8), respectively (Navarro et al., 1993).

$$Ash\ content\ (\%) = \frac{weight\ of\ ash}{oven\ dry\ weight} \times 100 \quad (6)$$

$$OM\ (\%) = 100 - \text{Ash} \quad (7)$$

$$OC\ (\%) = 0.48 \times \text{OM} \quad (8)$$

Cellulose content was determined using a mixture of ethanol and nitric acid in a 4:1 ratio. A total of 2 g of each sample was placed in a conical flask, and 25 ml of the ethanol-nitric acid mixture was added. The flask was then placed in a water bath and heated for 15 minutes. This process was repeated four times, with an additional 15 ml of the mixture added each time. After the sequential extraction, the mixture was filtered, and the residue was placed in an oven for 24 hours. The percentage of cellulose was calculated by using Eq. (9):

$$Cellulose\ (\%) = \frac{weight\ of\ precipitate}{oven\ dry\ weight} \times 100 \quad (9)$$

Lignin content in the biomass samples was determined using sulfuric acid with a concentration of 72%. Initially, 5 g of the sample was weighed and placed in a Soxhlet extractor. To this, 15 ml of sulfuric acid was added to a beaker and then in a freezer for 2 hours. During this time, the mixture was periodically mixed every 15 minutes. Subsequently, the mixture was transferred to a conical flask, and 575 ml of distilled water was added. The flask was then heated for 4 hours. After heating, the mixture was filtered, and the residue was transferred to an oven. The percentage of lignin was calculated by using Eq. (10):

$$Lignin\ (\%) = \frac{weight\ of\ precipitate}{oven\ dry\ weight} \times 100 \quad (10)$$

The total phenol content was determined by the Folin-Ciocalteu method, which has already been described in previous work (Bikoro Bi Athomo et al., 2018). The total phenol content was calculated using Eq. (11):

$$Total\ Phenols\ (\%) = \frac{C \times D \times V}{1000 \times M_{dried}} \times 100 \quad (11)$$

where: C is the total phenol concentration (ppm), D is the degree of dilution (10), V is the volume of starting solution (30 ml), and M_{dried} is the mass of dry powder.

2.1.2. Fourier Transform Infrared Spectroscopy Analysis (FTIR)

FTIR spectroscopy analysis was conducted on the oven-dried samples of bagasse, kenaf bast fibers, and cotton stalks. The samples were dried at 105°C for 24 hours, and approximately 5 mg of the dried powder was placed into the device (Fig. 15). The analyses were performed using 64 scans, with a resolution of 4 cm^{-1} and in the range from 4000 to 400 cm^{-1}.

Figure 15: Fourier Transform Infrared Spectroscopy (FTIR) spectra

2.1.3. Thermogravimetric analysis (TGA)

The thermal degradation was performed using a thermogravimetric instrument (TGA Q50 Instrument), as shown in Fig. 16. Approximately 10 mg of samples were weighed and placed in a small pan in the device. The temperature program was from 30°C to 600°C at a heating rate of 10°C/min. The measurement was conducted under air with a 60 ml/min flux. All experiments were repeated three times to ensure accuracy and reproducibility.

Figure 16: Thermogravimetric analyzer (TGA)

2.1.4. Differential scanning calorimetry (DSC) analysis

The analysis was conducted on a DSC (TA Instruments, Q20) equipped with a rapid cooling system. The samples of bagasse, cotton stalks, and kenaf bast fibers were weighed (~5 mg) in standard aluminum pans, and data acquisitions were carried out using the Universal Analysis 2000 program (TA Instruments). Samples were first dried in an isotherm at 105 °C for 1 min followed by a cooling step at the rate of 10 °C/min. The experiment has been tested in a temperate range of (-50 to 250) °C. All experiments were repeated three times. Fig. 17 shows the Differential scanning calorimetry (DSC) analyzer.

Figure 17: Differential scanning calorimetry (DSC) analyzer

2.1.5. Higher heating value (HHV)

The bomb calorimetry device (Fig. 6) was used to accurately determine the higher heating value of the bagasse, kenaf bast fibers, and cotton stalk. ~1 g for each type of fiber was placed on the bomb for this test. Benzoic acid was used to calibrate the device, commonly used as a primary standard (Melville, 2014; Rojas & Valués, 2003). The experiments were carried out in triplicate, and the results were expressed as means ± SD.

CHAPTER 3

RESULTS AND DISCUSSION

3. Results and Discussion

3.1. Chemical characterization

The cellulose and lignin contents of bagasse, kenaf bast fibers, and cotton stalk are shown in Fig. 18. Among the three fibers studied, the highest % of Cellulose was achieved by the kenaf bast fibers (58.5%), which is similar to the value reported by Hamidon et al., 2019. However, it is in the normal range (44 to 57%) reported in the literature (Rowell et al., 2000). The bagasse reported a value of (50.6%), which was higher than the value reported in the previous study (Kanwal et al., 2019) (36.9%) and lower than the value recorded by Robles et al., 2015. The mean amount of cellulose in the cotton stalks (40.3%) was in line with the values in previous studies (A. Gupta et al., 2020; Hou et al., 2014). The differences among these values could be attributed to various parameters such as climatic conditions, soil chemical composition, plant variety, and age (Bledzki & Gassan, 1999). Natural fibers' mechanical, physical, and thermal properties are heavily influenced by their cellulose, hemicellulose, and lignin contents. Cellulose, the main structural component of plant cell walls and fibers, contributes to their strength and stability. Advanced mechanical properties are indicated by high cellulose content in fibers. In addition, understanding how cellulose content affects fiber thermal stability contributes to developing materials with enhanced heat resistance, expanding potential applications in various industries. It has been observed that the three fibers have a relatively high amount of cellulose, making them suitable for use in bioenergy and biocomposites since cellulose thermally degrades at approximately 300°C.

The lignin content in bagasse, cotton stalks, and kenaf bast fibers was 21.6%, 21.3%, and 10%, respectively. Bagasse had the highest lignin amount, followed by cotton stalks, while kenaf bast fibers had the lowest percentage. The measured value of lignin content in bagasse was consistent with the findings of Edreis et al., 2017. The value of kenaf bast fibers was the same as that found in the previous study (Guillou et al., 2018). The lignin content of cotton stalks was approximately equivalent to that determined in the literature (J. Li et al., 2016).

The results of the total phenol content of bagasse, kenaf bast fibers, and cotton stalks revealed that the fibers with the highest phenols content were the cotton stalks with a value of 6%, followed by bagasse with a value of 1.7%, and kenaf bast fibers with a value of 1.3%. The cotton stalks contain high amounts of phenols that have potential applications in various fields, including producing high-value products such as bio-based tannin adhesives, chemicals, and

pharmaceuticals. The phenolic compound is essential in protecting the biocomposite materials from fungi (Bhattacharya et al., 2010). Phenolic compounds possess antimicrobial and antifungal properties, making them natural defense mechanisms against biological degradation. Phenolic compounds play a crucial protective role in applications where biocomposite materials are exposed to high humidity, moisture, or outdoor environments conducive to fungal growth. Additionally, their presence could enhance the final adhesive-fibers network in future work targeting the production of biocomposites based on natural matrices such as tannins.

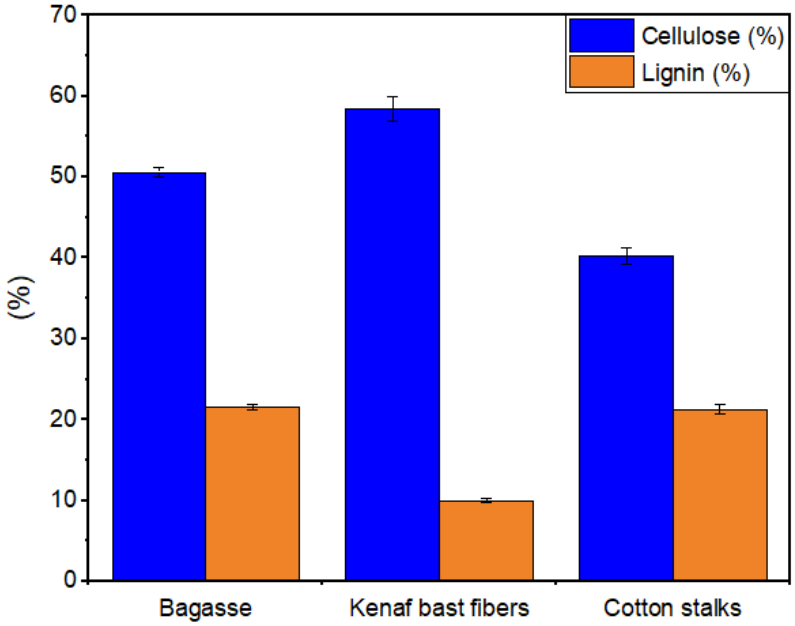

Figure 18: Cellulose and lignin contents of the bagasse, kenaf bast fibers, and cotton stalks.

The equilibrium moisture content (EMC) at 65% relative humidity and 20°C obtained for the bagasse, kenaf bast fibers, and cotton stalks are shown in Tab. 5. The results revealed 7.8%, 8.5%, and 8.4% for bagasse, kenaf bast fibers, and cotton stalks. The fibers' moisture content varies due to atmospheric conditions, plant age, soil quality, and preservation method. These results were lower than previous observations by Spinacé et al., 2009, who noticed that the moisture content of the fibers under normal atmospheric conditions ranged from 9.1% to 12.1%. It is worth noting that the three fibers understudy were found to be more dried than solid wood particles stored under the same moisture conditions (MC around 11%). This could be due to the dry weather conditions in Sudan during the collection of the fibers, where the temperature was above 40°C. The fibers' high moisture content is undesirable for many applications, including biocomposites and bioenergy

production. Water-repellent additions may not always be efficient and require advanced technology to reduce adverse effects ((BMBF) et al., 2018).

The results of the ash content of bagasse, kenaf bast fibers, and cotton stalks are shown in Tab. 5. The ash percentage was 8%, 2.5%, and 5.2%, respectively. The ash content of bagasse was higher than that of kenaf bast fibers and cotton stalks, exceeding the value reported in the literature (Edreis et al., 2017). The ash content of kenaf bast fibers was approximately in line with the value observed by Hamidon et al., 2019, which was (2-5)%. The cotton stalks showed lower ash content than previous works (A. Gupta et al., 2020; Xie et al., 2019). These differences can be attributed to the difference in chemical composition and the nature of the soil in which plants were grown (Hamza et al., 2013; Khiari et al., 2010). High ash content may affect biocomposites' mechanical properties, making transformation difficult. Low ash content is recommended for bioenergy production, where high heat output is desired (Platače & Adamovičs, 2014).

Table 5: Moisture content (H%), dry matter (DM%), ash content (%), organic matter (OM%), and organic carbon (OC%) of the fiber samples

Fibers	H (%)[a]	DM (%)[a]	Ash (%)[a]	OM (%)[a]	OC (%)[a]
Bagasse	7.8 ± 0.07	92.2 ± 0.07	8 ± 0.12	92 ± 0.12	44. ± 0.06
Kenaf bast fibers	8.5 ± 0.03	91.5 ± 0.03	2.5 ± 0.08	97.5 ± 0.08	46.8 ± 0.04
Cotton stalks	8.4 ± 0.14	91.6 ± 0.14	5.2 ± 0.16	94.8 ± 0.16	45.5 ± 0.08

(%): percentages are given on a raw material dry basis.

[a] Values are means ± SD.

Table 6 shows the soluble extractives in cold and hot water of bagasse, kenaf bast fibers, and cotton stalks. The kenaf bast fibers present the lowest % of the extractives compared to bagasse and cotton stalks. In contrast, cotton stalks showed the highest extractive % in cold and hot water.

The percentages of the extractive content obtained with 1% sodium hydroxide for bagasse, kenaf bast fibers, and cotton stalks are shown in Tab. 6. The highest rate was obtained by bagasse (43%), followed by cotton stalks 31.2% and then kenaf bast fibers 16.7%. These values were approximately equal to values reported for non-wood and annual plants (Khiari et al., 2010). It is important to note that the bagasse had a high percentage of extractives because of the sugars on the surface of the fibers. The ethanol-soluble extractives for the fibers were 9.9%, 10.1%, and 9.5% of bagasse, kenaf bast fibers, and cotton stalks, respectively (Tab. 6). The value of bagasse was

lower than the value reported in previous work (Kanwal et al., 2019). The kenaf bast fibers and Cotton stalks showed higher values than the ones reported in previous studies (Saba et al., 2015) and (B. Zhou et al., 2020), respectively. Knowing the percentage of extractives is crucial because they impede the reaction between fibers and resins in composite manufacturing. Removing them also enhances mechanical and thermal stability by hindering water uptake by the resulting panels.

Table 6: The percentage of soluble extractives of bagasse, kenaf bast fibers, and cotton stalk

	Bagasse	Kenaf bast fibers	Cotton stalks
Hot water extractives (%)[a]	13.9 ± 0.38	4.6 ± 0.08	15.3 ± 0.47
Cold water extractives (%)[a]	12 ± 0.15	2.6 ± 0.22	12.2 ± 1.19
Sodium hydroxide extractives (%)[a]	43 ± 0.29	16.7 ± 0.37	31.2 ± 0.39
Ethanol extractives (%)[a]	9.9 ± 0.18	10.1 ± 0.17	9.5 ± 0.14

(%): percentages are given on a raw material dry basis.

[a] Values are means ± SD.

3.2. Fourier transform infrared spectroscopy (FTIR) analysis

The FTIR analysis of the bagasse, kenaf bast fibers, and cotton stalks are shown in Fig. 19. The result achieved by the bagasse showed a high absorbance occurs at 3338 cm^{-1}, indicating the presence of a large amount of O–H groups in the lignocellulosic structure of the bagasse fibers. The absorptions related to groups O–H and C–H stretches are apparent, corresponding to the cellulose and hemicellulose structures and the aromatic and aliphatic chains in the lignin (Teixeira Cardoso et al., 2019). The band at 2891 cm^{-1} indicates the presence of a C–H group, at 1629 cm^{-1} of absorbed O–H or carbonyl bands, while the peak at 1423 cm^{-1} indicates the presence of a $-CH_2$ group, at 1319 cm^{-1} corresponds to the bending C–H. The Analysis also shows other vital absorptions related to groups, such as the C–O bond, which occurs at 1030 cm^{-1}, C=O at 1603 cm^{-1}, C=C at 1423 cm^{-1}, and 897 cm^{-1} indicating the presence of β-glycosidic bond. These profiles are pretty similar to what was reported in previous studies (Robles-García et al., 2018; Tronc et al., 2007).

The FTIR curve of the kenaf bast fibers shows that the band at 3334 cm^{-1} represents the O–H stretching vibration and hydrogen bond of hydroxyl groups. This is approximately in line with what was achieved by Rozyanty et al., 2021 and A. Guo et al., 2019a. The band at 2916 cm^{-1}

represents the C–H stretching vibration of methyl and methylene groups in cellulose and hemicelluloses (Saha et al., 2010). The band at 1728 cm^{-1} is attributed to the carbonyl C=O stretching frequency for aldehydes groups in lignin (Karimi et al., 2014; Rozyanty et al., 2021). The band at 1619 cm^{-1} is due to the C=C stretching of the aromatic ring of the lignin, and it is close to what was found in the literature (Rozyanty et al., 2021). The absorption band appeared at 1423 cm^{-1} and 1318 cm^{-1}, corresponding to the C–H bending and C–O stretching frequencies of hemicelluloses (Rozyanty et al., 2021). The band at 1237 cm^{-1} is attributed to the C–O and C=O stretching vibration of the acetyl group in hemicelluloses and lignin (A. Guo et al., 2019b). The band at 1155 cm^{-1} is due to C–O–C asymmetrical stretching in cellulose and hemicelluloses (A. Guo et al., 2019b; Tuerxun et al., 2019). The strong band at 1024 cm^{-1} is attributed to the C–O and C–C stretching frequencies of xylans. The band is also assigned to the C–O stretching, originating from the C–O–CH_3 groups, confirming lignin's presence (Rozyanty et al., 2021). The band at 896 cm^{-1} is attributed to β-Glycosidic linkage in cellulose (Karimi et al., 2014). The band at 668 cm^{-1} is attributed to cellulose's C–OH out-of-plane bending (A. Guo et al., 2019b).

The FTIR analysis of the cotton stalks showed the following results: The band observed at 3757 cm^{-1} is likely associated with isolated hydroxyl groups (Schramm, 2020). Isolated hydroxyl groups represent hydroxyl (OH) functional groups that do not bond hydrogen with adjacent molecules or functional groups (H. Lin et al., 2012). The band at 3336 cm^{-1} is attributed to the hydrogen-bonded O–H stretching vibration (Rahbar Shamskar et al., 2016). The band at 2920 cm^{-1} indicates the presence of a C–H group. The band at 1745 cm^{-1} is attributed to the carbonyl C=O stretching frequency for aldehydes groups in lignin. The bands in the range of ~1607 cm^{-1} are linked to lignin and C=C of aromatic compounds (A. Gupta et al., 2020). The absorption band at 1424 cm^{-1} is attributed to the C–H bending and C–O stretching frequencies of hemicelluloses. The band at 1234 cm^{-1} is attributed to the C–O and C=O stretching vibration in hemicelluloses and lignin (Gaur et al., 2016). The band at 1151 cm^{-1} is ascribed to the C–O–C asymmetrical stretching in cellulose structure (Wu et al., 2016). The band at ~1031 cm^{-1} shows the presence of C=O and C–C at 599 cm^{-1}, which are attributed to cellulose (Sasmal et al., 2012).

The curves of bagasse, kenaf bast fibers, and cotton stalks showed similarities and congruence. For instance, the absorption of O-H groups showed similar values, but differences were observed in other groups, such as C-O, which was more potent in kenaf bast fibers than in bagasse and cotton stalks. These variations are due to the chemical structure of the fibers (Coletti et al., 2021).

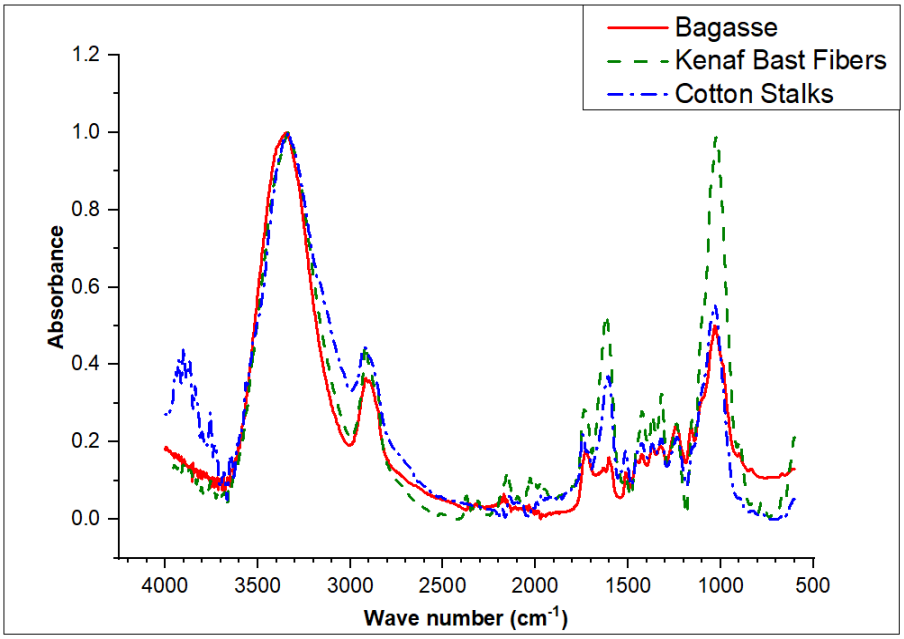

Figure 19: FTIR spectra of bagasse, kenaf bast fibers, and cotton stalk

3.3. Thermogravimetric analysis (TGA)

In thermogravimetric Analysis (TGA), there are two critical curves: the thermogravimetry (TG) curve and the derivative thermogravimetry (DTG) curve. The TG curve shows the change in a sample's mass when subjected to controlled heating or cooling, while the DTG curve represents the rate of change of mass concerning temperature and is derived from the TG curve. The thermogravimetric analysis curves for bagasse, kenaf bast fibers, and cotton stalks exhibited a similar pattern of mass loss concerning temperature. The TG and DTG curves analysis showed that kenaf bast fibers have better thermal stability than bagasse and cotton stalks. Furthermore, bagasse displayed more excellent thermal stability than cotton stalks, as depicted in Figs 20 and 21. Based on the TG and DTG curves, it was observed that the temperature range between 30°C and 100°C was associated with removing water from the fibers. No significant mass loss was observed between 100°C and 200°C, indicating that the fibers were thermally stable in this temperature range (Corrêa et al., 2010; Hamza et al., 2013). At a temperature of 200°C, bagasse lost 7.7% of its weight, kenaf bast fibers lost 6.3%, and cotton stalks lost 10%. These results strongly indicate that volatile components were released from the samples.

During the temperature range of 200°C to 400°C, the decomposition of the bio-macromolecule chains was observed. Specifically, the degradation of hemicelluloses occurred within the temperature range of 250°C to 315°C, while the degradation of cellulose took place between 315°C and 370°C (Candido & Gonçalves, 2019). Lignin degradation was observed to occur within the

temperature range of 280°C to 500°C. This temperature range signifies the thermal decomposition of lignin, a complex polymer found in plant cell walls. During pyrolysis, lignin degrades, releasing volatile compounds and forming char residue (Tanobe et al., 2010). The degradation temperature of the fibers can be determined by analyzing the maximum peaks on the derivative thermogravimetry (DTG) curves (Ouajai & Shanks, 2005). In this study, the degradation temperatures for bagasse, kenaf bast fibers, and cotton stalks were approximately 321.5°C, 354°C, and 289.5°C, respectively. These temperatures represent the points at which the fibers undergo significant thermal decomposition and weight loss. Identifying degradation temperatures provides insight into fiber thermal stability, crucial for biomass utilization and energy production applications. Factors such as chemical composition, crystallinity, and moisture content affect the thermal degradation of fibers.

The exceptional thermal stability of cellulose makes it the primary component of natural fibers. Kenaf bast fibers, which have a higher cellulose content, exhibit higher degradation temperatures due to cellulose's inherent heat resistance and structural integrity (Sharma & Varma, 2014). Indeed, the thermal degradation behavior of fibers can be influenced by factors beyond cellulose content, lignin, and hemicellulose content. As a result, fibers with a higher cellulose content are more resistant to thermal decomposition and can withstand higher temperatures before undergoing significant degradation. This characteristic makes cellulose-rich fibers desirable for various applications that involve exposure to elevated temperatures, such as thermal insulation, fire-resistant materials, and biocomposites.

Lignin is a complex polymer known to have higher thermal stability than cellulose. Therefore, fibers with a higher lignin content are generally more resistant to thermal degradation. On the other hand, hemicellulose, a branched polysaccharide, exhibits lower thermal stability than cellulose and lignin. The temperature range of 400 to 600°C, the thermal degradation of lignin and other organic components took place. During this phase, the remaining organic matter undergoes decomposition, forming residues with high molecular weight (Hamza et al., 2013). This thermal degradation process includes the carbonization of degraded compounds from cellulose, hemicellulose, and lignin, as well as the condensation of aromatic rings in the lignin structure. These reactions form charred residues and transform organic compounds into more stable carbonaceous structures. The presence of aromatic rings in lignin promotes condensation reactions, leading to the formation of carbon-rich structures. These thermal events occurring in the temperature range of 400 to 600°C are crucial for understanding the behavior of biomass materials during high-temperature processes such as pyrolysis and carbonization (Candido & Gonçalves, 2019).

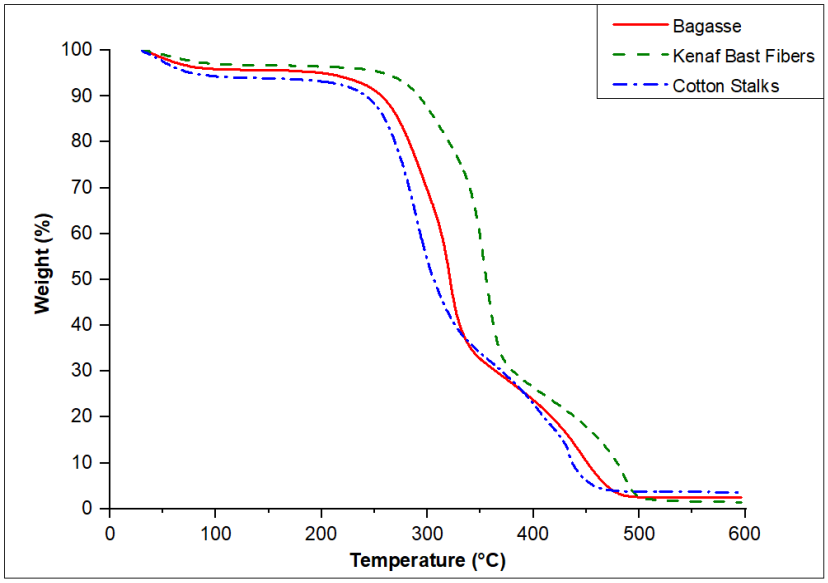

Figure 20: TG curves of the bagasse, kenaf bast fibers, and cotton stalks

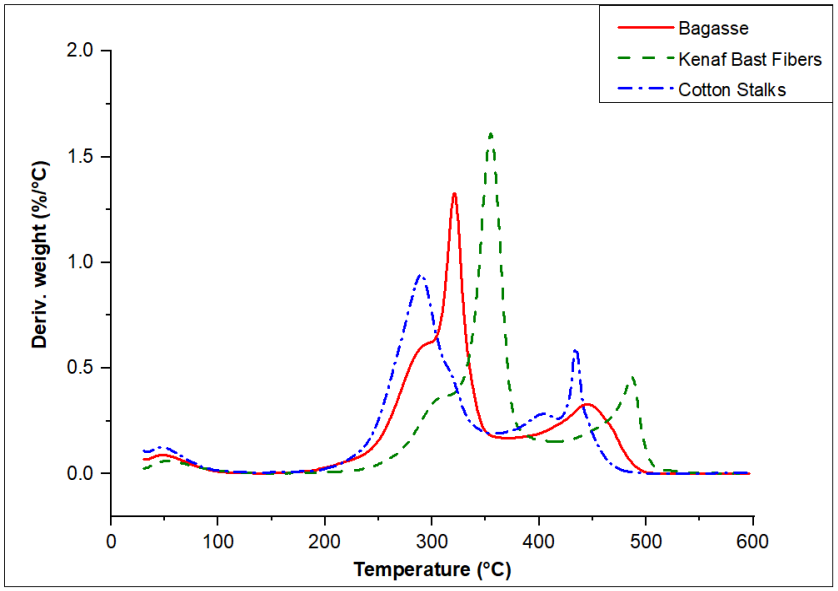

Figure 21: DTG curves of the bagasse, kenaf bast fibers, and cotton stalks

3.4. Differential scanning calorimetry (DSC) analysis

The DSC analysis of the three fibers is illustrated in Fig. 22. The curves show the glass transition (T_g) of the studied fibers, which is an endothermic event, and it represents the softening point of the material, as mentioned by S. Singh et al., 2013. The parameter significantly impacts the material's mechanical and thermal characteristics. The differences in chemical composition, molecular structure, and thermal behavior of materials contribute to their varying T_g. Valuable

insights into material behavior and performance can be gained by understanding the T_g in various applications. The glass transition temperature (T_g) was 81°C for bagasse, 66.3°C for cotton stalks, and 64.5°C for kenaf bast fibers. It is worth noting that the moisture content can affect the glass transition temperature (Zimeri and Kokini, 2002).

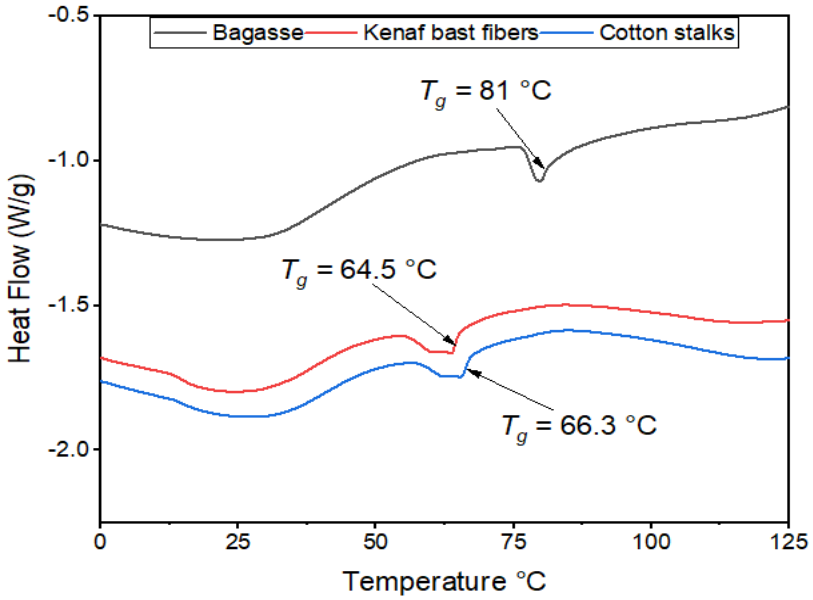

Figure 22: DSC curves for the bagasse, kenaf bast fibers, and cotton stalks

3.5. Higher heating value (HHV)

The bagasse fibers had the highest heating value compared to kenaf bast fibers and cotton stalks in bomb calorimetric analysis, as shown in Fig. 23. Bagasse fibers reported a value of 17.36 MJ/Kg, which was higher than the value recorded by Boumanchar et al., 2017 and lower than the value observed by Cordeiro et al., 2013. The value obtained for kenaf bast fibers was 16.61 MJ/Kg, approximately equal to that observed by Yub Harun et al., 2019. The cotton stalks showed a value of 17.08 MJ/Kg, slightly lower than the bagasse value. This value was similar to that reported in the previous work (Munir et al., 2010). The difference in moisture content of fibers affects biomass combustion by causing water evaporation, which reduces heating value. Therefore, as the moisture content of biomass increases, its heating value decreases (Demirbas, 2007). Techniques like pyrolysis, gasification, and combustion can convert biomass into energy sources with potential uses. Assessing biomass's higher heating value (HHV) before and after conversion is crucial.

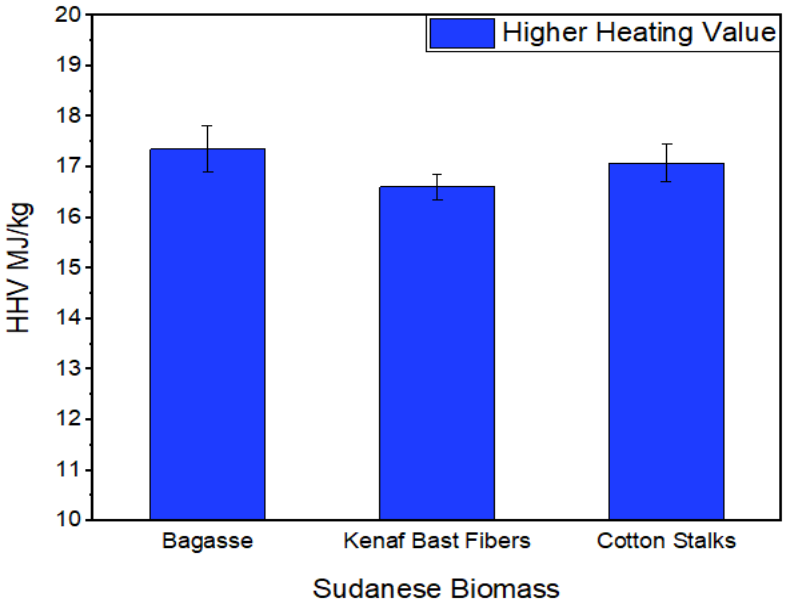

Figure 23: Higher heating values of bagasse, kenaf bast fibers, and cotton stalks

CHAPTER 4

CONCLUSION

4. Conclusion

The potential of bagasse, kenaf bast fibers, and cotton stalk for producing biocomposites and bioenergy was analyzed by examining their chemical properties and thermal behavior. The results aligned with the studies available in the literature, indicating their suitability for these applications.

The moisture content of bagasse, kenaf bast fibers, and cotton was determined to be 7.8%, 8.5%, and 8.4%, respectively. The ash content of bagasse fibers was 8%, while kenaf bast fibers had 2.5% and cotton stalks had 5.2%. Bagasse had the highest extractive content (43%) using 1% sodium hydroxide, followed by cotton stalks (31.2%) and kenaf bast fibers (16.7%). The percentage of ethanol-soluble extractives in bagasse, kenaf bast fibers, and cotton stalks was 9.9%, 10.1%, and 9.5%, respectively. Among the fibers, kenaf bast had the highest cellulose content at 58.5%, followed by bagasse at 50.6% and cotton stalks at 40.3%. In contrast, lignin content was highest in bagasse (21.6%), followed by cotton stalks (21.3%), whereas kenaf bast fibers had the lowest percentage at 10%. The abundance of lignin presents potential opportunities for lignin-derived products. Analysis of phenol content revealed that cotton stalks had the highest amount (6%), followed by bagasse (1.7%) and kenaf bast fibers (1.3%). The results obtained from Fourier transform infrared spectroscopy (FTIR) were consistent with previous studies.

The thermogravimetric analysis showed that the fibers remained stable up to 200°C. Degradation occurred between 200°C and 400°C. Kenaf bast fibers' high cellulose content resulted in excellent stability in this range. The degradation temperatures were determined as 321°C for bagasse, 354°C for kenaf bast fibers, and 289°C for cotton stalks. These findings have significant implications for the biocomposite materials and understanding of these fibers' thermal behavior and stability in bioenergy production. Differential scanning calorimetry (DSC) analysis determined the glass transition temperatures of the material, which indicates the temperature at which the material changes from a rigid, glassy state to a more flexible, rubbery state. Fibers' glass transition temperature (T_g) was measured as 81°C for bagasse, 66.3°C for cotton stalks, and 64.5°C for kenaf bast fibers. Furthermore, the higher heating values were determined as 17.36 MJ/kg for bagasse, 16.61 MJ/kg for kenaf bast fibers, and 17.08 MJ/kg for cotton stalks, aligning with previous studies. These results provide valuable insights into the potential sustainable applications of these fibers, enhancing our understanding of their properties and performance.

The next part investigates the possibility of producing 100% eco-friendly boards for interior fitments (including furniture) for use in dry conditions. It also aims to evaluate and compare the mechanical, physical, and thermal properties of individual and blended fiber particleboards made from bagasse, cotton stalk, and kenaf bast fibers using two natural matrices: tannins and casein. In addition, the next part investigates the possibility of producing foam from different types of tannins.

Part III. Biocomposites production and characterization of their mechanical, physical, and thermal properties

CHAPTER 1

INTRODUCTION

1. Introduction

Biomass residues from agricultural waste are increasingly considered valuable for manufacturing composite materials. Numerous agricultural by-products, such as crop residues, wood waste, straw, and bagasse, offer highly efficient, environmentally sustainable, and renewable alternatives that are also cost-effective (H. A. M. Saeed et al., 2017). The scientific community is researching ways to produce wood-based materials using renewable resources to address environmental and economic concerns. Thanks to their exceptional performance, particleboards are popularly used as a cost-effective alternative to solid wood or plywood (Gumowska et al., 2021; Holt et al., 2014).

Forest and agricultural products are transformed into particleboard materials using appropriate technologies (Archanowicz et al., 2013). Composite materials are efficiently produced through processing steps, including forming, drying, matting, pre-pressing, and hot pressing. Adhesives are commonly employed during hot pressing to ensure the fibers are effectively bonded together (Halvarsson et al., 2009). Particleboard manufacturing for green chemistry is now yielding reduced or zero formaldehyde emissions. This renewed interest in the industry should be taken seriously and acted upon with immediate effect to ensure a safer and healthier environment for all (Nunes de Oliveira Júnior et al., 2023; Owodunni et al., 2020; Wronka & Kowaluk, 2022). Substituting synthetic adhesives with casein and tannin is a crucial bio-based solution for particleboard bonding (Ndiwe et al., 2019). The attractiveness of particleboard for residential construction, furniture manufacturing, and interior design (wall and ceiling cladding) has continued to increase (Nourbakhsh, 2010). De Almeida et al., 2017 mention that materials' physical and mechanical properties are fundamental in determining their applications and uses.

The principal objective of this part is to produce 100% biocomposites for interior fitments (including furniture) for use in dry conditions. The study aimed to evaluate and compare particleboards made from three fiber types (bagasse, cotton stalk, and kenaf bast) using natural matrices of tannins and casein. The particleboards were manufactured using individual fibers, and then the fibers blended. In addition, this part aimed to produce foam from different types of tannins such as maritime pine and mimosa tannins. The study found that particleboards made from bagasse and cotton stalks had superior mechanical and physical properties than those made from kenaf bast fibers. In addition, the casein adhesive leads to better mechanical properties and lower physical properties of the particleboards. The results conclusively determined that utilizing individual fibers

results in superior mechanical and physical properties compared to blended fibers. This is an indisputable fact that should be acknowledged and acted upon accordingly. All particleboards made from casein and tannin, whether from individual or blended fibers, exhibited favorable thermal properties, indicating their appropriateness for insulation.

CHAPTER 2

MATERIALS AND METHODS

2. Materials and methods

2.1. Materials

The Sugarcane bagasse, cotton stalks, and kenaf bast fibers were used without any further treatments. Mimosa condensed tannin ACACIA was supplied by GREEN'ING Company. Maritime pine samples were collected from the Lands forest in the Mont de Marsan area. Commercial maritime pine tannins are provided by the Biolandes and DRT Phénopin company. Casein was supplied by ACROS ORGANICS Company Hexamethylenetetramine (99%) and sodium bicarbonate were purchased from Fisher Scientific (France). All the products were used as received.

2.2. Methods

2.2.1. Fibers preparation

Sugarcane bagasse, cotton stalks, and kenaf bast fibers were cleaned and cut into small pieces (10 to 20 mm) using a laboratory hammer mill, then they were placed into the oven at 105°C for 24 hours to reduce the moisture content to less than 5%.

2.2.2. Preparation of the bio-based binding materials

An aqueous solution of 35 % concentration was prepared from the spray dried powder of commercial mimosa, ACACIA tannins. The initial pH was raised to 9. 6.5% of hexamethylenetetramine (hexamine) was added as a hardener on the tannin solids extract. An aqueous solution of 30% casein was used, while sodium bicarbonate (25% w\w of casein) was added as a hardener. 15% of each adhesive (of the weight of the panel) was used.

2.2.3. Manufacturing of particleboards

Particleboards were manufactured at the Materials Science and Engineering department laboratory, SGM, Institute of Technology of the University, IUT, Pau University and the Adour Region, UPPA. Single-layer laboratory particleboards of 200×200×20 mm^3 dimensions bonded with two types of adhesives, tannin, and casein were produced. The particleboards were manufactured using a pressing cycle of maximum pressure of 2.5 MPa, different pressing time durations of 480s, 240s, 120s, and 60s, and a pressing temperature of 180°C were used. The target density was 0.6 $g.cm^{-3}$. To bond the particleboards, a 15% proportion of each adhesive, based on the weight of the panel, was utilized.

2.2.3.1. Determination of mechanical properties

The mechanical properties of the produced panels, modulus of rupture (MOR), modulus of elasticity (MOE), and internal bond (IB) were tested using a (3R) universal testing machine (SYNTAX). The MOR and MOE were determined according to European standards (EN 310) and IB according to (EN 319).

2.2.3.2. Determination of physical properties

The water absorption and (WA) thickness swelling (TS) properties of the particleboards were determined using test specimens with dimensions of 50mm x 50mm. The measurements were conducted according to the European standard (EN 317). These tests provide information on the dimensional stability and water resistance of the particleboards, which are important considerations for their performance in various applications.

2.2.3.3. Determination of thermal properties

The thermal analysis of the particleboards was conducted using the hot disk thermal analyzer TPS 1500 S system. Test specimens with dimensions of 50mm x 50mm were prepared for analysis. The thermal conductivity of the particleboards was measured using a probe with a radius of 6.403 mm (Ref. 5501, Kapton insulated sensor). The measurements were performed in triplicate for each panel to ensure accuracy and reliability. The obtained thermal conductivity values were then compared with the European standard (EN 12664) to assess the thermal performance of the particleboards.

2.2.4. Foam production

2.2.4.1. Extraction of maritime pine tannins from bark

The bark maritime pine (*Pinus pinaster*) samples were ground into a powder with a RETSCH grinder, resulting in a particle size of approximately 60 mesh. Subsequently, the samples were dried at 70°C overnight. A 50g sample was then mixed with 500 mL of a 70/30% water/acetone mixture using a magnetic stirrer operating at 500 rpm for 3 hours. Afterward, the mixture was filtered, and a rotavator with a water bath at 60°C and a vacuum set to 556 mbar was employed to recover the acetone. The tannin powder was obtained through a freeze-dryer.

2.2.4.2. Foam formulation

The tannin-based foam was prepared in a plastic beaker by thoroughly mixing 30 g of tannins with a liquid mixture containing furfuryl alcohol (AF), water, glyoxal, polyethylene glycol 400 (PEG400), PEG35-CO, 1-methoxy-2propanol (Dowanol PM), and pentane. Following this, the catalyst (pTSA) was added, and the preparation was mixed for 20 s. The induction time was only a few seconds, and then the liquid expanded, and the foam slowly expanded. Once the foam reached its final volume, the foam with the skin was left to dry overnight to complete

polymerization. This method is extensively described in previous work (Lacoste, Pizzi, Laborie, et al., 2014). The method was tested, and the quantities of components were adjusted to achieve the desired foam formulation. Tab. 7 illustrates the foam components and formulation.

Table 7: Tannin-based foam formulation

Tannins	AF	Water	Glyoxal	PEG400	Pentane	Dowanol PM	PEG35-CO	pTSA
30	20	4	5	6	5	1.8	1-2	11

Where AF is Furfuryl alcohol, PEG-400 is polyethylene glycol 400, Dowanol is 1-methoxy-2propanol ether, PEG35-CO is Polyethylene glycol, and pTSA is para-toluene sulfonic acid.

2.2.4.3. Foam characterization

The universal machine tested a specimen measuring 50mm x 50mm of Acacia tannin foam for its mechanical properties. The thermal conductivity of the specimen was measured by a hot disk using a probe with a radius of 6.403 mm (Ref. 5501, Kapton insulated sensor). In addition, the density of the produced foam was measured.

CHAPTER 3

RESULTS AND DISCUSSION

3. Results and discussion

3.1. Individual fibers particleboards

3.1.1. Casein-based adhesives

3.1.1.1. Modulus of rupture (MOR)

Figure 24 illustrates the results of the modulus of rupture (MOR) determined for the casein particleboards. The MOR values show the particleboards' flexural strength and ability to withstand applied loads without breaking. Among the three fibers tested, the bagasse particleboard had the highest MOR value of 15.6 $N.mm^{-2}$, followed by the cotton stalks (14.4 $N.mm^{-2}$). Both values exceeded the EN standard's minimum requirements for particleboard use in interior fitments and furniture under dry conditions (11 $N.mm^{-2}$). The MOR value of bagasse particleboard aligns with values reported in previous literature (Pothula, 2016). Nyang et al., 2019 also reported close values of MOR when using Euphorbia sap as a natural binder. However, the values obtained were in line with those obtained by Flávia Maria Silva Brito (Brito et al., 2021) for particleboard made from treated bagasse fibers and UF adhesive, which is known for its emission problems.

The MOR value obtained for particleboard made from cotton stalks was slightly lower than the value reported in the previous study (Kadja et al., 2011) when they used a bone-based adhesive at a comparable level. However, it is essential to note that the MOR value of cotton stalks particleboard made with casein adhesive was within the range of values achieved by cotton stalks particleboard with emulsifiable polymeric isocyanate adhesive when used at 12%. The result indicates that the particleboard with casein adhesive still shows satisfactory performance in terms of its mechanical strength. When comparing casein adhesive and emulsifiable polymeric isocyanate adhesive, casein performs better than emulsifiable polymeric adhesive. However, it is also important to remember that Emulsifiable polymeric isocyanate adhesive has disadvantages, such as toxicity and cost. In contrast, casein adhesive offers advantages such as non-toxicity, cost-effectiveness, and easy availability. Based on the results, casein adhesive is preferable due to its positive environmental image compared to conventional binders, which can cause ecological problems. Although more information is needed on the use of casein adhesive in particleboard production, the results of this study show its promising performance. In particular, using casein adhesive with bagasse and cotton stalks produced particleboards with favorable properties suitable for various applications such as furniture, interior fitting, and insulation.

Unexpectedly, the kenaf bast fibers particleboard exhibited the lowest MOR value of 2.8 $N.mm^{-2}$. This value is below the minimum requirements specified in the EN standards for interior fitments. A possible explanation for this is the low weight of kenaf bast fibers compared to bagasse and cotton stalk fibers. The lower density of kenaf bast fibers may result in a larger volume of fibers being used to manufacture the panels, possibly leading to inadequate coverage by the adhesives. Insufficient fiber-adhesive interaction can lead to a weaker bond and lower mechanical strength of the particleboard. In addition, the lower pressure during the manufacturing process could also contribute to the lower MOR value observed in the kenaf bast fibers particleboard. Higher pressure during the pressing phase can improve the consolidation and bonding of the fibers, resulting in better mechanical properties of the particleboard.

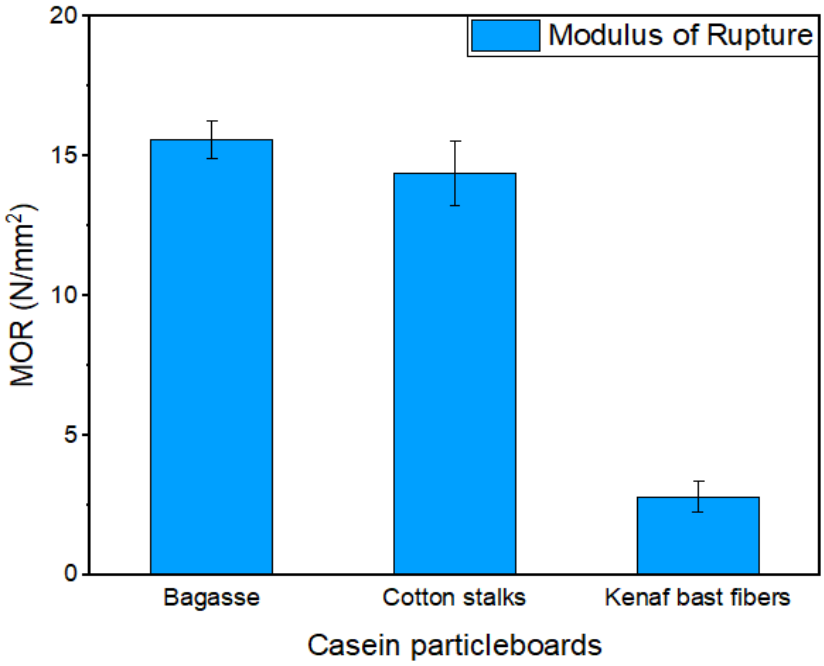

Figure 24: Modulus of rupture of bagasse, cotton stalks, and kenaf bast fibers particleboards made of casein

3.1.1.2. Modulus of elasticity (MOE)

The casein particleboards made from bagasse and cotton stalks had a modulus of elasticity (MOE) of 2316 $N.mm^{-2}$ and 2230 $N.mm^{-2}$, respectively (Fig. 25). These values exceeded the value recommended by the EN standard (1600 $N.mm^{-2}$) and indicated the stiffness of the particleboards.

The MOE of bagasse was similar to the value given by Pothula (Pothula, 2016), who used the modified blue-green algae protein as an adhesive material, which could be costly. Interestingly,

these values were higher than those obtained when bagasse and cotton stalks particleboards were made with the harmful UF (Brito et al., 2021) and Soybean adhesive (X. Chen et al., 2015).

The particleboards made from kenaf bast fibers did not reach the standard value for the modulus of elasticity, measured at 433 $N.mm^{-2}$. However, it is noteworthy that this value was still higher than reported in the literature (Paridah et al., 2015). As mentioned above, the inadequate performance of the kenaf bast fibers particleboard can be attributed to the low weight of the fibers, which resulted in a large volume of fiber compared to the amount of adhesive used. As a result, the boards had less intimate contact and loose bonding. The result aligns with Escobar (W. G. Escobar, 2008), who indicated that voids per unit area in kenaf bast fiber particleboards could lead to failure under load, resulting in lower strength properties. Kenaf particleboard has been made from 100% kenaf bast fibers, suggesting that using the entire kenaf stem without separating the fibers could result in panels with improved strength properties (Halip et al., 2019). This approach eliminates the cost of manually separating fibers and allows for utilizing the entire kenaf stalk in producing particleboard.

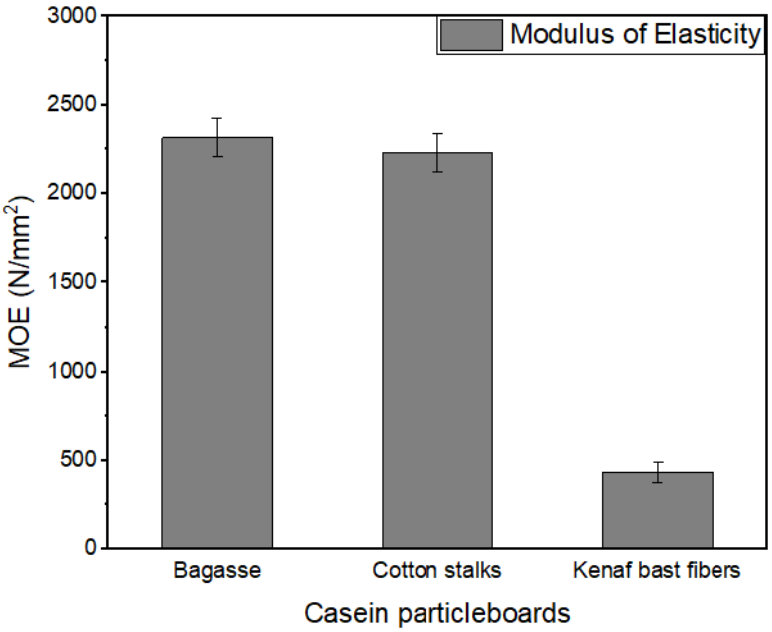

Figure 25: Modulus of elasticity of bagasse, cotton stalks, and kenaf bast fibers particleboards made of casein

3.1.1.3. Internal bond (IB)

The results of the internal bond are shown in Fig. 26. The casein particleboards made from bagasse and cotton stalks gave internal bond values (IB) of 0.39 $N.mm^{-2}$ and 0.36 $N.mm^{-2}$, respectively.

These values exceeded the EN standard requirements of 0.35 N.mm^{-2} for furniture and interior fitment, indicating a strong bond between the particles and good overall strength of the particleboards. The findings indicate that the casein adhesive has successfully linked the interparticle bonding, leading to elevated IB values and desirable particleboard performance. The lowest IB value was measured for the kenaf bast fibers particleboard (0.07 N.mm^{-2}). The low IB value could be because the volume of the kenaf bast fibers was large, and therefore they were only loosely compacted.

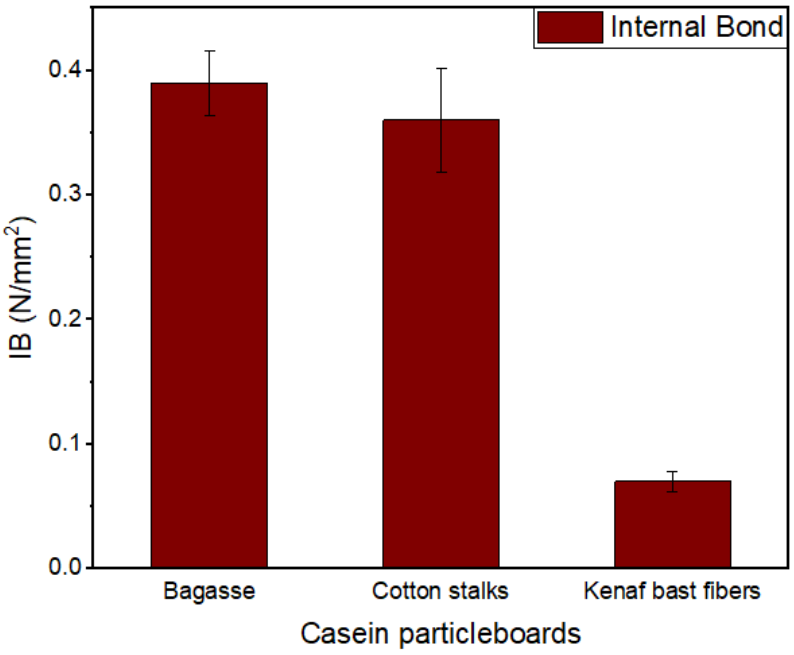

Figure 26: Internal bond of bagasse, cotton stalks, and kenaf bast fibers particleboards made of casein.

3.1.1.4. Water adsorption and thickness swelling

Table 8 shows the casein particleboards' water adsorption and thickness swelling values. The water absorption values were measured at 2 and 24 hours, indicating a high absorption level. The WA percentage values for bagasse particleboard were 75% and 118% after 2 and 24 hours, respectively. The values were higher for cotton stalk particleboard at 96.3% and 137%, respectively, followed by kenaf bast particleboards with 192% and 214%, respectively. Due to its high solubility in water, casein can be readily washed out as an adhesive, making it an excellent choice for the eco-friendly furniture industry (M. Guo & Wang, 2016a). The type of fiber, the adhesive matrix, and the manufacturing process can significantly influence the water absorption properties of particleboard (Moubarik, Mansouri, et al., 2013; Moubarik, Pizzi, et al., 2013).

The casein adhesive particleboards exhibited a thickness swelling (TS) that exceeded the EN 317 standard requirements (8% and 14% after 2 and 24 hours, respectively). The bagasse casein particleboard showed 8.9% and 14.4% after 2 and 24 hours, respectively. These values were slightly higher compared to the standard requirements. The cotton stalk particleboard TS also showed a percentage of 9.3% and 19.3% after 2 and 24 hours, respectively, exceeding the standard requirements. However, the values of the cotton stalks particleboard were lower than in the previous work (Guler & Ozen, 2004). The kenaf bast fiber particleboards had significantly higher TS values than reported in the literature (Kalaycioglu & Nemli, 2006), with values of 50.6% and 70.9% for 2 hours and 24 hours, respectively, indicating poor dimensional stability and high susceptibility to water absorption. High TS values in casein particleboards lead to swelling and moisture absorption, negatively impacting their dimensional stability and suitability for outdoor use.

Table 8: The water absorption and thickness swelling for the casein particleboards

Casein adhesive Particleboards	WA (%) 2h Means ± SD	WA (%) 24h Means ± SD	TS (%) 2h Means ± SD	TS (%) 24h Means ± SD
Bagasse	75 ± 7.6	118 ± 14	8.9 ± 2.5	14.4 ± 4.36
Cotton stalks	96.3 ± 8.7	137 ± 13.5	9.3 ± 2.7	19.3 ± 3.92
Kenaf bast fibers	192 ± 13	214 ± 19.38	50.6 ± 3.66	70.9 ± 7.3

3.1.1.5. Thermal properties

Thermal conductivity is crucial in determining whether a material is appropriate for thermal insulation and construction. Several factors influence heat transfer through a solid polymer, including the density, thickness, and diameter of the cells or voids in the material (Issaoui et al., 2021). The thermal conductivity of particleboard is highly influenced by its density, thickness, cell size, and void distribution. These factors must be carefully considered to ensure optimum thermal performance (Lacoste et al., 2015).

The thermal conductivity results of the particleboards made of bagasse, kenaf bast fibers, and cotton stalks glued with casein show good thermal conductivity, below EN's standard value (0.12 W/m. K). The thermal conductivity of the bagasse particleboard exhibited a value of 0.082 W/m. K. Cotton stalks particleboard had a value of 0.056 W/m. K, while kenaf bast fibers recorded a value of 0.089 W/m. K, as shown in Fig. 27. The lower thermal conductivity values can limit heat transfer effectively, making them suitable for enhancing thermal insulation in various applications. Manufacturing infrastructure materials with natural fibers offers numerous advantages. Most importantly, it reduces the carbon footprint by utilizing renewable sources. Moreover, these natural

fibers possess exceptional mechanical properties, rendering them a viable substitute for traditional materials. Furthermore, using natural fibers is frequently cost-effective, leading to affordable materials (Chakraborty et al., 2013; Olivito et al., 2014). Optimizing particleboards' thermal conductivities is crucial for enhancing building energy efficiency and comfort. This can be achieved by adjusting density, cell structure, and thickness during manufacturing.

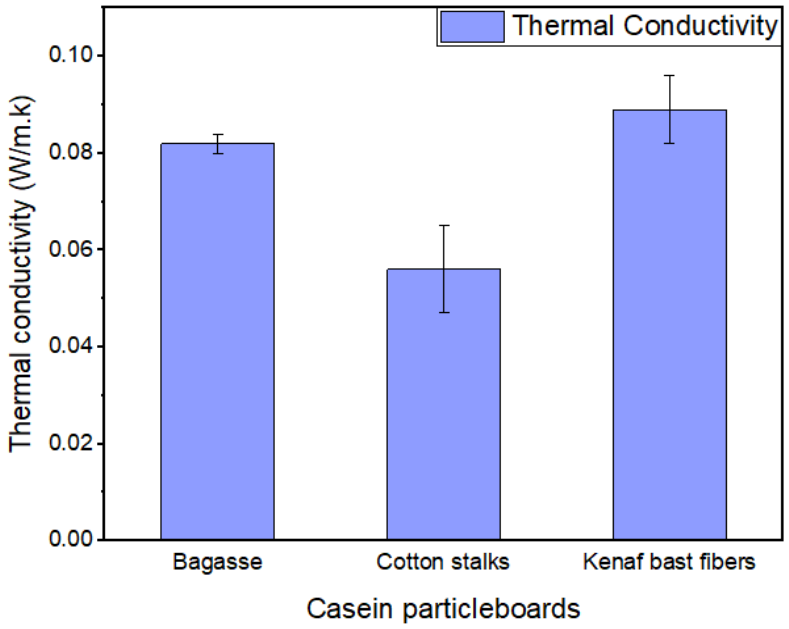

Figure 27: Thermal conductivity of bagasse, cotton stalks, and kenaf bast fibers particleboards made of casein

3.1.2. Tannin-based particleboards

3.1.2.1. Modulus of rupture (MOR)

The MOR values for particleboards made from tannins are depicted in Figure 28. The results showed that the values were lower compared to casein. This could be because the three studied fibers had an acidic pH, which lowered the pH of the overall system (glued particles). As a result, the boards had poorer mechanical properties. The tannin was cured at a strongly alkaline pH and formed a good bond with the fiber particles. This phenomenon was previously reported by Z. Osman et al., 2009. Although the pH of the tannin adhesives was raised, the tannins condensed automatically at room temperature (Z. Osman, 2013) and (became a thick solution) and so did not spread well on the fibers, which were not evenly covered with the adhesives, making clots and spots on the boards.

In contrast, casein's isoelectric pH balancing positive and negative charges makes it highly soluble in alkaline pH, allowing for complete coverage when uniformly sprayed onto fibers. In addition, sodium bicarbonate, used as a hardener and added in an amount of 25%, balanced the acidic pH of the fibers. Casein, a heterogeneous polymer, can efficiently establish a strong network through heat treatment using a hot press, which is not achievable by tannins (Vachon et al., 2000). Again, bagasse particleboard had the highest MOR value (8.8 $N.mm^{-2}$) among the fibers studied, followed by cotton stalks (8.4 $N.mm^{-2}$), which are slightly lower than bagasse, while kenaf bast fibers scored the lowest value (1.6 $N.mm^{-2}$). This could be because both bagasse and cotton stalks have a small volume compared to kenaf bast fibers, and both contain shorter fibers that fill the voids and give more compact, stronger boards. The bagasse and cotton particleboard had a lower MOR value than those reported in previous studies (Abd El-Sayed et al., 2019; T. T. Nguyen et al., 2020). Although the values obtained did not meet the EN standard value (11 $N.mm^{-2}$), they could be used as a healthy panel for thermal insulation.

In the previously mentioned studies, the researchers used smaller particle sizes of 4 and 8 mm, respectively, which yielded better qualities. In addition, the bagasse fibers were pre-treated with polymethyl methacrylate (PMMA), and the researcher used paraformaldehyde as a hardener which can cause the emission of UF. This study used hexamine as a hardener to avoid UF emissions and produce 100% green panels without costly pre-treatment.

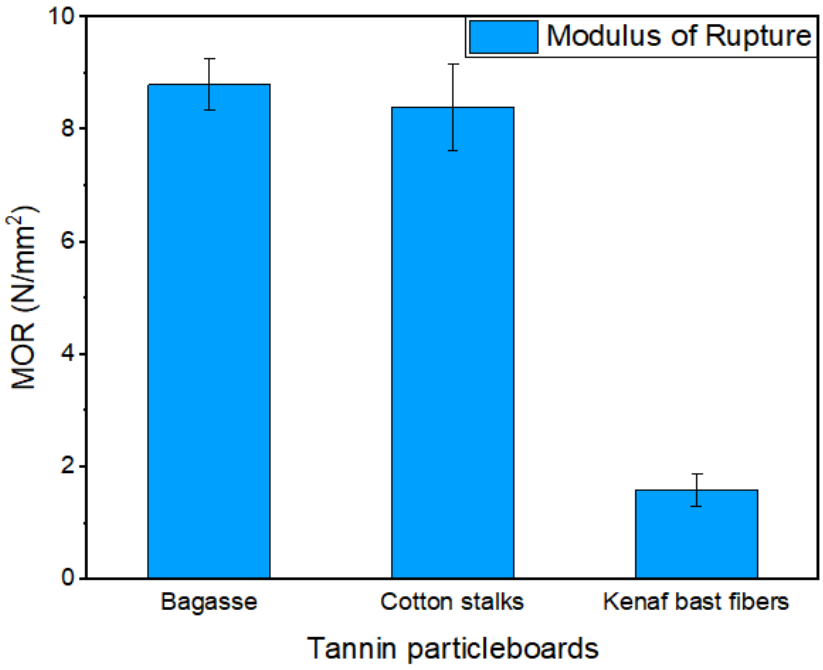

Figure 28: Modulus of rupture of bagasse, cotton stalks, and kenaf bast fibers particleboards made of tannin

3.1.2.2. Modulus of elasticity (MOE)

The modulus of elasticity of the tannin particleboards was lower than the standard value. It was 1263 N.mm^{-2} for bagasse, 1401 N.mm^{-2} for cotton stalks, and 577 N.mm^{-2} for bast kenaf fibers particleboards (Fig. 29). It is worth noting that the limited availability of studies on cotton stalks and kenaf bast fibers particleboards using tannin and casein adhesives makes it challenging to compare the results directly. However, most studies used a UF adhesive and reported better mechanical properties than the results obtained in this study, as reported by Nazerian et al. (Nazerian et al., 2018) and Grigoriou et al. (Grigoriou et al., 2000).

According to Ndazi et al. (Ndazi et al., 2006), kenaf fibers particleboard represents only 0.04% of annual world production. This suggests that while kenaf has limited use as a raw material for particleboard production, there is potential for further research and development to exploit its advantages as a sustainable and renewable resource.

Based on the results of the modulus of rupture (MOR) and modulus of elasticity (MOE), it can be concluded that the casein adhesive particleboards have excellent reactivity with the fibers studied, especially bagasse and cotton stalks. The casein adhesive showed improved adhesion between the fibers and the casein particles, resulting in higher MOR and MOE values than the tannin adhesive. This shows that the casein adhesive bonds better with the fibers studied, resulting in enhanced mechanical performance of the particleboards (Mahieu & Leblanc, 2017).

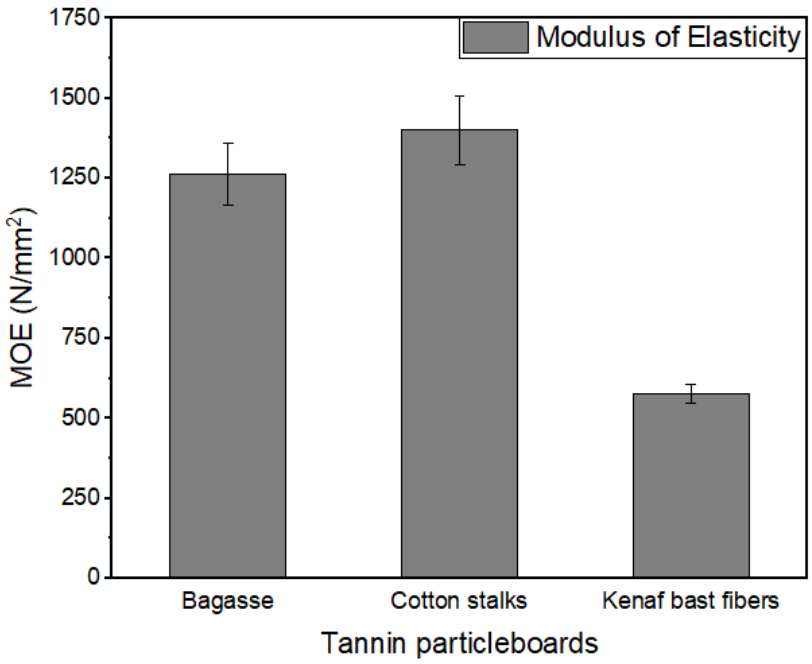

Figure 29: Modulus of elasticity of bagasse, cotton stalks, and kenaf bast fibers particleboards made of tannin

3.1.2.3. Internal bond (IB)

The tannin particleboards made from bagasse, cotton stalks, and kenaf bast fibers had lower internal bonding (IB) values than the standard requirements. The value IB was 0.22 $N.mm^{-2}$ for bagasse particleboard, 0.21 $N.mm^{-2}$ for cotton stalk particleboard, and 0.04 $N.mm^{-2}$ for kenaf bast fiber particleboard (Fig. 30). These values indicate that the particleboards did not have the desired internal bond strength. The tannin adhesive might have led to less effective particle bonding, resulting in lower IB values. Sala et al., 2021, reported that internal bonding depends on the density and homogeneity of the fibers and the mixing process. As mentioned before, due to auto condensation at room temperature, the thick tannin adhesive posed a challenge in evenly distributing it on the fibers.

Increasing the lignin content of fibers can improve particleboard's mechanical properties. Lignin is an essential part of plant cell walls, providing structural support. When exposed to heat and moisture, it can undergo chemical reactions that create new bonds between lignin and other components, enhancing its binding capacity and improving the mechanical properties of particleboard. Heat also causes lignin to act as a binder during the pressing process, contributing to overall mechanical property enhancement (Mahieu et al., 2021). It should also be noted that kenaf bast fibers have a low lignin content compared to bagasse and cotton stalks (Rowell et al., 2000), which may explain the low mechanical properties of kenaf bast fiber particleboards. On the other hand, the high compaction of fibers in bagasse leads to faster heat transfer and stronger adhesive curing in the core layer, resulting in higher mechanical properties (Tabarsa et al., 2011). The compact structure of bagasse fibers enables efficient heat transfer, leading to superior performance compared to other fibers.

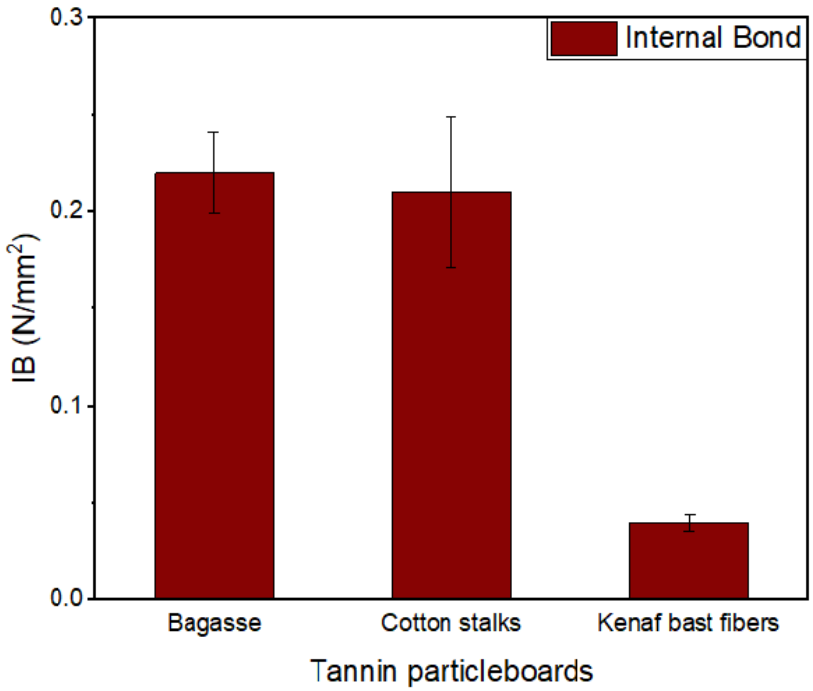

Figure 30: Internal bond of bagasse, cotton stalks, and kenaf bast fibers particleboards made of tannin

3.1.2.4. Water adsorption (WA) and thickness swelling (TS)

Table 9 shows the results from WA and TS for the tannin particleboards. Except for the bagasse particleboard, after 2 hours, the water absorption was lower than the casein particleboard. The WA percentage of bagasse particleboard was 86.4% after 2 hours and 110.3% after 24 hours. These values were higher than those reported in the literature (Abd El-Sayed et al., 2019). On the other hand, the cotton stalks particleboards exhibited WA percentages of 79.2% after 2 hours, which was slightly lower than the bagasse particleboards, and 115.3% after 24 hours. The kenaf bast fiber particleboards had the highest water absorption, with percentages of 170% after 2 hours and 193.1% after 24 hours.

The bagasse particleboard made with tannin glue showed a thickness swelling (TS) of 5 % and 7.4 % for 2 hours and 24 hours, respectively. The cotton stalks tannin particleboard recorded 3% and 10.3% TS values for 2 and 24 hours, respectively. These values were lower than the EN standard values. On the other hand, the Kenaf bast fiber particleboard with tannin glue did not meet the standard requirements, with values of 32.1% and 48.6% for 2 and 24 hours, respectively. As mentioned by Chiang et al., 2014, the rate of water absorption in particleboards is affected by several factors, including fiber and matrix type, environmental conditions (temperature and humidity), water distribution within the boards, water-matrix interaction, board porosity, and fiber

volume fraction. These factors can influence the particleboards' general water absorption properties and swelling behavior (Moubarik, Mansouri, et al., 2013; Moubarik, Pizzi, et al., 2013).

The internal bond strength (IB) directly impacts its physical properties, significantly improving its specific physical. This relationship is highlighted in the earlier study by Paridah et al. (Paridah et al., 2014). The stronger bond between particles can lead to lower porosity and higher density, affecting water absorption, thickness swelling, and dimensional stability. It is vital to balance achieving satisfactory mechanical properties and maintaining acceptable physical properties when manufacturing particleboard. It is worth noting that bagasse and cotton stalks particleboards had good physical properties due to their fiber structure and higher IB compared to kenaf bast fibers.

The type of adhesive used in particleboard production affects the boards' physical properties. The tannin glue particleboards showed good physical properties compared to casein particleboards. This difference can be attributed to casein's relatively lower water resistance than tannin. However, the water resistance of casein adhesive can be improved by increasing the proportion of hardeners in the range of 15 % to 25 % (Pothula, 2016). Therefore, optimizing the adhesive formulation is crucial to achieving the desired balance between improved mechanical and physical properties in particleboard production. The adhesive plays an essential role in binding the fibers and determines the overall quality of the particleboard (Ayrilmis et al., 2012).

In the industrial production of particleboard, small amounts of wax and hydrophobic substances (such as paraffin or wax emulsions) are commonly added to improve board properties such as water resistance, dimensional stability, and reduced thickness swelling due to reduced moisture absorption. This information is supported by the results found in the literature (Halvarsson et al., 2009; Moubarik et al., 2010). Additionally, according to Nourbakhsh (Nourbakhsh, 2010), heat treatment can improve dimensional stability but may affect particleboard's mechanical properties.

Table 9: The water absorption and thickness swelling for the tannin particleboards

Tannin adhesive Particleboards	WA (%) 2h Means ± SD	WA (%) 24h Means ± SD	TS (%) 2h Means ± SD	TS (%) 24h Means ± SD
Bagasse	86.4 ± 5.3	110.3 ± 13	5 ± 1.1	7.4 ± 3.5
Cotton stalks	79.2 ± 5.9	115.3 ± 14.5	3 ± 1.12	10.3 ± 3.3
Kenaf bast fibers	170 ± 10.1	193.1 ± 17	32.1 ± 6.6	48.6 ± 5.9

3.1.2.5. Thermal conductivity

The results for the thermal conductivity of the tannin particleboards made from bagasse, kenaf bast fibers, and cotton stalks were below the standard value of EN (0.12 W/m. K), which is desirable

for insulation applications. The bagasse particleboards recorded a thermal conductivity value of 0.057 W/m. K. On the other hand, cotton stalks particleboard had a value of 0.05 W/m. K. Among the particleboards, the highest thermal conductivity was found in the Kenaf bast fiber particleboard with a value of 0.083 W/m.K (Fig. 31). The particleboards studied have the potential to be a healthier and viable alternative to currently used insulation materials, according to these results (D. T. Liu et al., 2012). Insulation materials with lower thermal conductivity values can reduce heat loss or gain through buildings, maintain stable indoor temperatures, and save energy on excessive heating or cooling.

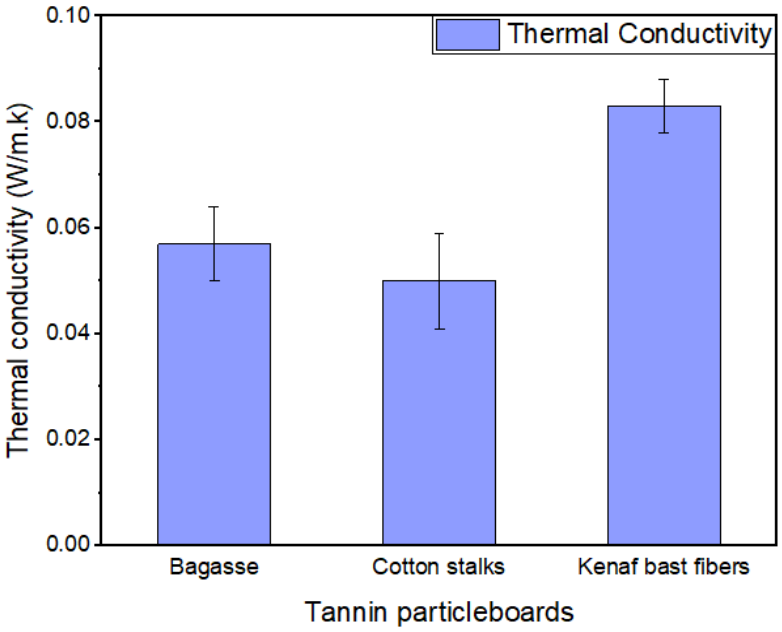

Figure 31: Thermal conductivity of bagasse, cotton stalks, and kenaf bast fibers particleboards made of tannin

3.2. Fibers blended particleboards

This part of the study aimed to evaluate the effect of blending the three fibers on the mechanical and physical properties of the produced panels. The three fibers were blended in the ratio 50:50 (w/w) for the binary fiber particleboards and 40:30:30 (w/w/w) for the triple particleboard for bagasse, cotton stalks, and kenaf bast fibers, respectively, as follows:

- Bagasse/Cotton Stalks (B/CS)
- Bagasse/Kenaf Bast Fibers (B/KBF)
- Cotton Stalk/Kenaf Bast Fibers (CS/KBF)
- Bagasse/Cotton Stalks/Kenaf Bast Fibers (B/CS/KBF)

The major goal is to meet the needs of these materials and to secure the sustainability of the particleboard industry using the three fibers. The results analyzed the alterations in mechanical, physical, and thermal properties caused by fiber blending in comparison to the particleboards made from single fibers.

3.2.1. Casein-based adhesive

3.2.1.1. Modulus of rupture (MOR)

The values of modulus of rupture (MOR) for the blended particleboards are illustrated in Fig. 32. The B/CS casein particleboard exhibited a value of 14.28 N.mm^{-2}, while the B/KBF particleboard recorded 9.2 N.mm^{-2}. The CS/KBF particleboard showed a slightly lower MOR of 8.8 N.mm^{-2}. In contrast, the triple fibers particleboards B/CS/KBF had the lowest MOR value of 5.6 N.mm^{-2}. It is worth noting that the value of the MOR for the B/CS particleboard exceeded the minimum requirements of EN standards (11 N.mm^{-2}) for board use in interior fitments (including furniture) in dry conditions. This may due to their high compression capacity resulting from their full coverage by the adhesives used. On the other hand, the addition of kenaf bast fibers deteriorated the mechanical properties of bagasse and cotton stalks when blended with them. This is because of its low density and the large volume of the fibers which was inadequately covered by the casein adhesives and resulted in a weak bond (Oliveira et al., 2016). It is worth noting that these values were compatible with those found in the literature (Brito and Bortoletto, 2020).

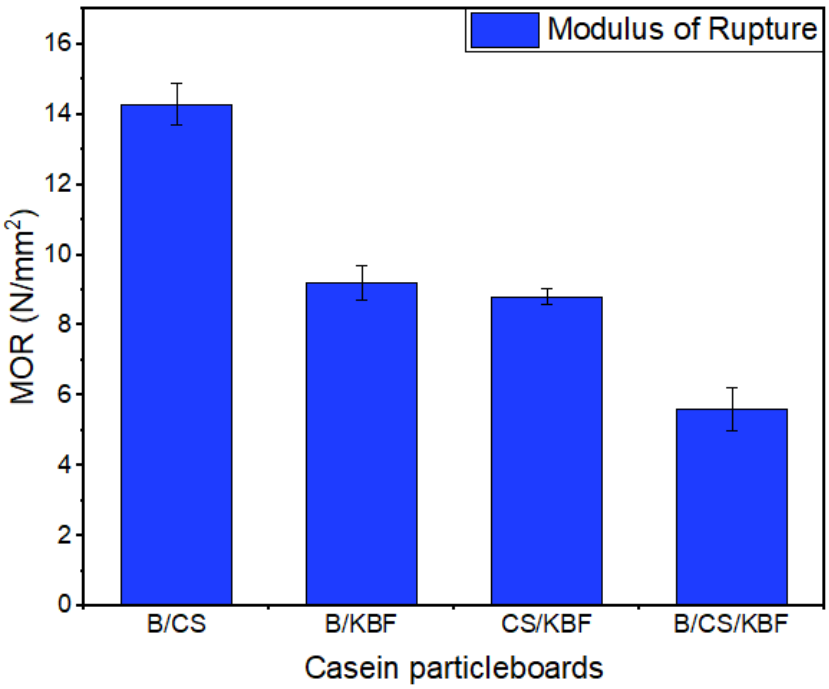

Figure 32: Modulus of rupture of the blended particleboards made from casein adhesive

3.2.1.2. Modulus of elasticity (MOE)

Figure 33 displays the modulus of elasticity (MOE) for the blended casein particleboards. The B/CS particleboard showed again the highest MOE value of 2212 N.mm^{-2}, followed by B/KBF with 1625 N.mm^{-2}. Both B/CS and B/KBF particleboards exceeded the minimum requirement for the European standard (1600 N.mm^{-2}). In contrast, CS/KBF recorded a value of 1363 N.mm^{-2}, and the triple particleboard had the lowest value of 1067 N.mm^{-2}. It has been reported that the addition of the bagasse to other fibers such as corn stalks always gave acceptable improved results (Hajihassani et al., 2022; Iswanto et al., 2021). It has been observed that the, CS/KBF and triple fiber particleboards did not meet the standard value. There is a lack of studies on particleboards made from cotton stalks and kenaf bast fibers that use tannin and casein adhesives, making direct result comparison difficult. It should be noted that the boards made from B/CS and B/KBF gave excellent MOE values, however, when the three fibers blended, the effect of KBF which has a large volume appeared as the amount of the adhesive was not enough to produce full coverage, and hence decrease the internal bond which adversely affected all the mechanical and physical properties. Studies on Kenaf particleboards that used the whole stem showed that the pressing cycle affected the mechanical properties when UF was used as adhesives (Kalaycioglu and Nemli, 2006).

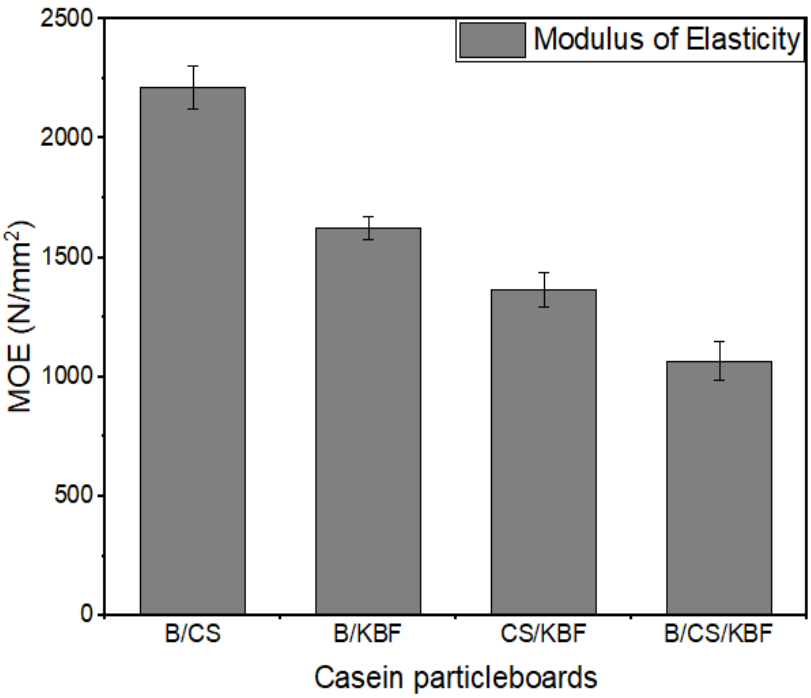

Figure 33: Modulus of elasticity of the blended particleboards made from casein adhesive

3.2.1.3. Internal bond (IB)

The internal bond (IB) values of the particleboard made from the blended fibers were analyzed and presented in Figure 34. Among the particleboards made with casein, the B/CS particleboard demonstrated the highest IB value (0.36 $N.mm^{-2}$), meeting the standard requirement. Lower IB values (0.23 $N.mm^{-2,}$ 0.22 $N.mm^{-2}$) were achieved when the kenaf bast fibers were added to the bagasse and cotton stalks respectively. The triple fibers particleboards showed the lowest IB value of 0.14 $N.mm^{-2}$. As previously discussed by Escobar (W. G. Escobar, 2008), the presence of voids per unit area in kenaf bast fiber particleboards can cause them to fail under load, resulting in lower strength properties. The poor performance of kenaf bast fibers can be attributed to their low weight, leading to a larger fiber volume than the amount of adhesive used. This behavior results in less intimate contact and loose bonding when blended with bagasse and cotton stalks in particleboards.

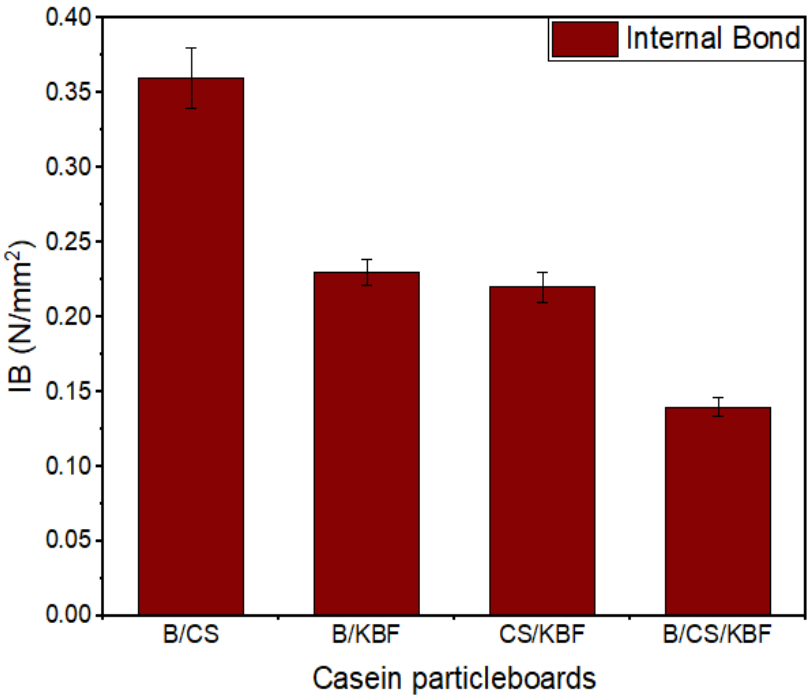

Figure 34: Internal bond of the blended particleboards made from casein adhesive

3.2.1.4.Water adsorption (WA) and thickness swelling (TS)

Based on the findings, the blended particleboards had low physical properties, particularly when kenaf bast fibers were mixed with bagasse and cotton stalks. This is because of the low density of kenaf bast fibers, which have a higher water uptake than other fibers. The water absorption and thickness swelling values for the blended casein particleboards are displayed in Tab. 10. The WA for blended particleboards had values of (82.7 and 115.4) % for B/CS particleboard, (149 and 166) % for B/KBF, (156.7 and 182.6) % for CS/KBF, and (116.34 and 141.9) % for the triple fiber

particleboards at 2 hours and 24 hours. Among the different types of casein particleboards, B/CS particleboard had the lowest value at 10.9% after 2 hours and 21.9% after 24 hours. The B/KBF particleboard achieved thickness swelling values of (28.6 and 38.7) %. The CS/KBF particleboard showed the highest thickness swelling value. It recorded 39% after 2 hours and 53.4% after 24 hours. The triple fibers' particleboard showed (21.9 and 33.7) % after 2 and 24 hours, respectively. Meanwhile and as previously stated, the casein particleboards have a greater tendency to swell and absorb moisture. This can affect their ability to retain their form and strength when used outdoors.

It is worth noting that none of the particleboards met the required TS standards of 8% (2h) and 14% (24h). This is likely because the low-density, particularly kenaf bast fibers, being loosely bonded with the adhesive, react more with water and swell (Wronka et al., 2021). On the other hand, bagasse and cotton stalks, being less penetrative by water, may have contributed less to the particleboard's overall thickness swelling. These thickness swelling values indicate that further optimization of the particleboard composition and adhesive selection is necessary to improve their water resistance and meet the standard requirements. Again, these particle boards are not suitable for the conditions where they may be exposed to water. However, their use indoors for furniture or thermal insulation is recommended.

Table 10: The water absorption and thickness swelling for the blended particleboards made of casein adhesive

Casein adhesive Particleboards	WA (%) 2 h Mean ± S. D	WA (%) 24 h Mean ± S. D	TS (%) 2 h Mean ± S. D	TS (%) 24 h Mean ± S. D
B/CS	82.7± 7.2	115.4 ± 9.8	10.9 ± 1.5	21.9 ± 0.66
B/KBF	149 ± 2.34	166 ± 10.96	28.6 ± 1.52	38.7 ± 1.9
CS/KBF	156.7 ± 2.7	182.6 ± 13	39 ± 0.9	53.4 ± 2.5
B/CS/KBF	116.34 ± 2.7	141.9 ± 10.64	21.9 ± 1	33.7 ± 1.4

Values are means ± SD.

3.2.1.5. Thermal conductivity

The thermal conductivity of blended casein particleboards showed similar results with minor variations among different types of fibers and adhesives, as depicted in Fig. 35. The B/CS recorded a value of 0.076 W/m.k, while the B/KBF particleboard exhibited the lowest value of 0.075 W/m.k. The CS/KBF particleboards had a value of 0.077 W/m.k. The triple fiber particleboards Presented the highest thermal conductivity value of 0.080 W/m.k among the particleboards. According to (Lacoste et al., 2015), the thermal conductivity of particleboard is influenced by board density, thickness, and the size and distribution of its cells or voids. It is important to note that all blended

casein particleboards meet the standard requirement of having a thermal conductivity lower than 0.12 W/m.k, making them suitable for insulation applications.

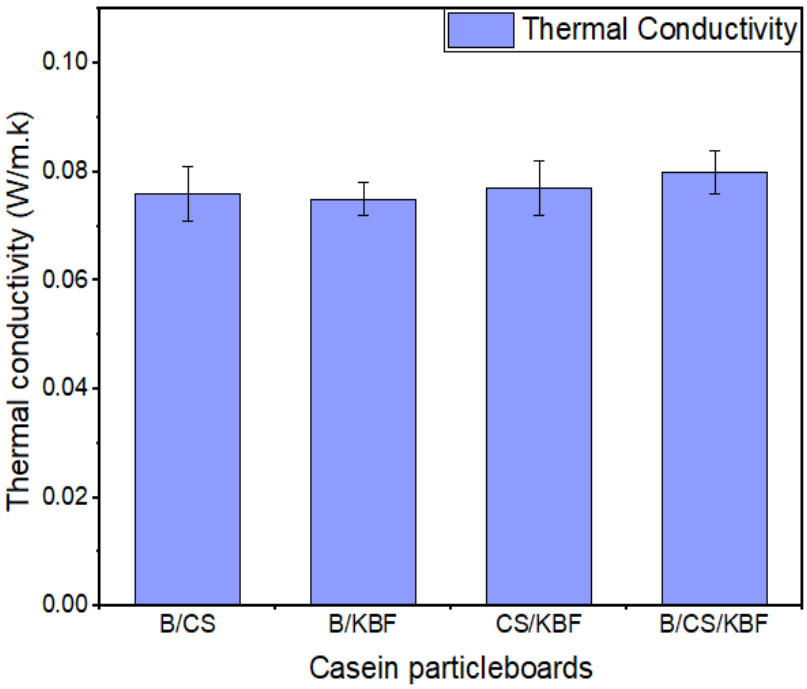

Figure 35: Thermal conductivity of the blended particleboards made from casein adhesive

3.2.2. Tannin-based adhesive

3.2.2.1. Modulus of rupture (MOR)

Figure 36 illustrates the MOR of the blended particleboards made from tannin. B/CS particleboard exhibited the highest MOR with a value of 10 $N.mm^{-2}$, followed by B/KBF with a value of 8.4 $N.mm^{-2}$. While CS/KBF had a value of 7.2 $N.mm^{-2}$, and triple fiber particleboard recorded the lowest value (5.2 $N.mm^{-2}$). Furthermore, all the tannin particleboards failed to meet the required MOR standard. It has been reported that increasing the tannin percent and tannins concentration could improve the properties of the produced particleboard. In addition, attention should also be paid to the pH of the glued particles (Z. Osman et al., 2009). It worth noting that in this study no pretreatment for the fiber had been done and the pH of the tannins was increased from 5 to 9 which was turned to be insufficient for the production of particleboard with improved mechanical properties. It has also been reported by Gisip, 2023 that increasing the resin content is one way to enhance the mechanical properties of particleboards, as it improves the bonding of particles and results in better overall performance. With a higher volume of adhesive, stronger bonds are formed, and the resin also fills the gaps between particles, reducing the chance of particle separation and improving the board's integrity. Optimizing the resin content is critical in particleboard production from agricultural residues and natural fibers to achieve the desired balance between enhanced

mechanical properties and other performance factors. It is imperative to ensure proper formulation and optimization to achieve optimal results (Ayrilmis et al., 2012).

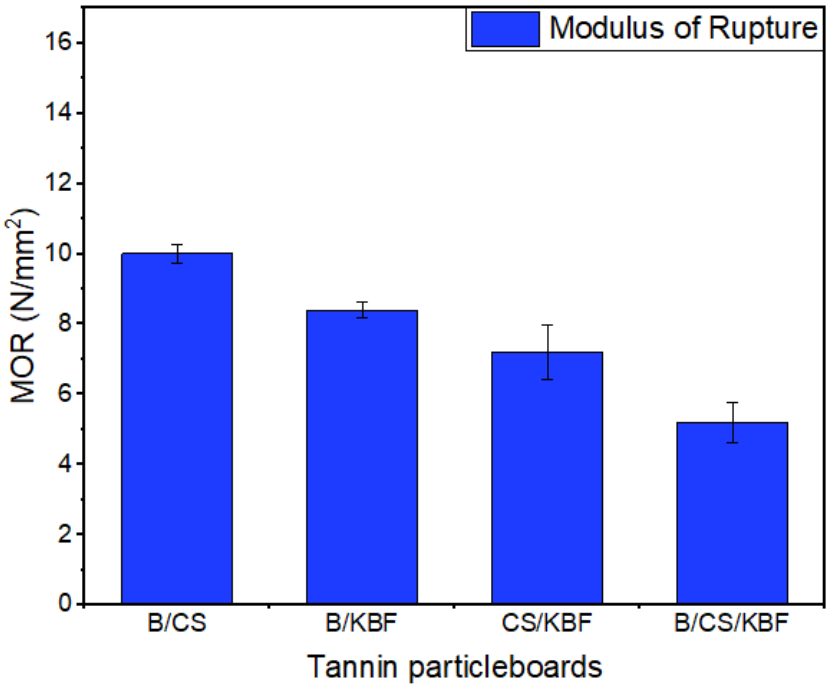

Figure 36: Modulus of rupture of the blended particleboards made from tannin adhesive

3.2.2.2. Modulus of elasticity (MOE)

Figure 37 shows the MOE values for the blended tannin particleboards. The highest MOE value was achieved by B/CS particleboard with a value of 1549 $N.mm^{-2}$, followed by CS/KBF with 1435 $N.mm^{-2}$, and then B/KBF with 1301 $N.mm^{-2}$. In contrast, triple fiber particleboards had the lowest value of 805 $N.mm^{-2}$. None of the tannin particleboards met the standard requirement. It can be observed that the values for blended tannin particleboards were lower than those of casein particleboards.

As mentioned in the individual fiber particleboards and based on the study reported by Osman et al. (Z. Osman et al., 2009), the studied fibers had an acidic pH. It decreased the overall pH of the system. Consequently, the boards' mechanical properties were poorer. The tannin cured effectively at a strongly alkaline pH and formed a good bond with the fiber particles, as observed in individual fiber particleboards. Due to this, tannin autocondensed at room temperature (Z. Osman, 2013), and the solution became thick, making it a challenge to cover evenly the fibers. Increasing the density of particleboards improves their mechanical properties, according to a study (Xu et al., 2003). A denser structure can handle more weight and resist deformation, resulting in

better strength and stiffness. When determining the optimal board density, it is vital to consider the specific application and requirements to achieve the desired mechanical properties.

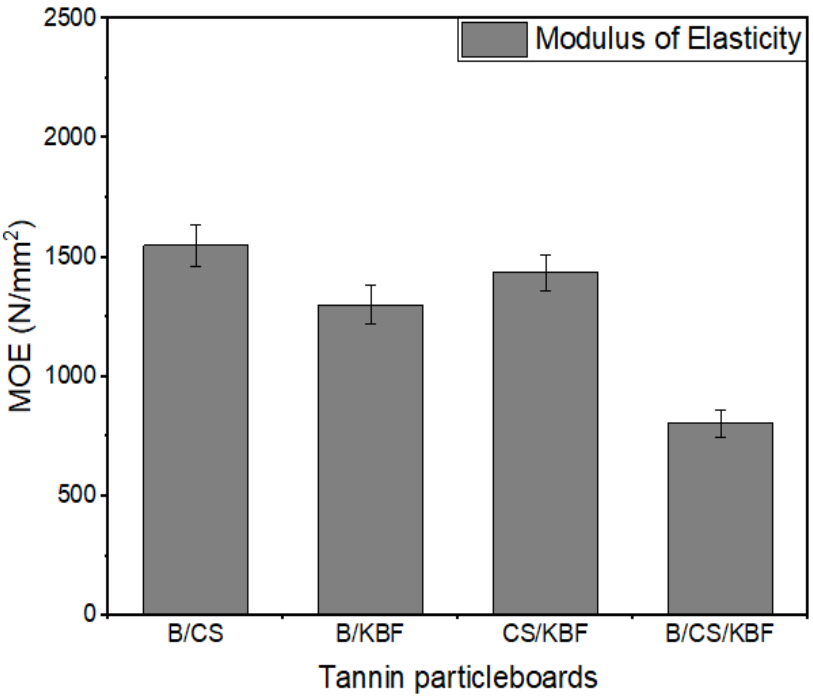

Figure 37: Modulus of elasticity of the blended particleboards made from tannin adhesive

3.2.2.3. Internal bond (IB)

The internal bond of the particleboards made from tannin is demonstrated in Figure 38. All the tannin particleboards did not meet the standard value for the internal bond (0.35 $N.mm^{-2}$). The highest IB value was achieved by B/CS particleboards with a value of 0.25 $N.mm^{-2}$, followed by B/KBF with 0.21 $N.mm^{-2}$, and CS/KBF with 0.18 $N.mm^{-2}$, while the triple fiber particleboards had the lower value of 0.13 $N.mm^{-2}$.

The combination of kenaf bast fibers, bagasse, and cotton stalks decreases mechanical properties when compared to B/CS particleboard. As previously mentioned, this is due to the low density of kenaf bast fibers and their poor coverage by the adhesives (Kowaluk, 2014). The low density results in a less compact structure and weaker bonding between fibers and glue, leading to lower mechanical properties. Similarly, the low reactivity with adhesives can also hinder the formation of strong bonds, resulting in weaker particleboards. The addition of bast kenaf fibers may have detrimentally impacted the bonding and structural integrity of the particleboards, resulting in a significant decline in their mechanical performance. Based on the results, the casein adhesive was more successful than the tannin adhesive in improving the internal bond of blended

particleboards. As mentioned before the reaction between the fibers and the tannins required alkaline media.

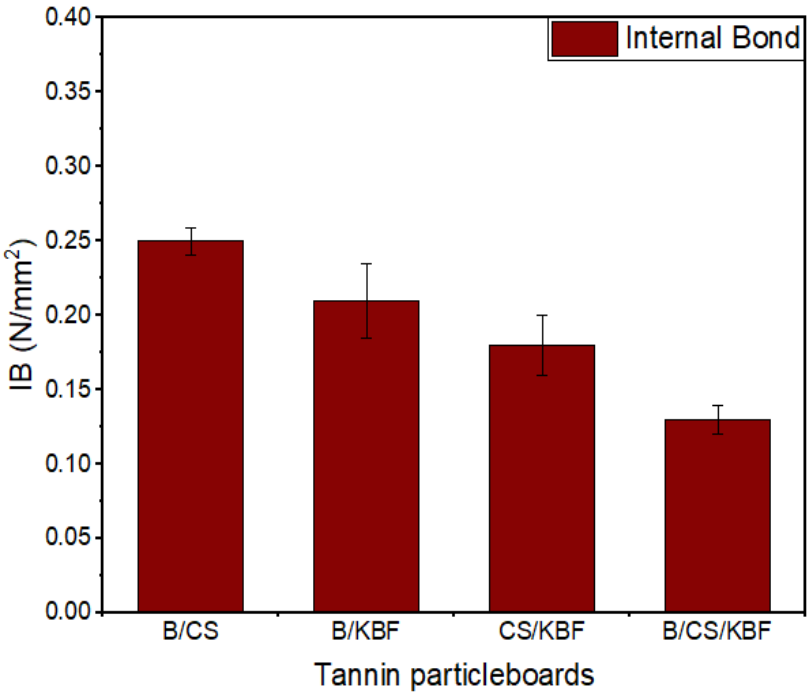

Figure 38: Internal bond of the blended particleboards made from tannin adhesive

3.2.2.4. Water adsorption (WA) and thickness swelling (TS)

Based on water adsorption results, tannin adhesive in blended particleboards reduced water absorption more than casein adhesive. This indicates that using tannin adhesive could improve the physical characteristics of the blended particleboards. The values of WA for B/CS particleboards were 75.4% and 103.1% after 2 and 24 hours, respectively. For B/KBF, the values were 93.3% and 120.5%, while for CS/KBF, it was 90.5% and 133.9%. Triple fiber particleboards had values of 96.7% and 113.7%. The TS of blended particleboards was measured at 2 and 24 hours (Tab. 11). Results for B/CS, B/KBF, CS/KBF, and triple fiber particleboard were (9.15 and 17.2) %, (18.9 and 22.4) %, (20.12 and 28) %, and (20.5 and 28.3) %, respectively. These variations in the results may due to the type of fibers used. Chiang et al., 2014, identified several factors affecting water absorption in particleboards, such as fiber type, environmental conditions, water distribution within the particleboard, interaction between water and matrix, porosity, and fiber volume fraction.

Particleboards of various fiber types can become more porous, allowing water to seep in and causing expansion. Blended fiber boards have higher water absorption and swelling than those made of only one type. The varying abilities of different fibers to absorb water may result in

differences in water uptake and swelling extent. Reducing the size of fibers used in particleboard composition is essential to enhance its quality. Smaller fibers facilitated better distribution within the board, leading to stronger particle bonding and improved physical characteristics like increased strength and reduced water absorption. As mentioned earlier, the use of waxes can reduce the amount of water that particleboards absorb. According to (Halvarsson et al., 2009), waxing particleboards can enhance their water resistance and stability by repelling water and forming a protective layer on the surface, preventing water from seeping into the board's structure. It is important to mention that in this study no wax was added to the produced particleboard in order to understand the reaction of these fibers with the water absorption.

Table 11: The water absorption and thickness swelling for the blended particleboards made of tannin adhesive

Tannin adhesive Particleboards	WA (%) 2 h Mean ± S. D	WA (%) 24 h Mean ± S. D	TS (%) 2 h Mean ± S. D	TS (%) 24 h Mean ± S. D
B/CS	75.4 ± 9.32	103.1 ± 8.8	9.15 ± 0.74	17.2 ± 0.7
B/KBF	93.3 ± 3.74	120.5 ± 9.9	18.9 ± 0.6	22.4 ± 0.86
CS/KBF	90.5 ± 3.9	133.9 ± 15.6	20.12 ± 1.2	28 ± 1.3
B/CS/KBF	96.7 ± 12.8	113.7 ± 11.5	20.5 ± 0.48	28.3 ± 0.58

Values are means ± SD.

3.2.2.5. Thermal conductivity

The thermal conductivity of blended tannin particleboards is shown in Fig. 39. The highest thermal conductivity values were observed in the B/KBF and CS/KBF particleboards, which recorded 0.086 W/m. k. The B/CS particleboard had the lowest thermal conductivity value at 0.075 W/m. k, while the triple particleboard recorded 0.08 W/m.k. It is important to note that all particleboards met the standard requirement of having a thermal conductivity lower than 0.12 W/m. k. These results suggest that all the blended tannin particleboards are suitable for use as insulating materials.

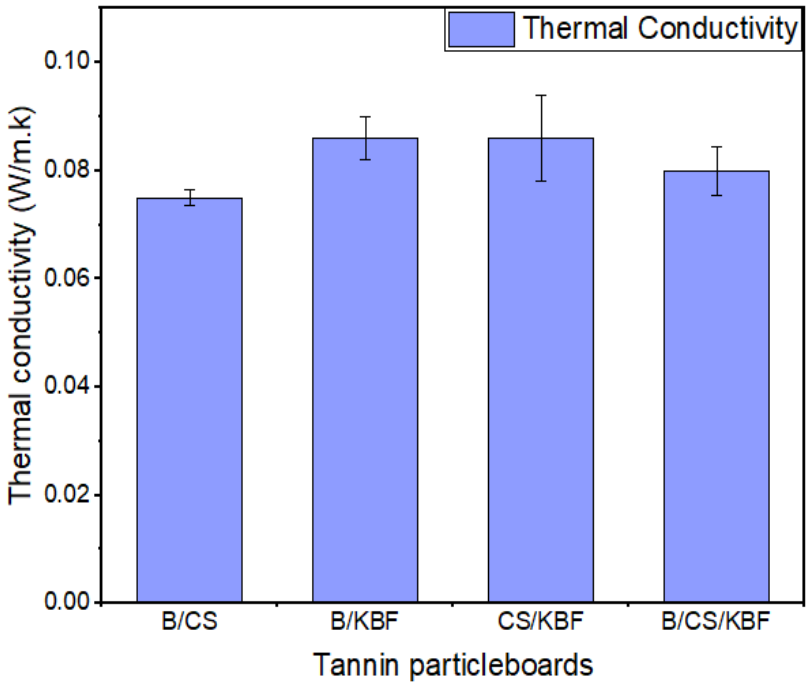

Figure 39: Thermal conductivity of the blended particleboards made from tannin adhesive.

3.3. Foam Production

The formulation described by (Lacoste, Pizzi, Laborie, et al., 2014) effectively produced foam from acacia mimosa tannin-based, and it required no adjustments (Fig. 40a). To produce a larger volume of foam, the quantities were doubled to formulate the foam in cake molds. However, when using maritime pine tannins extracted in the laboratory with smaller quantities of tannins (0.5 to 1g), the resulting mixture was non-uniform, and the foam appeared solid (Fig. 40b). It was evident that the chemical quantities were not suitable and required readjustment. This discrepancy could be attributed to the extraction process or the structure and components of the tannins extracted.

Furthermore, it was observed that when Biolandes maritime pine tannins from bark were utilized, the mixture did not expand to produce foam (Fig. 40c). In contrast, the foam produced from DRT Phénopin pine tannins (Fig. 40d) exhibited a shape similar to that of foam produced from acacia mimosa tannins. These results are useful for further formulation work. According to (Szczurek et al., 2014), many factors can affect foam production such as chemical components, tannins structure, and its reactivity, mixture speed, and duration.

The issue of foam color is a noteworthy concern in this study. The foams produced had a very dark color, ranging from dark gray to black for the acacia tannins foam and dark brown for the maritime pine tannins foam. This coloration, although unattractive, can be attributed to the extensive polymerization process and the significant use of furfuryl alcohol in the foam formulation. Efforts are underway to explore

methods to modify and improve this color, including reducing the quantity of furfuryl alcohol or incorporating new substances into the formulations that could help regulate the color. Some experiments involved adding hexamine to the formulation, resulting in foams with a reddish-to-brown. However, the addition of hexamine slowed down the foaming process, and the foams did not expand adequately.

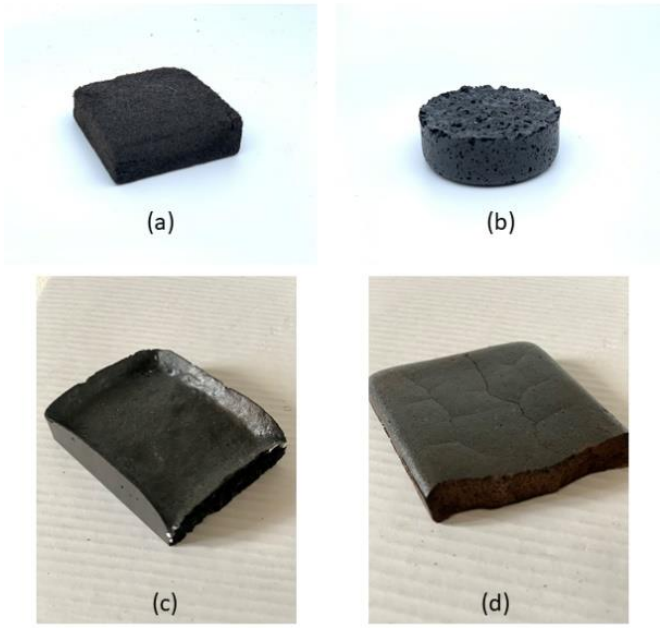

Figure 40: Tannins-based foams (a) mimosa tannins, (b) maritime pine tannins, Biolandes pine tannins, and DRT pine tannins.

3.3.1. Foam characterization

The density, flexion strength, modulus of rupture, compressive strength, and thermal conductivity of produced Acacia mimosa foam are illustrated in (Tab. 12). The density and the thermal conductivity were lower than the previous work reported by (Lacoste et al., 2015) which used maritime pine tannin (0.116 g/cm^3).

Table 12: The density, flexion strength, modulus of rupture, compressive strength, and thermal conductivity of Acacia mimosa tannin foam

Flexion strength	Modulus of rupture	compressive strength (N)	Thermal conductivity	Density
7.2 N	0.10 MPa	575 N	0.022 W/m.k	0.07 g/cm^3

CHAPTER 4

CONCLUSION

4. Conclusion

In this part, the mechanical, physical, and thermal properties of particleboards made of sugarcane bagasse (B), cotton stalks (CS), and kenaf bast fibers (KBF), using casein and tannin adhesives at the loading level of 15% (w/particles) were investigated. The aim was to produce 100% biocomposites suitable for interior fitments, including furniture and thermal insulating materials. The Particleboards were manufactured with individual and blended fibers. The particleboard properties were tested and compared to European standards. A pressing cycle of maximum pressure of 2.5 MPa, different pressing time durations of 480s, 240s, 120s, and 60s, and a pressing temperature of 180°C were used, while the target density was 0.6 $g.cm^{-3}$.

The achieved results provided insights into the mechanical, physical, and thermal properties of particleboards made of these fibers with casein and tannin adhesives, highlighting the importance of fiber type and adhesive selection in achieving the desired properties. The type of fibers and adhesive used significantly impacted particleboard's mechanical, physical, and thermal properties. Casein adhesive produced better mechanical properties with bagasse and cotton stalks. It allowed the production of 100% green boards that exceeded the minimum values recommended by standard (EN 312) for boards for interior fitments, including furniture and thermal insulating materials. In general, particleboards made from individual particles displayed superior mechanical and physical characteristics compared to particleboards made from blends of particles.

Compared to tannin adhesive particleboards, both individual and blended particleboards made with casein adhesive had higher values for modulus of rupture (MOR), modulus of elasticity (MOE), and internal bond (IB). Casein particleboards have lower physical properties compared to tannin particleboards. However, these properties can be enhanced by increasing the hardener content and utilizing hydrophobic substances such as paraffin or wax emulsions. In contrast, tannin adhesives perform optimally in an alkaline environment, necessitating a pre-treatment to convert their acidic pH to alkaline.

Kenaf bast fiber particleboard had lower mechanical and physical properties than bagasse and cotton stalk particleboards due to its low density which resulted in a large volume of these fibers compared with the other. Blending kenaf bast fibers with bagasse and cotton stalks reduced particleboards' mechanical and physical properties leading to poorer bonding qualities. Examining

the utilization of whole stalk kenaf fibers is crucial, as it can offer exceptional mechanical and physical outcomes without requiring an expensive retting process.

In terms of thermal conductivity, both individual and blended fiber particleboards, regardless of the adhesive type, meet the standard requirements (EN 12664). This indicates their suitability for insulation applications. Based on current findings, it is imperative to note that kenaf bast fiber particleboards are only suitable for insulation applications.

The study concluded that it is possible to produce 100% green composites from the three studied fibers and some of them were suitable for furniture and interior fitment applications. However, attention should be paid in a future study to the notes taken by this study.

Regarding the foam production, Acacia mimosa tannin produces a foam that had good properties compared to the literature, while the results of extracted maritime pine, DRT Phénopin, and commercial maritime pine (Biolandes) were not satisfactory and require further experimentation and improvements in future work.

The next part investigates using Sudanese biomass (bagasse, cotton stalks, and kenaf bast fibers) through slow pyrolysis for bioenergy applications. The study evaluates the resulting biochar's yield and thermal properties for potential energy applications. In addition, bio-oil obtained from the process is analyzed with FT-IR and GC–MS to explore its composition.

Part IV. Slow pyrolysis of the bagasse, cotton stalks, and kenaf bast fibers and its products

CHAPTER 1

INTRODUCTION

1. Introduction

Biomass is the fourth primary energy source after coal, oil, and natural gas. Its carbon neutrality and vast reserves have gained significant attention from domestic and international researchers (H. Li et al., 2019). The conversion of biomass involves different technologies that aim to transform the energy stored in organic matter into usable forms of energy. The processes can be categorized into two main types: biological and thermochemical conversion (Iliopoulou et al., 2007). Various types of biomass are highly promising feedstocks for producing clean energy and chemicals due to their potential use in thermal and biological conversion pathways (Güleç et al., 2022). High temperatures and rapid conversion rates characterize thermochemical conversion processes. The primary pathways for thermochemical conversion are combustion, gasification, and pyrolysis (Gonçalves et al., 2016; Kuba et al., 2018).

Pyrolysis is a highly effective process that can efficiently break down large polymer chains into lighter compounds (Prajapati et al., 2023). Pyrolysis can convert biomass into more valuable and clean products, including gas, liquid bio-oil, and solid biochar (Zhang et al., 2007). During pyrolysis, biomass's hemicellulose, cellulose, and lignin structures undergo thermal degradation in an oxygen-free environment. Biochar exhibits higher stability and lower reactivity as compared to uncharred biomass. It has a much lower reactivity and a much longer residence time in the soil, which can lead to long-term carbon sequestration. In addition to its use in generating electricity or heat, biochar has an inherent energy value that maximizes the energy efficiency of the pyrolysis process (Gaunt and Lehmann, 2008). Pyrolysis of biomass can result in the creation of bio-oil, which is a complex blend of organic compounds. The composition of bio-oil can differ depending on the type of biomass and the pyrolysis conditions applied. Bio-oil contains various compounds, including alcohols, aldehydes, ketones, acids, esters, phenolics, and furans (Bertero et al., 2014). These compounds are derived from the complex chemical reactions that occur during the pyrolysis process, which involves the breakdown of the three main components of biomass: cellulose, hemicellulose, and lignin (Czernik and Bridgwater, 2004). The utilization of bio-oil has gained significant interest in various fields due to its potential applications (Tiilikkala et al., 2014). The bio-oil can be used as a fuel in various combustion processes, directly or after further processing. This includes upgrading or blending with conventional fuels. It can be utilized in heating systems, power generation, or even as a transportation fuel, providing a renewable alternative to fossil fuels

(Mathew & Zakaria, 2015; Pimenta et al., 2018). The gas generated during pyrolysis can be an energy source for various applications. The mixture contains high CO_2, CO, CH_4, H_2, and C_2 hydrocarbon levels. In some cases, the gas is used to sustain the pyrolysis process, providing the necessary heat for the reaction. The gas can also dry the biomass feedstock before introducing it into the pyrolysis reactor (Becidan et al., 2007). The produced gas mixture can fuel engines and turbines (Policella et al., 2019).

This part explores the potential of Sudanese bagasse, cotton stalks, and kenaf bast fibers for producing bioenergy via slow pyrolysis. The study evaluates the potential of biochar derived from these fibers as an energy source by analyzing their yield and thermal characteristics, including proximate, ultimate, and calorific analysis. In addition, the bio-oil obtained from the pyrolysis process is analyzed using FT-IR and GC-MS to determine its composition and potential uses.

CHAPTER 2

MATERIALS AND METHODS

2. Materials and methods

2.1. Sample preparation

In the laboratory, the sugarcane bagasse, cotton stalks, and kenaf bast fibers underwent cleaning and cutting to an approximate length of 5cm. A sample of 150g of each fiber type was utilized for every pyrolysis experiment.

2.2. Macro TGA set-up and parameters

The macro thermogravimetric analyzer, TGA (Fig. 41) is composed of a muffle furnace with a volume of 75 liters, capable of reaching temperatures up to 850°C. The furnace was hermetically sealed to prevent the loss of volatile materials during the pyrolysis reactions. The pressure within the muffle furnace was maintained below 0.5 bars. A basket was placed inside the furnace to hold the selected fiber sample. The basket was positioned on a scale that enables the continuous measurement of the mass loss of the biomass during the experiment. The device was operated under N_2 atmosphere with a flow rate controlled by valves and monitored using flow meters. The heater is utilized to preheat the outer gas stream to a temperature of 35°C. Subsequently, the gaseous mixture consisting of the pyrolysis products and the unreacted portion of the introduced gas stream was directed toward a condenser to facilitate the condensation of tars and their accumulation in the receiver. The condenser was circulated with cold water from a cooling bath (2°C). Uncondensed gases were directed toward a cotton filter to separate any aerosols and solid residues effectively and then to the gas vent line. The macro TGA is equipped with 16 thermocouples and connected to software to measure the temperature accurately.

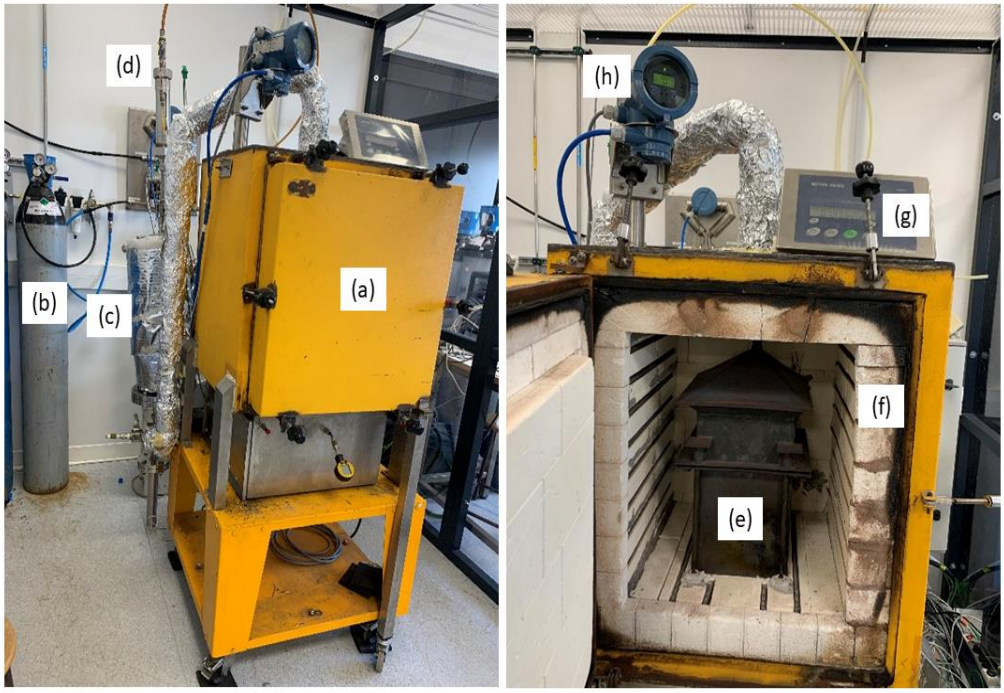

Figure 41: Experimental set-up of macro thermogravimetric reactor: (a) main reactor, (b) nitrogen gas supply, (c) condensation system, (d) filter and gases vent line, (e) pyrolysis basket, (f) muffle furnace, (g) sensitive balance, and (h) gas flowmeter.

The experimental procedure involved utilizing a heating cycle that started with a temperature of 30°C and gradually increased to a maximum temperature of 500°C at a heating rate of 10°C/min. The samples were dried at 110°C for 60 minutes to eliminate the moisture content. Then the temperature was gradually increased until it reached 500°C and maintained at this level for 60 minutes; Fig. 42 illustrates the diagram of temperature vs. time for the pyrolysis cycle. A nitrogen flow rate of 13.1 g/min was used to carry away the reactor's organic vapors and gas products generated from the pyrolyzed fibers. The nitrogen gas acts as a carrier gas and prevents oxidation of the biomass by excluding oxygen from the system. The yield of both char (CY) and pyrolysis liquid (LY) was calculated by determining the weight ratio of the final product to the weight of the initial fiber according to Eq. 12 and 13, respectively (Boer et al., 2020; R. K. Mishra et al., 2022). The gaseous product was not recovered in this study. The pyrolysis experiment was conducted in triplicate for each fiber type.

$$CY\ (\%) = \frac{m_{\ biochar}}{m_{\ biomass}} \times 100 \tag{12}$$

$$LY\ (\%) = \frac{m_{\ liquid}}{m_{\ biomass}} \times 100 \tag{13}$$

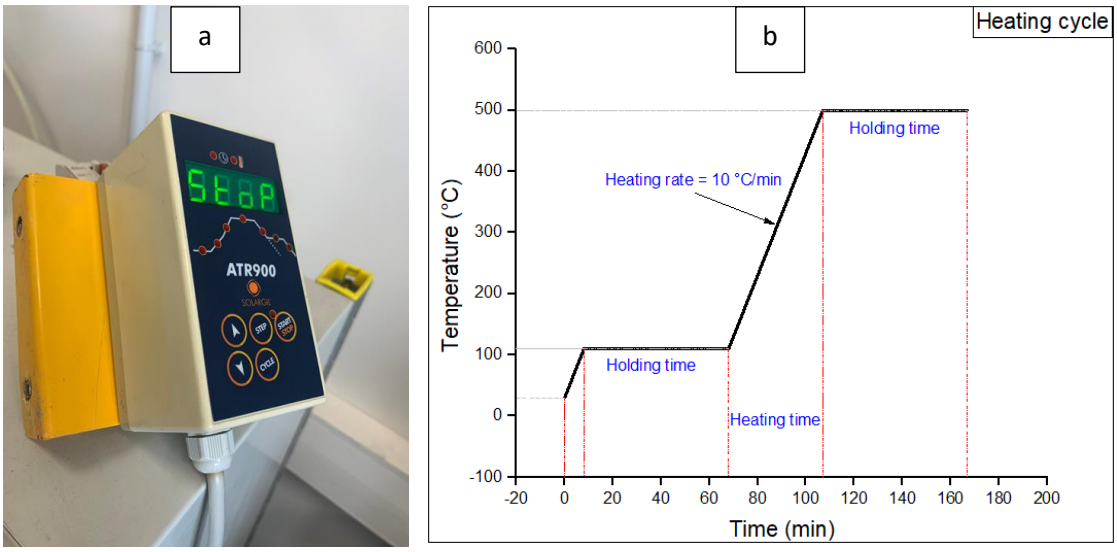

Figure 42: a) temperature controller and b) heating cycle

2.3. Biomass and biochar characterization

2.3.1. Proximate analysis

The proximate analysis assessed each of the three fibers and biochar's moisture, volatile matter, fixed carbon, and ash content. The moisture content of the samples was measured using a moisture content analyzer. Using a muffle furnace, the biomass and biochar ash content was determined under the TAPPI standard methods. The volatile matter was measured by heating the samples to 900°C for 7 minutes using covered crucibles (Boer et al., 2020; Mierzwa-Hersztek et al., 2019). The fixed carbon content of the samples was determined by computing the difference between the ash and volatile matter content.

2.3.2. Ultimate analysis

The content of carbon (C), hydrogen (H), and nitrogen (N) in both biomass and biochar was assessed through elemental analysis by using a CHNS elemental analyzer under ISO 21663:2020 standards. The oxygen content (O) was determined through the difference between the total weight percentage of all analyzed elements and the sum of the weight percentages of carbon, hydrogen, and nitrogen. The ratios of O/C and H/C were subsequently calculated using the obtained weight percentages and the atomic weights of the corresponding elements (Kharel et al., 2019; Pereira et al., 2013).

2.3.3. Higher heating value (HHV)

Higher Heating Value measures the amount of energy released when a fuel is burned completely, taking into account the heat released from the water vapor formed during the combustion process (X. Yang et al., 2017). The higher heating value of biomass and biochar was determined using a bomb calorimeter device (PARR 6200). Approximately 1 gram of each type of sample was utilized for this test. The device was calibrated using benzoic acid, commonly used as a primary standard (Melville, 2014; Rojas & Valués, 2003). The experiments were conducted in triplicate, and the outcomes were reported as means ± SD.

2.3.4. Ash recovery (AR)

Ash recovery refers to the amount of inorganic ash that remains in the solid biochar phase after pyrolysis. This is important because the ash content of biochar can affect its properties and potential applications. High ash content may reduce the biochar's effectiveness as a soil amendment or for other uses. According to (Ghysels et al., 2019), the ash recovery conducted from the ash content of biomass, the ash content of biochar, and the biochar yield, as illustrated in Eq. 14:

$$AR\ (\%) = \frac{Ash_{\ biochar}}{Ash_{\ biomass}} \times CY \tag{14}$$

2.3.5. Energy yield (EY) and energy density (EY)

The energy yield (EY) can be mathematically expressed as the amount of energy produced from the biochar $HHV_{biochar}$ relative to the amount of energy input from the original biomass $HHV_{biomass}$ multiplied by the biochar yield (Eq. 15) (X. Yang et al., 2017). Efficiency in biomass conversion processes is determined by how effectively the energy contained in the biomass is captured and converted into a usable form. A higher energy yield indicates that a more significant proportion of the energy content in the biomass is successfully harnessed and transformed into a valuable energy product. The energy density (ED) is determined by dividing the energy yield by the biochar yield (Eq. 16).

$$EY = \frac{HHV_{\ biochar}}{HHV_{\ biomass}} \times CY \tag{15}$$

$$ED = \frac{EY}{CY} \tag{16}$$

2.3.6. Thermogravimetric analysis (TGA)

The thermal degradation was performed using a thermogravimetric instrument (TGA Q50 Instrument). Approximately 10 mg of the sample was weighed and placed in a small pan in the device. The temperature program was from 30 to 800 °C at a heating rate of 20°C/min. The measurement was conducted under air with a 60 ml/min flux.

2.4. Pyrolysis liquid separation

During the pyrolysis process, the resulting pyrolysis liquid can be separated into two phases based on density. The lower phase, called the aqueous phase, primarily contains water-soluble products, including small hydrocarbons and acids. These components are soluble in water and contribute to the aqueous phase with low calorific values (H. Li et al., 2016). The upper phase is an organic phase, known as pyrolysis oil or bio-oil, consisting of organic compounds rich in various constituents. This bio-oil phase contains complex organic compounds, including liquid hydrocarbons, phenols, aldehydes, ketones, and other volatile organic compounds (R. K. Mishra et al., 2022). Separating the pyrolysis liquid into these two phases allows further analysis and utilization of the different components based on their properties and applications. Many solvents, such as dichloromethane (H. Li et al., 2016), ethyl acetate (Modak et al., 2023), and diethyl ether, can separate the bio-oil from the aqueous phase. In this study, diethyl ether was used with a ratio of 0.5:1 to pyrolysis liquid.

2.5. Characterization of bio-oil

2.5.1. Fourier transform infrared spectroscopy (FTIR) spectra

The Fourier transform infrared spectroscopy (FTIR) was obtained using a PerkinElmer Frontier spectrophotometer with a diamond/ZnSe crystal operating in attenuated total reflection (ATR) mode. The bio-oil samples were placed into the device, and the analyses were performed with 64 scans, with a resolution of 4 cm^{-1} and in the range from 4000 to 400 cm^{-1}.

2.5.2. Gas chromatography-mass spectrometry (GC–MS)

The analysis was done using a PerkinElmer GC-MS device, with the following parameters: DB-5MS (30 m 0.32 mm 0.5 µm); injection temperature of 300 °C; column oven temperature program: 60 °C (held for 5 min.), then ramped to 270 °C (at 10 °C/min, held for 5 min). The carrier gas was high-purity Helium at a constant flow rate of 20 ml min^{-1}. The MS scan was conducted on an electron impact ionization mode (70 eV) with the m/z range from 50 to 450. The samples were diluted by dichloromethane with a 10:1 (m/v) ratio, and 1 µL of the sample was injected each time.

CHAPTER 3

RESULTS AND DISCUSSION

3. Results and discussion

3.1. Biomass characterization

The proximate, ultimate, and calorific analysis of bagasse, cotton stalks, and kenaf bast fibers are resumed in Tab. 11. Proximate analysis is a technique used to determine the chemical composition of the material by measuring the amount of moisture, volatile matter, fixed carbon, and ash content (Park et al., 2023). Bagasse exhibited a moisture content of 6.8%, a volatile matter content of 76.6%, a fixed carbon content of 19.3%, and an ash content of 4.1%. These values were consistent with those found in the literature (Boer et al., 2020). Cotton stalks recorded a moisture content of 7.7%, a volatile matter of 73.3%, a fixed carbon content of 21.5%, and a 5.2% ash content. The cotton stalks' values were in range with those presented by (A. Gupta et al., 2020). On the other hand, kenaf bast fibers exhibited a moisture content of 7.3%, a volatile matter content of 84.8%, a fixed carbon content of 12.7%, and an ash content of 2.5%. These values were close to those reported in the literature (Harussani & Sapuan, 2022). Among the three studied fibers, the Cotton stalks exhibited a slightly higher moisture and ash content, this may due to the presence of the large inner pith large consists of thin-walled parenchyma cells that are known as hydrophobic short fibers (Tutus et al., 2010).

The fuel ratio is an essential parameter in biomass pyrolysis. The fuel ratio was calculated as the weight percentage of volatile matter divided by the weight percentage of fixed carbon in the biomass sample. A low fuel ratio indicates that a high proportion of the biomass is volatile matter, which can lead to lower heating values and greater instability during pyrolysis. A fuel ratio of 1 or less is considered very low, indicating that the biomass is highly volatile and may require additional processing to stabilize the pyrolysis process (Chae et al., 2020). The fuel ratio of bagasse, cotton stalks, and kenaf bast fibers was 0.25, 0.29, and 0.15, respectively (Tab. 11).

The ultimate analysis is a technique used to determine the elemental composition of a sample, usually by measuring the percentages of carbon, hydrogen, nitrogen, sulfur, and oxygen present in the material (Dhyani & Bhaskar, 2018). Bagasse had 44.5% of carbon, 5.6% hydrogen, 0.34% nitrogen, 0.26% of sulfur, and 49.4% of oxygen. The ultimate analysis of cotton stalks was: 46.1% carbon, 5.7% hydrogen, 0.72% nitrogen, 0.13% sulfur, and 47.3% oxygen. Kenaf bast fibers exhibited a carbon content of 45.7%, hydrogen of 5.8%, nitrogen of 0.28%, sulfur of 0.15%, and

oxygen of 48.1%. The ultimate values of bagasse, cotton stalks, and kenaf bast fibers were compared to the other studies, as shown in Tab. 13.

The O/C ratio was measured for three different materials. Bagasse had a ratio of 0.83, cotton stalks had a ratio of 0.77, and kenaf bast fibers biochar had a ratio of 0.79. The H/C ratios were also determined for these materials, with values of 1.5 for bagasse and kenaf bast fibers and 1.48 for cotton stalks. These values were consistent with those found in previous research, shown in Tab. 13.

The higher heating measures the energy released when a substance is burned (Petráš et al., 2019; M. Singh et al., 2020). The HHVs of bagasse, cotton stalks, and kenaf bast fibers were: 18 MJ/kg, 18.6 MJ/kg, and 18.2 MJ/kg, respectively. The analysis indicates that the current biomass exhibits similarities to other biomass documented in various research studies.

Table 13: Proximate, ultimate analysis, O/C ratio, H/C ratio, and higher heating values of bagasse, cotton stalks, and kenaf bast fibers.

Characteristics	Bagasse	Ref [1]	Cotton stalks	Ref [2]	Kenaf bast fibers	Ref [3]
Proximate analysis						
Moisture content (MC)	6.8	8.5	7.7	-	7.3	4.4
Volatile matter (VM)	76.6	82.4	73.3	74	84.8	83.05
Ash content	4.1	4.2	5.2	6.5	2.5	1.15
Fixed carbon (FC)[a]	19.3	13.4	21.5	19.5	12.7	15.80
Fuel ratio (FC/VM)	0.25	0.16	0.29	0.26	0.15	0.19
Ultimate analysis						
Carbon (C)	44.5	47.3	46.1	39.58	45.7	47.32
Hydrogen (H)	5.6	5.7	5.7	5.98	5.8	5.20
Nitrogen (N)	0.34	0.4	0.72	0.37	0.28	0.38
sulfur (S)	0.26	-	0.13	< 0.5	0.15	<0.02
Oxygen (O)[a]	49.4	46.7[b]	47.3	47.57	48.1	47.1
O/C	0.83	0.74	0.77	0.9	0.79	0.75
H/C	1.5	1.43	1.48	1.8	1.5	1.3
HHV (MJ/kg)	18	18.1	18.6	15.8	18.2	18.54

Ref. [1]: (Boer et al., 2020), Ref. [2]: (A. Gupta et al., 2020), and Ref. [3]: (Harussani & Sapuan, 2022)

[a] calculated by difference

[b] (oxygen + sulfur)

3.2. Pyrolysis parameters and product yields

The temperature-time relationship was closely monitored during the experiment and followed the expected pattern, as shown in Fig. 43. The temperature and time curves were almost identical, with minimal delay. The nitrogen inlet and outlet gases curves for pyrolyzed bagasse, cotton stalks, and kenaf bast fibers displayed two primary peaks. The first peak represented water vapor, which can originate from the moisture content in the feedstock and the breakdown of oxygen-containing functional groups within the biomass structure, such as hydroxyl (-OH) groups. This dehydration reaction forms water as a byproduct and other volatile gases (Czernik and Bridgwater, 2004). At the same time, the second peak denoted the vaporized gaseous mixture containing both the pyrolysis products and nitrogen.

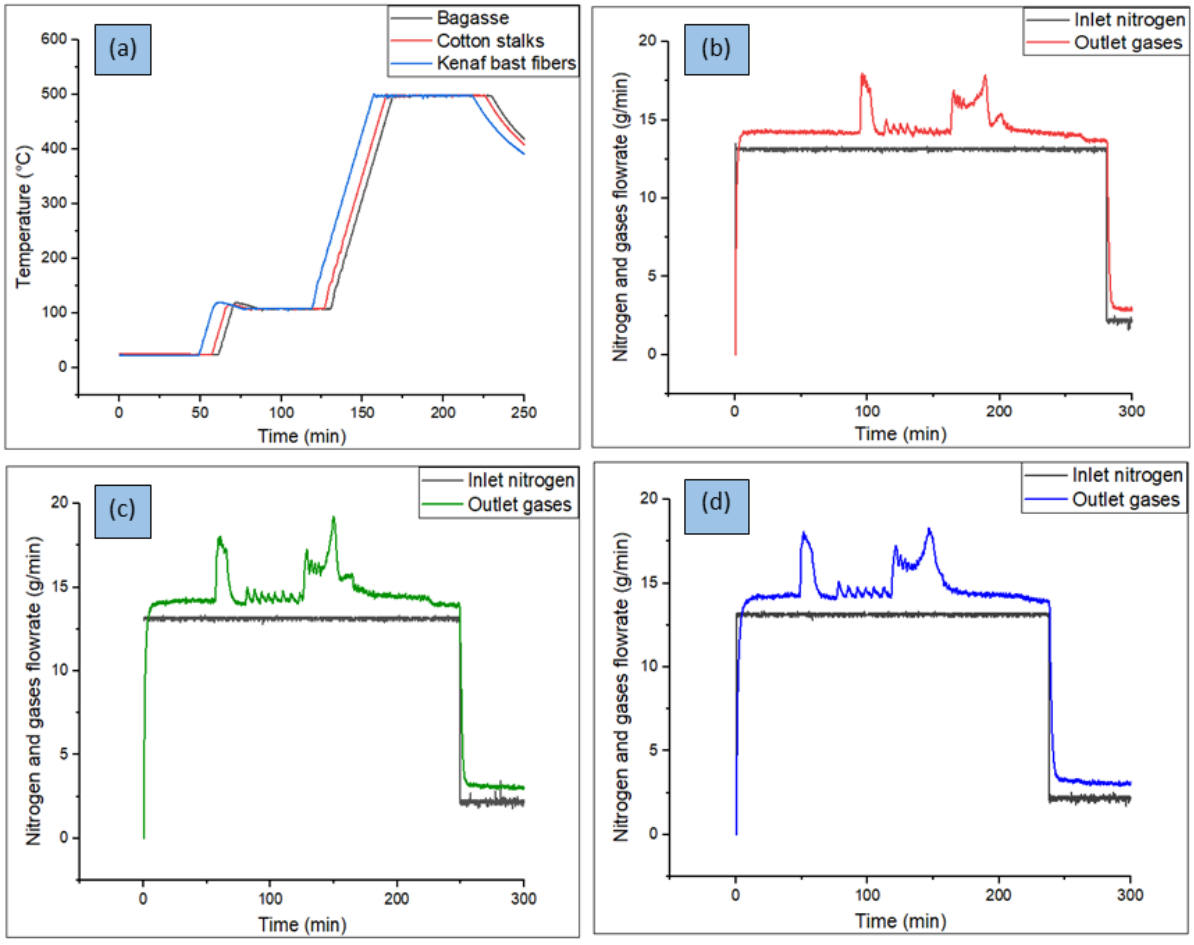

Figure 43: a) temperature as a function of time, b) nitrogen and gases flowrate of bagasse experiment, c) cotton stalks, and d) kenaf bast fibers

3.3. Biochar and pyrolysis liquid yield

Biochar and pyrolysis liquid obtained from the pyrolysis of bagasse, cotton stalks, and kenaf bast fibers are displayed in Fig. 44. The biochar and pyrolysis liquid yield were calculated using Eqs (12) and (13). The amount of biochar and pyrolysis liquid produced during the process depends on various factors, such as the type of biomass used, their particle size (S. Mishra and Upadhyay, 2021), the reactor employed, and the process conditions, including temperature, pressure, heating rate, and residence time (Iwuozor et al., 2022).

The results indicated that cotton stalks had the highest biochar and pyrolysis liquid yield, with values of 31.9% and 14%, respectively, followed by bagasse with 28% and 11.6%. Kenaf bast fibers had the lowest result, with 22.9% and 11.1% for biochar and pyrolysis liquid, respectively. The bagasse biochar yield was equal, while the liquid yield was lower than reported in the literature (Boer et al., 2020), which used the same temperature and heating rate, while the liquid yield percentage was lower. The cotton stalks' biochar and pyrolysis liquid yield were lower than the values stated in the literature (Makavana et al., 2020; Shah & Valaki, 2022). Previous studies utilized similar temperature and heating rate parameters, but their particle size was smaller than what was used in the current study. The biochar yield of kenaf bast fibers was higher than in previous work (Harussani & Sapuan, 2022) for the same parameters.

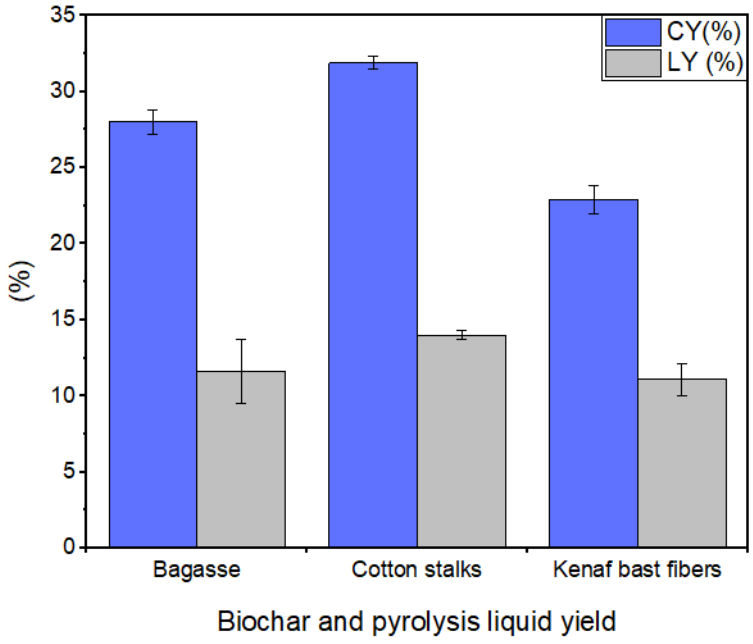

Figure 44: Biochar (CY) and pyrolysis liquid yield (LY) of bagasse, cotton stalks, and kenaf bast fibers.

A higher biochar yield is promoted by lower pyrolysis temperatures while increasing the temperature decreases biochar yield and increases gas and liquid yield. According to the previous study (Glushkov et al., 2021), the yield of biomass pyrolysis products can be enhanced by considering specific conditions for each product category. If the goal is to increase the char yield, it is better to use low heating rates and temperatures during the pyrolysis. This promotes the formation of solid carbonaceous material (char) rather than further decomposition into gases or liquids. In contrast, it is recommended to employ high heating rates with an average temperature and short residence time for higher liquid yield. These conditions facilitate the rapid breakdown of biomass into liquid products. The yield of biomass pyrolysis can be increased by optimizing the heating rates, temperatures, and residence times according to the desired product.

During slow pyrolysis, there is a low mass loss of biomass, and significant conversion occurs within the temperature range of 300°C to 500°C. The influence of heating rate on char yield is particularly substantial at temperatures below 400°C. The high biochar yield at lower temperatures suggests that the biomass has undergone only partial pyrolysis (Katyal et al., 2003). At higher temperatures, where char production is the primary objective, the effect of the heating rate becomes less significant. In such cases, the reduction in char yield at higher heating rates can be attributed to the secondary cracking of pyrolysis vapors and the secondary decomposition of the char (Carrier et al., 2011). It is worth mentioning that not all of the heavy tar produced during pyrolysis was recovered completely. Some heavy tar was trapped in the condensation system, although the amount was negligible. To ensure clarity and avoid ambiguity, the term "pyrolysis liquid" used in this study refers explicitly to the condensed liquid obtained from the tar pot, excluding the portion trapped in the condensation system.

3.4. Higher heating values and energy analysis of biochar

The higher heating value of bagasse, cotton stalks, and kenaf bast fibers biochar showed that the bagasse biochar had the highest value, followed by kenaf bast fibers and cotton stalks, as shown in Tab. 14. Bagasse biochar reported a value of 28.4 MJ/Kg, more elevated than others found in the literature (Boer et al., 2020; Carrier et al., 2011; Mesa-Perez et al., 2005; Varma & Mondal, 2017). The value obtained for kenaf bast fibers was 28.2 MJ/Kg. In comparison, cotton stalks showed a value of 26.7 MJ/kg, higher than the value reported by the previous work (Shah & Valaki, 2022). The high heating value of biochar makes it desirable for various fuel applications. In the current study, the biochar obtained from the pyrolysis of bagasse, cotton stalks, and kenaf bast fibers demonstrated elevated heating values comparable to those documented in previous studies conducted under similar conditions.

The energy yield (EY) and energy density (ED) were calculated using Eqs (15) and (16), respectively. Among the biochar produced, cotton stalks biochar exhibited the highest energy yield, measuring 45.9%. Bagasse biochar followed closely with 44.2%, and kenaf bast fibers biochar recorded a slightly lower value of 35.4%. Regarding energy density, bagasse biochar achieved the highest value (1.58), while cotton stalks and kenaf bast fibers biochar had energy density values of 1.44 and 1.55, respectively.

Table 14: Higher heating value, energy yield, and energy density of bagasse, cotton stalks, and kenaf bast fibers biochar

Biomass	HHV (MJ/kg)[a]	Energy yield (%)	Energy density
Bagasse	28.4 ± 0.47	44.2	1.58
Cotton stalks	26.7 ± 0.15	45.9	1.44
Kenaf bast fibers	28.2 ± 0.7	35.4	1.55

[a] Values are mean ± SD.

3.5. Proximate and ultimate analysis of biochars

Table 15 presents the proximate and ultimate analysis results of the biochar samples. The bagasse biochar had 23.8% volatile matter content, while the cotton stalks biochar had only 8.1%. The highest volatile matter content was recorded in the kenaf bast fibers biochar, which had 28.2%. The value of bagasse biochar was higher than what was previously reported in a study by Boer et al. (Boer et al., 2020). The value of cotton stalks was also slightly higher than what was reported in a previous study by Kumar (Kumar et al., 2021). On the other hand, the kenaf bast fibers' value was higher than reported in earlier work (Harussani and Sapuan, 2022).

Regarding ash content, bagasse biochar had a value of 11.6%, lower than found in the literature (Boer et al., 2020). Cotton stalks biochar had 15%; this value was lower than reported before (Venkatesh & Venkateswarlu, 2013). Kenaf bast fibers biochar exhibited the lowest ash content with a value of 9.3%, which was lower than what was recorded in previous work (Harussani & Sapuan, 2022).

Fixed Carbon denotes the solid residue that remains after the volatile matter and moisture has been eliminated from biomass. This residual carbon content in biomass remains after pyrolysis and is regarded as the primary source of energy within the biomass (Posom & Sirisomboon, 2017). The fixed carbon content was 64.7%, 76.9%, and 62.5% for bagasse, cotton stalks, and kenaf bast fibers biochar. These values represent the percentage of fixed carbon in the respective biochar samples after accounting for the volatile matter and ash content.

The ultimate analysis of the bagasse biochar revealed that it consists of approximately 72.3% carbon (C), 2.7% hydrogen (H), 0.55% nitrogen (N), 24.1% total oxygen (O), and 0.41% of sulfur (S), these values were comparable with the values reported in a previous study (Varma & Mondal, 2017). Cotton stalks had a 70.8% of carbon (C), 2.7% of hydrogen (H), 1.1% of nitrogen (N), 25.1% of oxygen (O), and 0.36% of sulfur (S). Kenaf bast fibers exhibited a composition of approximately 75.9% carbon (C), 3% hydrogen (H), 0.94% nitrogen (N), 20.5% oxygen (O), and 0.11% sulfur (S). Carbon, hydrogen, and sulfur values were higher than in the literature (A. A. H. Saeed et al., 2021). It is important to note that these percentages are approximate values and can vary depending on the specific characteristics of the samples being analyzed. According to the previous work (Pereira et al., 2013), carbon and hydrogen contents are essential criteria for assessing fuel's calorific value and power generation potential, while oxygen decreases the calorific value of the energy. On the other hand, fuel's low nitrogen and sulfur content is essential from an environmental perspective (Demirbaş & Demirbaş, 2004). Nitrogen and sulfur compounds present in fuel can contribute to the formation of air pollutants when the fuel is burned.

The ash recovery of biochar was calculated by dividing the ash content of the biochar by the ash content of the corresponding biomass and then multiplying it by the biochar yield (Ghysels et al., 2019). For bagasse, the ash recovery was determined to be 78.9%. This means that approximately 78.9% of the ash in the bagasse was retained in the resulting biochar. For cotton stalks, the ash recovery value was 91.6%, indicating that a higher proportion of the ash content was preserved in the biochar. In comparison, kenaf bast fibers had an ash recovery value of 88.7%. These values provide insights into the effectiveness of the biochar production process in retaining the ash components from the original biomass.

Table 15: Proximate and ultimate analysis of bagasse, cotton stalks, and kenaf bast fibers biochar

	Bagasse	**Cotton stalks**	**Kenaf bast fibers**
Proximate analysis (wt. %)			
Volatile matter	23.8 ± 1.1	8.1 ± 0.39	28.2 ± 0.66
Ash content	11.6 ± 0.07	15 ± 0.34	9.3 ± 0.3
Fixed carbon*	64.7 ± 1.2	76.9 ± 0.84	62.5 ± 0.76
Ash recovery (%)	78.9	91.9	88.7
Ultimate analysis (wt. %)			
C	72.3 ± 0.85	70.8 ± 0.7	75.9 ± 1.6
H	2.7 ± 0.03	2.7 ± 0.06	3 ± 0.06

N	0.55 ± 0.02	1.1 ± 0.03	0.94 ± 0.07
S	0.41 ± 0.01	0.36 ± 0.03	0.11 ± 0.02
O	24.1 ± 0.89	25.1 ± 0.69	20.5 ± 1.07
O/C	0.25	0.27	0.20
H/C	0.45	0.46	0.47

* calculated by the difference

The pyrolysis process induces chemical reactions that increase condensation and aromatization, resulting in changes in the O/C (carbonization degree) and H/C (aromatization degree) mole ratios. The O/C ratio provides information about the relative amounts of oxygen and carbon in biochar and can give insights into its chemical composition and potential properties (Kharel et al., 2019; Pereira et al., 2013). The O/C ratio of bagasse biochar was calculated to be 0.25. This value means that for every carbon atom in the biochar, there are approximately 0.25 oxygen atoms. Similarly, the O/C ratio for cotton stalks biochar was determined to be 0.27, indicating a slightly higher proportion of oxygen than carbon. Kenaf bast fibers biochar had an O/C ratio of 0.20, suggesting a lower oxygen content than carbon.

The H/C ratios of 0.45, 0.46, and 0.47 obtained for the biochar derived from bagasse, cotton stalks, and kenaf bast fibers indicate the relative hydrogen content compared to carbon. In biochar, the O/C and H/C ratios are typically lower than those of the biomass feedstock because carbon (C) is more resistant to degradation and remains in higher concentrations after pyrolysis. The loss of H and O during pyrolysis leads to higher carbon content and, consequently, lower O/C and H/C ratios in biochar (Boer et al., 2020). It is widely acknowledged that the O/C ratio in biochar should not exceed 0.4, and the H/C ratio should be below 0.6 (Mierzwa-Hersztek et al., 2019). It is worth mentioning that our results also confirmed these recommended values. The reduction in O/C and H/C ratios in biochar is a desirable outcome for specific applications, such as carbon sequestration or use as a solid fuel, as it increases the carbon content and stability of the char. However, it is essential to note that biochar's specific O/C and H/C ratios can vary depending on the pyrolysis conditions and biomass feedstock composition.

The comparison of the studied fibers' biochar properties with the critical properties for energy applications revealed exciting findings. Kenaf bast fibers biochar demonstrated favorable characteristics, including the lowest ash content, highest carbon content, highest H/C ratio, and lowest O/C ratio. These properties indicate its suitability as a fuel source, as they contribute to low impurities, high carbon content, and favorable combustion properties. On the other hand, cotton stalk biochar stood out with the highest fixed carbon content, which indicates its potential for stable and sustained combustion. Additionally, it exhibited the lowest volatile content, implying reduced

emissions during combustion. Bagasse biochar recorded the highest heating value (HHV). This signifies its potential for increased energy release during combustion, making it an attractive option for energy applications. It is essential to consider that while each biochar sample may excel in specific properties, the overall suitability for energy applications depends on a combination of these factors.

3.6. Thermogravimetric analysis (TGA)

The thermogravimetric analysis (TGA) curves for bagasse, kenaf bast fibers, and cotton stalks biochar exhibited similar patterns of mass loss as a function of temperature. However, the TG and DTG curves analysis revealed differences in the thermal stability of the biochar derived from these fibers. Fig. 45 illustrates the TG and DTG of the biochar derived from bagasse, cotton stalks, and kenaf bast fibers. Based on the curves, it was observed that the kenaf bast fibers biochar exhibited the highest degradation temperature compared to bagasse and cotton stalks biochar. This indicates that the kenaf bast fibers biochar is more thermally stable and can withstand higher temperatures before a significant mass loss occurs. The higher degradation temperature suggests a higher resistance to thermal decomposition. The cotton stalks biochar showed a higher degradation temperature than bagasse biochar. This implies that cotton stalks biochar is relatively more stable than bagasse biochar but less stable than kenaf bast fibers biochar.

The differences in thermal stability among the biochar can be attributed to various factors, including the composition of the original fibers, their lignocellulosic structure, and the presence of different chemical constituents. These factors influence the thermal degradation behavior and the temperature at which significant mass loss occurs. The information obtained from the TG and DTG curves provides insights into the thermal behavior of the biochar derived from bagasse, kenaf bast fibers, and cotton stalks. Understanding the thermal stability of biochar is vital for its potential applications, such as in energy generation, soil amendment, and carbon sequestration, as it determines its performance and behavior under different temperature conditions.

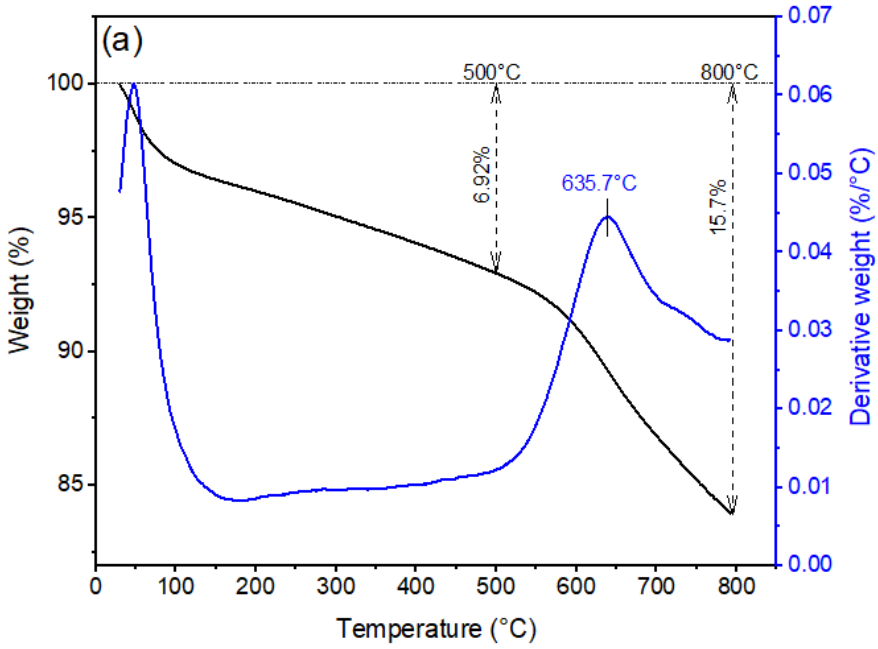
(a)
500°C
800°C
6.92%
635.7°C
15.7%
Weight (%)
Derivative weight (%/°C)
Temperature (°C)

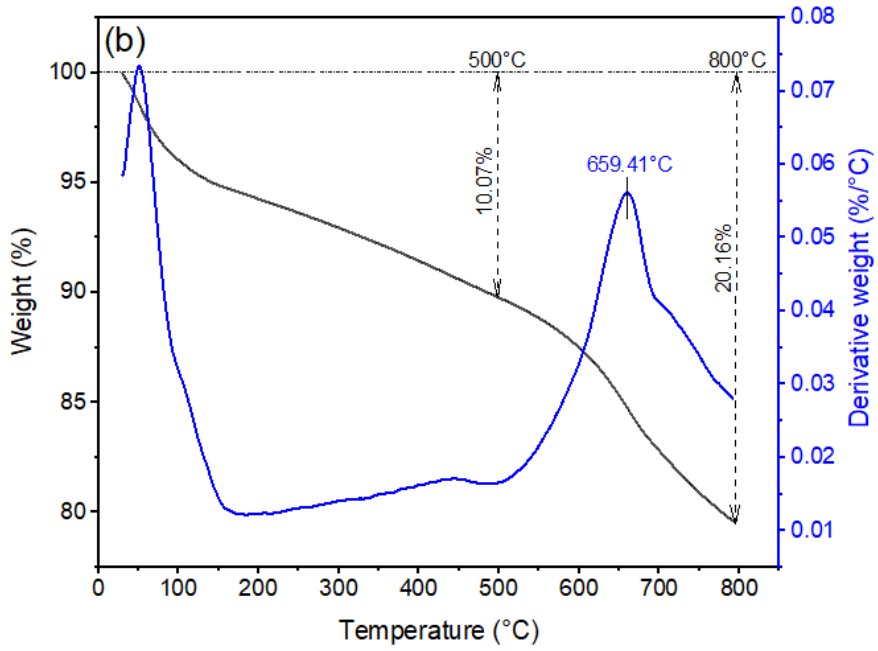
(b)
500°C
800°C
10.07%
659.41°C
20.16%
Weight (%)
Derivative weight (%/°C)
Temperature (°C)

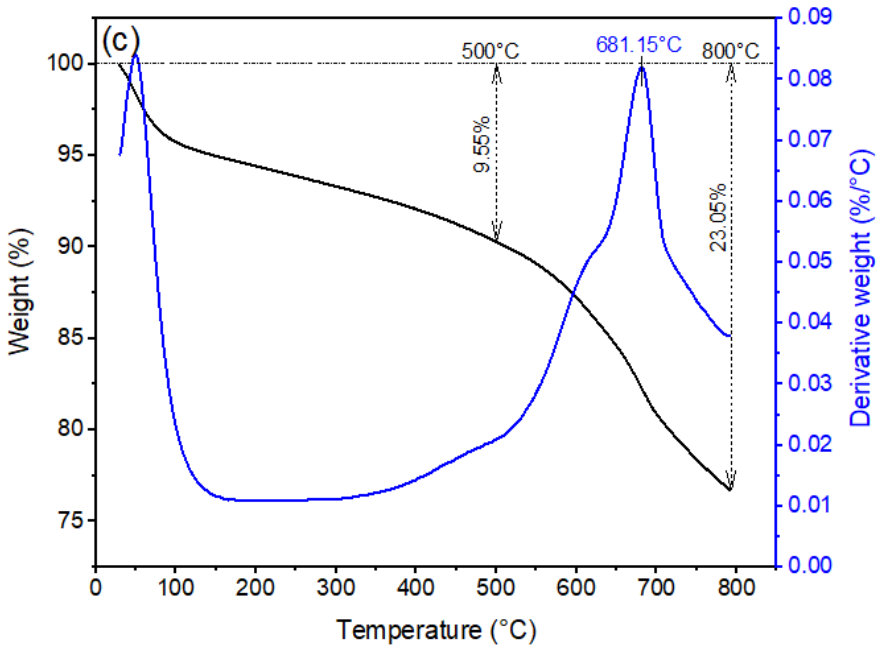

Figure 45: TG and DTG curves for a) bagasse, b) cotton stalks, and c) kenaf bast fibers biochar

Table 14 presents specific degradation temperatures of biochar. The degradation temperature of the bagasse biochar increased by 65.9% of the raw bagasse, cotton stalks biochar increased by 87.5%, while the degradation temperature of kenaf bast fibers increased by 76.1%. This means that the biochar can withstand higher temperatures before undergoing significant mass loss, indicating improved thermal stability and resistance to degradation. The increase in degradation temperature can be attributed to the structural and compositional changes that occur during the pyrolysis process. This biochar is enriched in carbon and has a higher thermal degradation resistance than the original biomass. The significant increase in the degradation temperature of the biochar indicates their improved thermal properties, making them suitable for applications where high-temperature stability is desired.

At a pyrolysis temperature of 500°C, the bagasse biochar showed a mass loss of 6.9% from its initial mass, indicating that only a relatively small portion of the biochar decomposed. Similarly, the cotton stalks biochar experienced a mass loss of approximately 10% at 500°C. The kenaf bast fibers biochar exhibited a mass loss of 9.55% at 500°C, indicating a comparable level of decomposition. These findings suggest that the biochar samples maintained their structural integrity significantly at the pyrolysis temperature. The degradation temperature and mass loss at 500°C and 800°C for both biochar and raw biomass were compared in Tab. 16.

Table 16: Degradation temperature mass loss at 500°C and 800°C for bagasse, cotton stalks, and kenaf bast fibers biochar and raw biomass

	Raw biomass			Biochar		
	D_T (°C)	W_{loss} at 500°C	W_{loss} at 800°C	D_T (°C)	W_{loss} at 500°C	W_{loss} at 800°C
Bagasse	383.09	82.72%	86.53%	635.7 °C	6.92%	15.7%
Cotton stalks	351.47	71.37%	77.27%	659.41 °C	10.07%	20.16%
Kenaf bast fibers	386.81	84.11%	79.72%	681.15 °C	9.55%	23.05%

D_T: degradation temperature and W_{loss} : means weight loss

3.7. Separation of the pyrolysis liquid

Figure 46 illustrates the separating process of the pyrolysis liquid into the aqueous phase and pyrolysis oil using diethyl ether. To ensure the complete extraction of organic components, the mixture was shaken vigorously and allowed to separate into phases for several minutes. This process was repeated thrice before recovering the diethyl ether with a rotary evaporator after separating it from the aqueous phase of the pyrolysis oil.

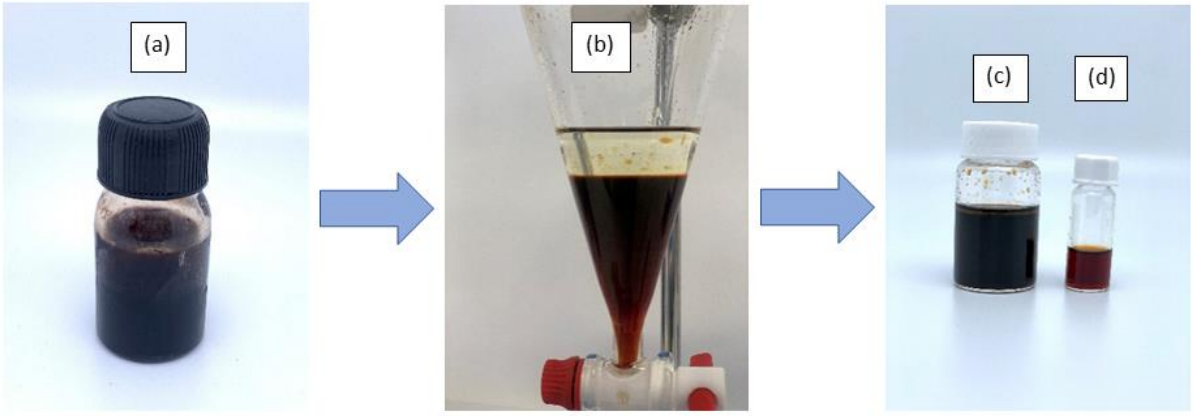

Figure 46: Pyrolysis liquid separation process, a) pyrolysis liquid, b) mixture of pyrolysis liquid and diethyl ether, c) aqueous phase, and d) extracted bio-oil

3.8. Characterization of the bio-oil

3.8.1. Fourier transform infrared spectroscopy (FTIR) spectra

FTIR spectra help detect and identify various functional groups and chemical bonds in bio-oil. The bands observed in the spectra exhibit varying intensities, which indicate the presence of different bonds and functional groups (Varma and Mondal, 2017). The intensity of the bands reflects the concentration or abundance of specific functional groups or bonds within the bio-oil sample. The

FTIR spectra analysis of the bio-oil of bagasse, cotton stalks, and kenaf bast fibers are illustrated in Fig. 47. The obtained curves demonstrated consistent or similar results among the pyrolysis oils containing phenols, alcohols, aldehydes, ketones, and other organic components.

Broad bands between 3600 to 3250 cm^{-1} corresponding to the O-H stretching vibration indicate the presence of alcohols and phenols in the bio-oil (W. Chen et al., 2016). The weak bands observed between 3100 and 2800 cm^{-1} correspond to C–H stretching vibrations, indicating alkanes (M. N. Islam et al., 1999). The bands between 1850 and 1580 cm^{-1} correspond to the C=O stretching vibrations, which show the presence of ketones or aldehydes (Boer et al., 2020; M. R. Islam et al., 2010). This region can also represent C=C stretching vibrations, which indicate alkenes and aromatics (M. K. Lee et al., 2010). The bands between 1500 and 1350 cm^{-1} correspond to the C-H and deformation vibrations (M. N. Islam et al., 1999; M. R. Islam et al., 2010). The presence of bands at around 1300 cm^{-1} can be attributed to primary, secondary, and tertiary alcohols and phenols. These bands arise from the C-O stretching vibrations and O-H deformations associated with these functional groups (Demiral et al., 2009). These functional groups may include esters, carboxylic acids, or ethers (Tsai et al., 2006).

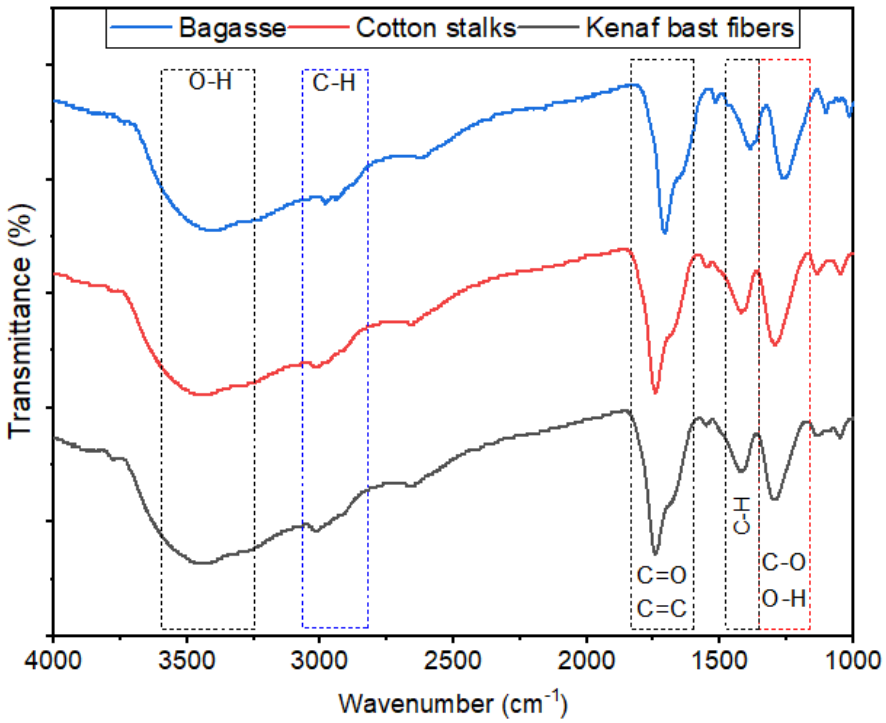

Figure 47: FTIR of pyrolysis oils from bagasse, cotton stalks, and kenaf bast fibers.

3.8.2. Gas chromatography-mass spectrometry (GC–MS)

The GC-MS analysis was performed to identify the chemical compounds in the bio-oils derived from bagasse, cotton stalks, and kenaf bast fibers. The results allowed for comparing the chemical compositions of the bio-oils obtained from these fibers. In Fig. 48, the GC-MS spectrum of the bio-oil typically displayed a plot showing the intensity (peak area) of the detected compounds as a function of their retention time. This provided a visual representation of the composition of the bio-oil and allowed for the identification and quantification of different chemical components. Tab. 17 illustrates a list of identified compounds present in the bio-oils, along with their corresponding percentage peak area, retention time, compound name, functional group, and molecular formula, was obtained. This analysis provided specific information about the compounds detected in the bio-oil samples.

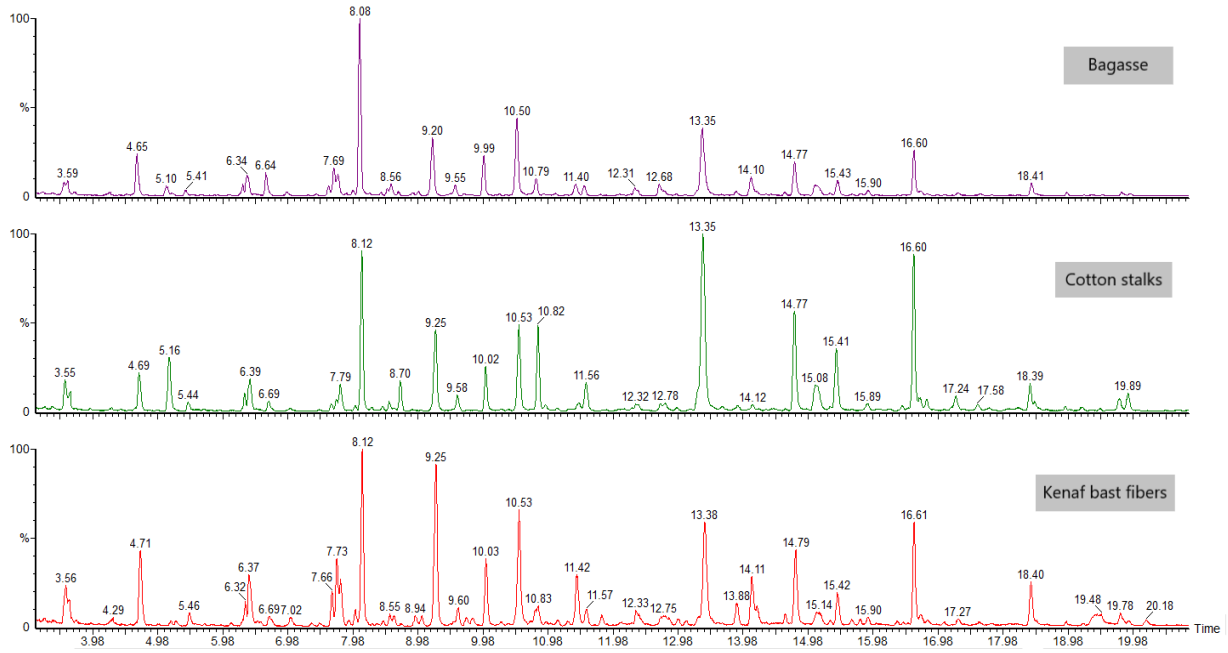

Figure 48: GC–MS curves of bagasse, cotton stalks, and kenaf bast fibers pyrolysis oil

The compounds present in the bio-oil derived from bagasse, cotton stalks, and kenaf bast fibers can be categorized into four main classes: phenols, ketones, aldehydes, and ethers. Phenols are the predominant class of compounds identified in the bio-oil (Barros et al., 2018b). In significant amounts, ketones, aldehydes, and others are also present. In addition to these major types, other minor compounds are identified in the bio-oil. These compounds belong to the classes of alcohols, acids, and an-hydro-sugars (Bertero et al., 2014). Although they may be present in smaller quantities compared to the major categories, their presence contributes to the overall composition

and characteristics of the bio-oil. According to previous work (Sun et al., 2011), the presence of alcohols, aldehydes, ketones, furfural, and furan in bio-oil is commonly observed. It can be attributed to the decomposition of biomass's cellulose and hemicellulose fractions during pyrolysis. On the other hand, aromatics, creosol, and phenol derivatives in bio-oil are attributed to the lignin degradation during the pyrolysis process (Yorgun and Yildiz, 2015). Phenol and its derivatives are crucial in manufacturing a wide range of products, contributing to industries such as textiles, plastics, adhesives, and automotive appliances (Varma and Mondal, 2017).

Table 17 presents the bio-oil compounds derived from bagasse, cotton stalks, and kenaf bast fibers, focusing on percentage areas above 0.40%. The table includes their names, molecular formulas, functional groups, peak areas, and retention times.

Table 17: Bio-oil compounds of bagasse, cotton stalks, and kenaf bast fibers, with their name, molecular formula, functional group, peak area, and retention time

Peak	Compound name	Formula	Functional group	Bagasse		Cotton stalks		Kenaf bast fibers	
				Area %	RT (min)	Area %	RT (min)	Area %	RT (min)
1	Phenol	C_6H_6O	P	15.85	8.08	8.19	8.12	8.3	8.12
2	Catechol	$C_6H_6O_2$	P	11.5	13.35	16.2	13.35	8.53	13.38
3	Phenol, 3-methyl-	C_7H_8O	P	9	10.5	5.28	10.53	7	10.53
4	3-Methylcyclopentane-1, 2-doine	$C_6H_8O_2$	K	6.8	9.2	5.28	9.25	9.32	9.25
5	Phenol, 2, 6-dimethoxy-	$C_8H_{10}O_3$	P	4.6	16.6	8.64	16.6	5.07	16.61
6	3-Cyclopentene-1-acetaldehyde, 2-oxo-	$C_7H_8O_2$	A	4.43	4.65	2.38	4.69	4.33	4.71
7	1, 2-Benzenediol, 4-methyl-	$C_7H_8O_2$	P	3.93	14.77	4.11	15.41	4.51	14.79
8	5-Hydroxymethylfurfural	$C_6H_6O_3$	F	2.86	14.1	-	-	2.96	14.11
9	2-Furancarboxaldehyde, 5-methyl-	$C_6H_6O_2$	F	2.58	7.69	0.52	7.73	2.89	7.73
10	2(5H) -Furanone	$C_4H_4O_2$	F	2.57	6.34	-	-	3.09	6.37
11	1, 2-Cyclopentanedione	$C_5H_6O_2$	K	2.29	6.64	-	-	-	-
12	Resorcinol monoacetate	$C_8H_8O_3$	HA	2.27	15.07	2.94	15.08	-	-
13	2-Cyclopenten-1-one, 3-methyl-	C_6H_8O	K	2.13	7.75	1.65	7.79	2.12	7.79
14	Phenol, 2-methoxy-	$C_7H_8O_2$	P	1.89	10.79	4.49	10.82	-	-
15	Maltol	$C_6H_6O_3$	P	1.64	11.4	0.72	11.46	3.21	11.42
16	3, 5-Dimethoxy-4-hydroxytoluene	$C_9H_{12}O_3$	P	1.63	18.41	1.59	18.39	2.69	18.4
17	Butanoic acid	$C_4H_8O_2$	AC	1.53	3.59	1.02	3.63	-	-
18	1, 4, 2, 5 Cyclohexanetetrol	$C_6H_{12}O_4$	AL	1.46	3.53	-	-	3.43	3.56
19	Phenol, 2, 5-dimethyl-	$C_8H_{10}O$	P	1.29	12.31	0.64	12.32	-	-
20	2-Cyclopenten-1-one, 2, 3-dimethyl-	$C_7H_{10}O$	K	1.25	9.55	0.97	9.58	1.11	9.6

21	2-Cyclopenten-1-one, 3-ethyl-2-hydroxy-	$C_7H_{10}O_2$	K	1.17	11.53	2.03	11.56	1.01	11.57
22	N-Butyl-tere-butylamine	$C_8H_{19}N$	N	1.15	8.56	-	-	-	-
23	2-Furanmethanol	$C_5H_6O_2$	F	1.09	5.1	3.43	5.16	-	-
24	2-Cyclopenten-1-one, 2-methyl-	C_6H_8O	K	0.85	6.28	0.75	6.31	0.98	6.32
25	2, 3-Pentanedione	$C_5H_8O_2$	K	0.83	7.61	-	-	1.42	7.66
26	1, 3-Benzenediol, 4, 5-dimethyl-	$C_8H_{10}O_2$	P	0.69	16.71	-	-	-	-
27	2-Propanone, 1-(acetyloxy)	$C_5H_8O_3$	C	0.62	5.41	0.58	5.44	0.71	5.46
28	2(5H) -Furanone, 5-methyl-	$C_5H_6O_2$	K	0.56	6.96	-	-	0.65	7.02
29	1, 4 : 3, 6-Dianhydro-α-d-glucopyranose	$C_6H_8O_4$	S	0.55	13.87	-	-	1.36	13.88
30	2-Pentanone, 1-(2 ,4, 6-trihydroxyphenyl)	$C_{11}H_{14}O_4$	P	0.5	23.68	-	-	-	-
31	Methylene chloride	CH_2CL_2	H	0.48	3.35	0.53	3.24	0.49	3.22
32	2-Butenoic acid	$C_4H_6O_2$	AC	0.48	4.23	-	-	-	-
33	1, 3-Benzenediol, 4-ethyl-	$C_8H_{10}O_2$	P	0.47	17.28	-	-	-	-
34	Benzene, 1, 2, 3-trimethoxy-5-methyl-	$C_{10}H_{14}O_3$	ET	0.46	19.79	0.99	19.76	1.01	19.78
35	1-Hydroxy-2-butanone	$C_4H_8O_2$	K	-	-	1.82	3.55	-	-
36	N-Cyano-2-methylpyrrolidine	$C_6H_{10}N_2$	N	-	-	2.18	6.39	-	-
37	2-Cyclopenten-1-one, 2-hydroxy-	$C_5H_6O_2$	K	-	-	0.65	6.69	0.65	6.69
38	3-Penten-2-one, 3, 4-dimethyl-	$C_7H_{12}O$	K	-	-	0.44	8.53	-	-
39	Furan-2-carbonyl chloride, tetrahydro-	$C_5H_7ClO_2$	F	-	-	1.49	8.7	-	-
40	Phenol, 2-methyl-	C_7H_8O	P	-	-	2.42	10.02	3.32	10.03
41	Cyclohexanone, 2-isopropyl-2, 5-dimethyl-	$C_{11}H_{20}O$	K	-	-	0.45	10.94	-	-
42	Phenol, 3, 4-dimethly-	$C_8H_{10}O$	P	-	-	0.66	12.78	-	-
43	Phenol, 2-(1-methylethoxy) -	$C_9H_{12}O_2$	P	-	-	0.44	14.12	-	-
44	1, 2-Benzenediol, 3-methoxy-	$C_7H_8O_3$	P	-	-	6.29	14.77	-	-
45	1, 4-Benzenediol, 2, 5-dimethyl-	$C_8H_{10}O_2$	P	-	-	0.84	16.68	-	-
46	1, 2-Benzenediol, 4-ethyl-	$C_8H_{10}O_2$	P	-	-	1.2	17.24	-	-
47	Benzaldehyde, 3-hydroxy-4-methoxy	$C_8H_8O_3$	A	-	-	0.49	17.58	-	-
48	2-Propanone, 1-(4-hydroxy-3-methoxyphenyl) -	$C_{10}H_{12}O_3$	P	-	-	1.21	19.89	-	-
49	1-(2, 6-dihydroxy-4-methoxphenyl) -1-butanone	$C_{11}H_{14}O_4$	P	-	-	0.85	23.61	-	-
50	Isocrotonic acid	C4H6O2	AC	-	-	-	-	0.59	4.29
51	2(5H) -Furanone, 3-methyl-	$C_5H_6O_2$	K	-	-	-	-	0.64	8.02
52	3-Hexen-2-one, 3-methyl-	$C_7H_{12}O$	K	-	-	-	-	0.45	8.55
53	1-Methyl-4-amino-4, 5(1H)-dihydro-1, 2, 4-triazole-5-one	$C_3H_6N_4O$	N	-	-	-	-	0.49	8.61
54	3, 4-Dihydro-6-methyl-2H-pyran-2-one	$C_6H_8O_2$	ES	-	-	-	-	0.61	8.94

55	2-Cyclohexen-1-one, 4, 4-dimethyl-	$C_8H_{12}O$	K	-	-	-	-	0.51	9.04
56	Heptane, 4-ethyl-	C_9H_{20}	HC	-	-	-	-	0.49	9.82
57	5-Octyn-4-one, 2, 2, 7, 7-tetramethyl-	$C_{12}H_{20}O$	K	-	-	-	-	1.77	10.83
58	Phenol, 2, 4-dimethly-	$C_8H_{10}O$	P	-	-	-	-	1.36	12.33
59	Phenol, 3-ethyl-	$C_8H_{10}O$	P	-	-	-	-	0.71	12.75
60	2, 3-Anhydro-d-mannosan	$C_6H_8O_4$	CH	-	-	-	-	1.04	14.19
61	1, 3-Dioxane-5-methanol, 5-ethyl-	$C_7H_{14}O_3$	ET	-	-	-	-	0.54	14.63
62	2-Cyclohexen-1-one, 5-methyl-2-(1-methylethyl) -	$C_{10}H_{16}O$	K	-	-	-	-	1.51	15.14
63	1, 2-Benzenediol, 4-methyl-	$C_7H_8O_2$	P	-	-	-	-	1.78	15.42
64	4-(2, 5-Dihydro-3-methoxyphenyl) butylamine	$C_{11}H_{19}NO$	N	-	-	-	-	0.5	15.9
65	1, 3-Benzenediol, 2, 5-dimethyl-	$C_8H_{10}O_2$	P	-	-	-	-	0.74	16.7
66	4-Ethylcatechol	$C_8H_{10}O_2$	P	-	-	-	-	0.48	17.27
67	β-D-Glucopyranose, 1, 6-anhydro	$C_6H_{10}O_5$	CH	-	-	-	-	1.39	19.42
68	4-O-Hexopyranosylhexose	$C_{12}H_{22}O_{11}$	CH	-	-	-	-	0.95	19.48
69	Melezitose	$C_{18}H_{32}O_{16}$	CH	-	-	-	-	0.44	20.18
70	Desaspidinol	$C_{11}H_{14}O_4$	P	-	-	-	-	1.77	23.61

where P: Phenol, K: Ketone, A: Aldehyde, F: Furan, HA: Hydroxyl and acetyl, AC: Acid, AL: Alcohol, N: Nitrogen content, C: Carbonyle, S: Sugar, H: Halogen atoms, ET: Ether, ES: Ester, HC: Hydrocarbon, and CH: Carbohydrate.

CHAPTER 4

CONCLUSION

4. Conclusion

Slow pyrolysis is an appealing technique for converting unstable biomass, such as sugarcane bagasse, cotton stalks, and kenaf bast fibers, into a stable, energy-rich product. This experimental investigation focused on the pyrolysis process of these fibers and aimed to identify the critical characteristics of the resulting biochar for potential bioenergy applications. Moreover, the study shed light on the composition and structure of the bio-oils obtained. The obtained biochar values for bagasse, cotton stalks, and kenaf bast fibers were consistent with previous literature reports. These biochars exhibited desirable properties for bioenergy applications, including low volatile and ash contents, high fixed carbon and carbon content, elevated H/C ratios, low O/C ratios, and increased heating values compared to earlier studies. The thermogravimetric analysis revealed a substantial increase in the degradation temperature of the biochars, indicating improved thermal stability and suitability for high-temperature applications. Among the studied fibers, kenaf bast fibers displayed the highest values for these properties, outperforming bagasse, and cotton stalks. This may be because the Kenaf fibers were retted the cleaned from any other parts such as the cortex. Furthermore, gas chromatography-mass spectrometry (GC-MS) analysis allowed identifying relevant bio-oil compounds. These compounds were classified into different classes, including phenols, ketones, aldehydes, furan, acids, carbohydrates, esters, ethers, alcohol, sugars, and nitrogen-containing compounds. This study indicated the potential and efficiency of bagasse, cotton stalks, and kenaf bast fibers in bioenergy production. The biochar derived from these fibers exhibited favorable properties, while the bio-oils demonstrated diverse compounds. These insights contribute to a better understanding of these biomass resources' energy applications and potential utilization.

Part V. Conclusion and perspective

CHAPTER 1

CONCLUSION AND PERSPECTIVE

1. Conclusions and perspectives

1.1. General conclusions

Utilizing biomass waste to produce biocomposite materials and bioenergy is a highly appealing option due to its abundance and cost-effectiveness, particularly regarding agricultural residue. Determining the potential applications of fibers requires critically analyzing their chemical and thermal properties. Chemical composition analysis of the three fibers was conducted according to the standards set by the Technical Association of the Pulp and Paper Industry (TAPPI). The Folin-Ciocalteu method was used to quantify total phenol content, while Fourier Transform Infrared Spectroscopy (FTIR) was utilized to evaluate light absorption by the bonds. To evaluate thermal stability and higher heating values, thermogravimetric analysis (TGA), differential scanning calorimetry (DSC), and bomb calorimetry were employed. The fibers under study exhibit enormous potential for biocomposite and bioenergy production, as evidenced by their chemical composition and thermal analysis. Bagasse boasts a cellulose content of 50.6% and a lignin content of 21.6%, kenaf bast fibers contain 58.5% cellulose and 10% lignin, while cotton stalks contain 40.3% cellulose and 21.3% lignin. TGA analysis reveals impressive degradation temperatures of 321°C for bagasse, 354°C for kenaf bast fibers, and 289°C for cotton stalks. DSC analysis reveals glass transition temperatures of 81°C for bagasse, 66.3°C for cotton stalks, and 64.5°C for kenaf bast fibers. The higher heating values, measured as 17.3 MJ/Kg, 16.6 MJ/Kg, and 17.1 MJ/Kg for bagasse, kenaf bast fibers, and cotton stalks, respectively, were remarkable.

Particleboard is a composite panel made from wood particles or other lignocellulosic materials, bonded with resin under heat and pressure to ensure a board with uniform texture and density suitable for various applications. In this study, particleboards were pressed using a pressing cycle of maximum pressure of 2.5 MPa, different pressing time durations of 480s, 240s, 120s, and 60s, and a pressing temperature of 180°C were used. The target density was 0.6 $g.cm^{-3}$. The panels were tested for their mechanical, physical, and thermal properties according to European standards EN (310), EN (317), and EN (12664). The study found that casein-based adhesive particleboards had higher mechanical properties and lower physical properties compared to tannin-based adhesives. Particleboards made from bagasse and cotton stalks with casein showed mechanical properties that exceeded EN standards. In contrast, kenaf bast fiber particleboards had lower mechanical and physical properties and did not meet standards. Tannin particleboards did not meet

European standards; however, the produced board is still suitable to be used as an insulator. Blended particleboards exhibited lower mechanical and physical properties compared to individual particleboards. Kenaf bast fiber lowered the bonding of particleboards when blended with bagasse and cotton stalks due to its low density and the large volume of the fibers which failed to be evenly covered by the adhesives. Thermal conductivities for individual and blended particleboards were below the EN standard. The study concluded that it is possible to produce low-cost, high-quality, and 100% green biocomposites for general applications, including furniture, interior fitments, and thermal insulation, from the three fibers studied. The production of foam using Acacia mimosa tannin has demonstrated favorable properties in comparison to existing literature. Conversely, outcomes obtained from extracted maritime pine bark, DRT Phénopin, and commercial maritime pine (Biolandes) were unsatisfactory, warranting further exploration and refinement in subsequent investigations.

Using biomass through slow pyrolysis is a promising method that can yield biochar and pyrolysis liquid, capable of energy densification and by-product valorization. Bagasse, cotton stalks, and kenaf bast fibers were pyrolyzed to produce biochar and pyrolysis liquid. The chosen pyrolysis parameters (temperature of 500°C with a heating rate of 10°C/min and a holding time of 60 minutes) generated biochars with favorable properties for bioenergy production. Cotton stalks had the highest biochar yield of 31.9% and 14% pyrolysis liquid, followed by bagasse with 28% biochar and 11.6% pyrolysis liquid, while, while Kenaf bast fibers had the lowest biochar yield at 22.9% and 11.1% pyrolysis liquid. The biochars underwent various analyses to determine their characteristics, including proximate analysis, ultimate analysis, higher heating value, and thermogravimetric analysis.

The fibers studied were compared to critical properties for energy applications, and it was found that their biochar properties were highly favorable. All biochars had remarkably low ash content, high carbon content, high H/C ratio, and low O/C ratio, making them ideal fuel sources with minimal impurities and excellent combustion properties. Among the studied biochars, kenaf bast fibers biochar exhibited the highest values of key properties for energy applications, making it the top choice. The higher heating value of the bagasse biochar increased by 57.8% of the raw bagasse, cotton stalks biochar increased by 43.5%, while the higher heating value of kenaf bast fibers increased by 55%. Biochars are capable of releasing significantly more energy than raw materials. The TG and DTG of the biochar driven from bagasse, cotton stalks, and kenaf bast fibers showed remarkable improvement with thermal stability and resistance to degradation, as the degradation temperature increased by 65.9%, 87.5%, and 76.1%, respectively, compared to the raw materials. It is worth noting that even at a pyrolysis temperature of 500°C, the biochar

exhibited only a relatively small portion of decomposition, meaning the biochar samples' structural integrity was preserved at the pyrolysis temperature.

The bio-oils were analyzed using FTIR and GC-MS to identify their composition. The FTIR spectra showed similar results for pyrolysis oils with phenols, alcohols, aldehydes, ketones, and other organic components. The GC-MS of the bio-oils from the three studied fibers showed many compounds such as phenol, ketone, furan, aldehyde, acid, nitrogen compounds, hydrocarbon, sugar, ester, and ether. The bio-oils from the three studied fibers contained similar compounds such as phenol, ketone, furan, aldehyde, acid, nitrogen compounds, hydrocarbon, sugar, ester, and ether.

1.2. Perspectives

Particleboard properties can be improved by adjusting density and particle size and by adding hydrophobic substances such as waxes. In addition, Optimizing the adhesive formulation is crucial to achieving the desired balance between mechanical and physical properties. Biomass for biofuels offers a wide range of uses in both domestic and the workplace and they are eco-friendly, sustainable and alternative to fossil fuels and its extensive use will benefit the entire planet due to their low cost and diverse applications. Before determining its potential uses, further research and analysis are necessary to understand bio-oil characteristics, such as its elevated acidity, poor stability, and substantial water content. Future research concerns should consider the pyrolysis of blended fibers or other biomass such as footstalks as an effective way of recycling. Attention should also be paid to the particle size, catalysts, and other factors that could improve the yield and qualities of bio-oil.

PUBLICATIONS AND CONGRESS

Publications

1. Wadah Mohammed, Zeinab Osman, Salah Elarabi, Bertrand Charrier "A Comprehensive Analysis of the Thermo-chemical Properties of Sudanese Biomass for Sustainable Applications". *Journal of Renewable Materials*, 2023.
2. **Communication in National Congress**
   a) Participation in the 8th annual meeting of Groupe de Recherche en science du Bois (GDR) 3544 – Epinal, 18-20 November 2019 - Oral presentation + Poster.
   b) Participation in the 9th annual meeting of Groupe de Recherche en science du Bois GDR 3544 – Grenoble, 18-20 November 2020 - Oral presentation + Poster.
   c) Participation in the National Congress of Research in CNRIUT'2021 – Lyon, 3-4 June 2021 - Oral presentation + Poster.

References

(BMBF), B. für B. und F., Fraunhofer-Gesellschaft, (LBF), F.-I. für B. und S., & Aachen, I. für T. (ITA)-R. (2018). Reinforcing plastics with renewable raw materials Less moisture in natural fibers. *Fraunhofer*, *February*, 1–3. https://www.fraunhofer.de/content/dam/zv/en/press-media/2018/February/ResearchNews/rn02_2018_LBF_Less moisture in natural fibers.pdf

Ab Karim, W. A. W., Moghadam, R. A., Mohd Salleh, M. A., & Alias, A. B. (2010). Air gasification of malaysia agricultural waste in a fluidised bed gasifier. *World Review of Science, Technology and Sustainable Development*, *8*(2–4), 100–113. https://doi.org/10.1504/WRSTSD.2011.044210

Abd El-Sayed, E. S., El-Sakhawy, M., Kamel, S., El-Gendy, A., & Abou-Zeid, R. E. (2019). Eco-friendly mimosa tannin adhesive system for bagasse particleboard fabrication. *Egyptian Journal of Chemistry*, *62*(5), 1177–1187. https://doi.org/10.21608/EJCHEM.2018.5413.1479

Adefris Legesse, A., Desalegn, D., Selvaraj, S. K., Paramasivam, V., & Chadha, U. (2022). Experimental Investigation of Sorghum Stalk and Sugarcane Bagasse Hybrid Composite for Particleboard. *Advances in Materials Science and Engineering*, *2022*. https://doi.org/10.1155/2022/1844004

Agblevor, F. A., & Besler, S. (1996). Inorganic compounds in biomass feedstocks. 1. Effect on the quality of fast pyrolysis oils. *Energy and Fuels*, *10*(2), 293–298. https://doi.org/10.1021/ef950202u

Aisien, F. A., Amenaghawon, A. N., & Bienose, K. C. (2015). Particle boards produced from cassava stalks: Evaluation of physical and mechanical properties. *South African Journal of Science*, *111*(5–6). https://doi.org/10.17159/sajs.2015/20140042

Ajala, E. O., Ighalo, J. O., Ajala, M. A., Adeniyi, A. G., & Ayanshola, A. M. (2021). Sugarcane bagasse: a biomass sufficiently applied for improving global energy, environment and economic sustainability. *Bioresources and Bioprocessing*, *8*(1). https://doi.org/10.1186/s40643-021-00440-z

Al Faruque, M. A., Salauddin, M., Raihan, M. M., Chowdhury, I. Z., Ahmed, F., & Shimo, S. S. (2022). Bast Fiber Reinforced Green Polymer Composites: A Review on Their Classification, Properties, and Applications. *Journal of Natural Fibers*, *19*(14), 8006–8021. https://doi.org/10.1080/15440478.2021.1958431

Amel, B. A., Paridah, M. T., Sudin, R., Anwar, U. M. K., & Hussein, A. S. (2013). Effect of fiber extraction methods on some properties of kenaf bast fiber. *Industrial Crops and Products*, *46*, 117–123. https://doi.org/10.1016/j.indcrop.2012.12.015

Archanowicz, E., Kowaluk, G., Niedzinski, W., & Beer, P. (2013). Properties of particleboards made of biocomponents from fibrous chips for FEM modeling. *BioResources*, *8*(4), 6220–6230. https://doi.org/10.15376/biores.8.4.6220-6230

Aristri, M. A., Lubis, M. A. R., Laksana, R. P. B., Sari, R. K., Iswanto, A. H., Kristak, L., Antov, P., & Pizzi, A. (2022). Thermal and mechanical performance of ramie fibers modified with polyurethane resins derived from acacia mangium bark tannin. *Journal of Materials Research and Technology*, *18*, 2413–2427. https://doi.org/10.1016/j.jmrt.2022.03.131

Ayrilmis, N., Kwon, J. H., & Han, T. H. (2012). Effect of resin type and content on properties of composite particleboard made of a mixture of wood and rice husk. *International Journal of Adhesion and Adhesives*, *38*, 79–83. https://doi.org/10.1016/j.ijadhadh.2012.04.008

Bacigalupe, A., & Escobar, M. M. (2021). Soy Protein Adhesives for Particleboard Production – A Review. *Journal of Polymers and the Environment*, *29*(7), 2033–2045. https://doi.org/10.1007/s10924-020-02036-8

Barros, J. A. S., Krause, M. C., Lazzari, E., Bjerk, T. R., do Amaral, A. L., Caramão, E. B., & Krause, L. C. (2018a). Chromatographic characterization of bio-oils from fast pyrolysis of sugar cane residues (straw and bagasse) from four genotypes of the Saccharum Complex. *Microchemical Journal*, *137*, 30–36. https://doi.org/10.1016/j.microc.2017.09.015

Barros, J. A. S., Krause, M. C., Lazzari, E., Bjerk, T. R., do Amaral, A. L., Caramão, E. B., & Krause, L. C. (2018b). Chromatographic characterization of bio-oils from fast pyrolysis of sugar cane residues (straw and bagasse) from four genotypes of the Saccharum Complex. *Microchemical Journal*, *137*, 30–36. https://doi.org/10.1016/j.microc.2017.09.015

Basso, M. C., Pizzi, A., Lacoste, C., Delmotte, L., Al-Marzouki, F. M., Abdalla, S., & Celzard, A. (2014). MALDI-TOF and 13C NMR analysis of tannin-furanic-polyurethane foams adapted for industrial continuous lines application. *Polymers*, *6*(12), 2985–3004. https://doi.org/10.3390/polym6122985

Batstone, D. (2021). *Sugarcane and the Creation of Carbon - Negative Hydrogen ought Leaders*. 1–5.

Becidan, M., Skreiberg, Ø., & Hustad, J. E. (2007). Products distribution and gas release in pyrolysis of thermally thick biomass residues samples. *Journal of Analytical and Applied Pyrolysis*, *78*(1), 207–213. https://doi.org/10.1016/j.jaap.2006.07.002

Bertero, M., Gorostegui, H. A., Orrabalis, C. J., Guzmán, C. A., Calandri, E. L., & Sedran, U. (2014). Characterization of the liquid products in the pyrolysis of residual chañar and palm fruit biomasses. *Fuel*, *116*, 409–414. https://doi.org/10.1016/j.fuel.2013.08.027

Bhattacharya, A., Sood, P., & Citovsky, V. (2010). The roles of plant phenolics in defence and communication during Agrobacterium and Rhizobium infection. *Molecular Plant Pathology*, *11*(5), 705–719. https://doi.org/10.1111/j.1364-3703.2010.00625.x

Bikoro Bi Athomo, A., Engozogho Anris, S. P., Safou-Tchiama, R., Santiago-Medina, F. J., Cabaret, T., Pizzi, A., & Charrier, B. (2018). Chemical composition of African mahogany (K. ivorensis A. Chev) extractive and tannin structures of the bark by MALDI-TOF. *Industrial Crops and Products*, *113*(July 2017), 167–178. https://doi.org/10.1016/j.indcrop.2018.01.013

Bledzki, A. K., Franciszczak, P., Osman, Z., & Elbadawi, M. (2015). Polypropylene biocomposites reinforced with softwood, abaca, jute, and kenaf fibers. *Industrial Crops and Products*, *70*, 91–99. https://doi.org/10.1016/j.indcrop.2015.03.013

Bledzki, A. K., & Gassan, J. (1999). Composites reinforced with cellulose based fibres. *Progress in Polymer Science*, *24*, 221–274. http://ac.els-cdn.com/S0079670098000185/1-s2.0-S0079670098000185-main.pdf?_tid=af34542c-0260-11e7-a49c-

00000aab0f27&acdnat=1488800173_c95596c7ddcc4673fe88c8ec84262bb9

Boer, F. D., Valette, J., Commandré, J. M., Fournier, M., & Thévenon, M. F. (2020). Slow pyrolysis of sugarcane bagasse for the production of char and the potential of its by-product for wood protection. *Journal of Renewable Materials*, *9*(1), 97–117. https://doi.org/10.32604/jrm.2021.013147

Bonawitz, N. D., & Chapple, C. (2010). The genetics of lignin biosynthesis: Connecting genotype to phenotype. *Annual Review of Genetics*, *44*, 337–363. https://doi.org/10.1146/annurev-genet-102209-163508

Boumanchar, I., Chhiti, Y., M'hamdi Alaoui, F. E., El Ouinani, A., Sahibed-Dine, A., Bentiss, F., Jama, C., & Bensitel, M. (2017). Effect of materials mixture on the higher heating value: Case of biomass, biochar and municipal solid waste. *Waste Management*, *61*, 78–86. https://doi.org/10.1016/j.wasman.2016.11.012

Boussetta, A., Benhamou, A. A., Charii, H., Ablouh, E. H., Mennani, M., Kasbaji, M., Boussetta, N., Grimi, N., & Moubarik, A. (2023). Formulation and Characterization of Chitin-Starch Bio-Based Wood Adhesive for the Manufacturing of Formaldehyde-Free Composite Particleboards. *Waste and Biomass Valorization*, *February*. https://doi.org/10.1007/s12649-023-02091-x

Boussetta, A., Benhamou, A. A., Ihammi, A., Ablouh, E. H., Barba, F. J., Boussetta, N., Grimi, N., & Moubarik, A. (2022). Shrimp waste protein for bio-composite manufacturing: Formulation of protein-cornstarch-mimosa-tannin wood adhesives. *Industrial Crops and Products*, *187*(PA), 115323. https://doi.org/10.1016/j.indcrop.2022.115323

Bridgwater, A. V., Carson, P., & Coulson, M. (2007). A comparison of fast and slow pyrolysis liquids from mallee. *International Journal of Global Energy Issues*, *27*(2), 204–216. https://doi.org/10.1504/IJGEI.2007.013655

Brito, F. M. S., & Bortoletto, G. (2020). Properties of particleboards manufactured from bamboo (Dendrocalamus asper). *Revista Brasileirade Ciencias Agrarias*, *15*(1), 1–10. https://doi.org/10.5039/AGRARIA.V15I1A7245

Brito, F. M. S., Júnior, G. B., & Surdi, P. G. (2021). Properties of particleboards made from sugarcane bagasse particles. *Revista Brasileirade Ciencias Agrarias*, *16*(1). https://doi.org/10.5039/AGRARIA.V16I1A8783

Cai, J., He, Y., Yu, X., Banks, S. W., Yang, Y., Zhang, X., Yu, Y., Liu, R., & Bridgwater, A. V. (2017). Review of physicochemical properties and analytical characterization of lignocellulosic biomass. *Renewable and Sustainable Energy Reviews*, *76*(October 2016), 309–322. https://doi.org/10.1016/j.rser.2017.03.072

Caillat, S., & Vakkilainen, E. (2013). Large-scale biomass combustion plants: An overview. In *Biomass Combustion Science, Technology and Engineering*. Woodhead Publishing Limited. https://doi.org/10.1533/9780857097439.3.189

Candido, R. G., & Gonçalves, A. R. (2019). Evaluation of two different applications for cellulose isolated from sugarcane bagasse in a biorefinery concept. *Industrial Crops and Products*, *142*. https://doi.org/10.1016/j.indcrop.2019.111616

Carrier, M., Hugo, T., Gorgens, J., & Knoetze, H. (2011). Comparison of slow and vacuum pyrolysis of sugar cane bagasse. *Journal of Analytical and Applied Pyrolysis*, *90*(1), 18–26. https://doi.org/10.1016/j.jaap.2010.10.001

Cesprini, E., Causin, V., De Iseppi, A., Zanetti, M., Marangon, M., Barbu, M. C., & Tondi, G. (2022). Renewable Tannin-Based Adhesive from Quebracho Extract and Furfural for Particleboards. *Forests*, *13*(11). https://doi.org/10.3390/f13111781

Chae, J. S., Kim, S. W., & Ohm, T. I. (2020). Combustion characteristics of solid refuse fuels from different waste sources. *Journal of Renewable Materials*, *8*(7), 789–799. https://doi.org/10.32604/jrm.2020.010023

Chakraborty, S., Kundu, S. P., Roy, A., Adhikari, B., & Majumder, S. B. (2013). Effect of jute as fiber reinforcement controlling the hydration characteristics of cement matrix. *Industrial and Engineering Chemistry Research*, *52*(3), 1252–1260. https://doi.org/10.1021/ie300607r

Chen, D., Cen, K., Zhuang, X., Gan, Z., Zhou, J., Zhang, Y., & Zhang, H. (2022). Insight into biomass pyrolysis mechanism based on cellulose, hemicellulose, and lignin: Evolution of volatiles and kinetics, elucidation of reaction pathways, and characterization of gas, biochar and bio-oil. *Combustion and Flame*, *242*(August 2022). https://doi.org/10.1016/j.combustflame.2022.112142

Chen, H., Liu, N., & Fan, W. (2006). Two-Step consecutive reaction model and kinetic parameters relevant to the decomposition of Chinese forest fuels. *Journal of Applied Polymer Science*, *102*(1), 571–576. https://doi.org/10.1002/app.24310

Chen, M. yi, Cheng, Y. ping, Li, H. ran, Wang, L., Jin, K., & Dong, J. (2018). Impact of inherent moisture on the methane adsorption characteristics of coals with various degrees of metamorphism. *Journal of Natural Gas Science and Engineering*, *55*(December 2017), 312–320. https://doi.org/10.1016/j.jngse.2018.05.018

Chen, W., Shi, S., Zhang, J., Chen, M., & Zhou, X. (2016). Co-pyrolysis of waste newspaper with high-density polyethylene: Synergistic effect and oil characterization. *Energy Conversion and Management*, *112*, 41–48. https://doi.org/10.1016/j.enconman.2016.01.005

Chen, X., Liu, H., Xia, N., Shang, J., Tran, V. C., & Guo, K. (2015). Preparation and properties of oriented cotton stalk board with konjac glucomannan-chitosan-polyvinyl alcohol blend adhesive. *BioResources*, *10*(2), 3736–3748. https://doi.org/10.15376/biores.10.2.3736-3748

Chiang, T. C., Osman, M. S., & Hamdan, S. (2014). Water Absorption and Thickness Swelling Behavior of Sago Particles Urea Formaldehyde Particleboard. *International Journal of Science and Research (IJSR)*, *3*(12), 1375–1379. https://www.ijsr.net/archive/v3i12/U1VCMTQ2Nzg=.pdf

Coletti, F., Romani, M., Ceres, G., Zammit, U., & Guidi, M. C. (2021). Evaluation of microscopy techniques and ATR-FTIR spectroscopy on textile fibers from the Vesuvian area: A pilot study on degradation processes that prevent the characterization of bast fibers. *Journal of Archaeological Science: Reports*, *36*(December 2020), 102794. https://doi.org/10.1016/j.jasrep.2021.102794

Cordeiro, L. G., El-Aouar, Â. A., & De Araújo, C. V. B. (2013). Energetic characterization of malt

bagasse by calorimetry and thermal analysis. *Journal of Thermal Analysis and Calorimetry*, *112*(2), 713–717. https://doi.org/10.1007/s10973-012-2630-x

Corrêa, A. C., de Teixeira, E. M., Pessan, L. A., & Mattoso, L. H. C. (2010). Cellulose nanofibers from curaua fibers. *Cellulose*, *17*(6), 1183–1192. https://doi.org/10.1007/s10570-010-9453-3

Czernik, S., & Bridgwater, A. V. (2004). Overview of applications of biomass fast pyrolysis oil. *Energy and Fuels*, *18*(2), 590–598. https://doi.org/10.1021/ef034067u

Dahmardeh Ghalehno, M., Nazerian, M., & Bayatkashkooli, A. (2011). Influence of utilization of bagasse in surface layer on bending strength of three-layer particleboard. *European Journal of Wood and Wood Products*, *69*(4), 533–535. https://doi.org/10.1007/s00107-010-0441-y

Dahou, T., Defoort, F., Khiari, B., Labaki, M., Dupont, C., & Jeguirim, M. (2021). Role of inorganics on the biomass char gasification reactivity: A review involving reaction mechanisms and kinetics models. In *Renewable and Sustainable Energy Reviews* (Vol. 135). https://doi.org/10.1016/j.rser.2020.110136

Danso-Boateng, E., & Achaw, O. W. (2022). Bioenergy and biofuel production from biomass using thermochemical conversions technologies—a review. In *AIMS Energy* (Vol. 10, Issue 4). https://doi.org/10.3934/energy.2022030

Davis, K., & Moon, T. S. (2020). Tailoring microbes to upgrade lignin. *Current Opinion in Chemical Biology*, *59*, 23–29. https://doi.org/10.1016/j.cbpa.2020.04.001

De Almeida, A. C., De Araujo, V. A., Morales, E. A. M., Gava, M., Munis, R. A., Garcia, J. N., & Cortez-Barbosa, J. (2017). Wood-bamboo particleboard: Mechanical properties. *BioResources*, *12*(4), 7784–7792. https://doi.org/10.15376/biores.12.4.7784-7792

de Galiza Barbosa, F., Galgano, S. J., Botwin, A. L., Lara Gongora, A. B., Sawaya, G., Baroni, R. H., & Queiroz, M. A. (2022). Genitourinary imaging. In *Clinical PET/MRI* (pp. 289–312). https://doi.org/10.1016/B978-0-323-88537-9.00012-X

Demiral, I., Atilgan, N. G., & Şensöz, S. (2009). Production of biofuel from soft shell of pistachio (Pistacia vera L.). *Chemical Engineering Communications*, *196*(1–2), 104–115. https://doi.org/10.1080/00986440802300984

Demirbas, A. (2007). Effects of moisture and hydrogen content on the heating value of fuels. *Energy Sources, Part A: Recovery, Utilization and Environmental Effects*, *29*(7), 649–655. https://doi.org/10.1080/009083190957801

Demirbaş, A., & Demirbaş, A. H. (2004). Estimating the calorific values of lignocellulosic fuels. *Energy Exploration and Exploitation*, *22*(2), 135–143. https://doi.org/10.1260/0144598041475198

Dhyani, V., & Bhaskar, T. (2018). A comprehensive review on the pyrolysis of lignocellulosic biomass. *Renewable Energy*, *129*, 695–716. https://doi.org/10.1016/j.renene.2017.04.035

Dobariya, U. D., Gojiya, D. K., Makavana, J. M., Kelaiya, S. V., Gadhiya, G. A., Dulawat, M. S., Vaja, K. G., & Chauhan, P. M. (2022). Influence of Temperature on the Production of Biochar from Cotton and Castor Feed Stalk in a Pyrolysis Process. *Current World Environment*, *17*(3), 634–642. https://doi.org/10.12944/cwe.17.3.12

Dziike, F., Linganiso, L. Z., Mpongwana, N., & Legodi, L. M. (2022). Biomass conversion into recyclable strong materials. *South African Journal of Science*, *118*(7/8). https://doi.org/10.17159/sajs.2022/9747

Ebnesajjad, S., & Landrock, A. H. (2015). Characteristics of Adhesive Materials. In *Adhesives Technology Handbook*. https://doi.org/10.1016/b978-0-323-35595-7.00005-x

Edreis, E. M. A., Li, X., Xu, C., & Yao, H. (2017). Kinetic study and synergistic interactions on catalytic CO2 gasification of Sudanese lower sulphur petroleum coke and sugar cane bagasse. *Journal of Materials Research and Technology*, *6*(2), 147–157. https://doi.org/10.1016/j.jmrt.2016.09.001

Edreis, E. M. A., Luo, G., & Yao, H. (2014). Investigations of the structure and thermal kinetic analysis of sugarcane bagasse char during non-isothermal CO 2 gasification. *Journal of Analytical and Applied Pyrolysis*, *107*, 107–115. https://doi.org/10.1016/j.jaap.2014.02.010

El Hajj, N., Dheilly, R. M., Goullieux, A., Aboura, Z., Benzeggagh, M. L., & Quéneudec, M. (2012). Innovant agromaterials formulated with flax shaves and proteinic binder: Process and characterization. *Composites Part B: Engineering*, *43*(2), 381–390. https://doi.org/10.1016/j.compositesb.2011.05.022

Elbadawi, M., Osman, Z., Paridah, T., Nasroun, T., & Kantiner, W. (2015). Properties of particleboards made from acacia seyal var. seyal using uf-tannin modified adhesives. *Cellulose Chemistry and Technology*, *49*(3–4), 369–374.

Ellatif Ahmed Habib, E. A. (2014). The usage of the Sugarcane Bagasse Ash in Sudanese Sugar Company as Pozzolanic-Cement Binder. *IOSR Journal of Engineering*, *4*(4), 54–60. https://doi.org/10.9790/3021-04435460

Engozogho Anris, S. P., Bikoro Bi Athomo, A., Safou-Tchiama, R., Leroyer, L., Vidal, M., & Charrier, B. (2021). Development of green adhesives for fiberboard manufacturing, using okoume bark tannins and hexamine–characterization by 1H NMR, TMA, TGA and DSC analysis. *Journal of Adhesion Science and Technology*, *35*(4), 436–449. https://doi.org/10.1080/01694243.2020.1808356

Farag, E., Alshebani, M., Elhrari, W., Klash, A., & Shebani, A. (2020). Production of particleboard using olive stone waste for interior design. *Journal of Building Engineering*, *29*(December). https://doi.org/10.1016/j.jobe.2019.101119

Ferdosian, F., Pan, Z., Gao, G., & Zhao, B. (2017). Bio-based adhesives and evaluation for wood composites application. *Polymers*, *9*(2). https://doi.org/10.3390/polym9020070

Ferreira, A. F. (2017). Biorefinery concept. *Lecture Notes in Energy*, *57*, 1–20. https://doi.org/10.1007/978-3-319-48288-0_1

Fertilizers, G. (2021). Catalysis for Clean Energy and Environmental Sustainability. In *Catalysis for Clean Energy and Environmental Sustainability* (Issue April). https://doi.org/10.1007/978-3-030-65017-9

Flores, H., Mentado, J., Amador, P., Torres, L. A., Campos, M., & Rojas, A. (2006). Redesigning the rotating-bomb combustion calorimeter. *Journal of Chemical Thermodynamics*, *38*(6), 756–759. https://doi.org/10.1016/j.jct.2005.08.008

Gabrielii, I., Gatenholm, P., Glasser, W. G., Jain, R. K., & Kenne, L. (2000). Separation, characterization and hydrogel-formation of hemicellulose from aspen wood. *Carbohydrate Polymers*, *43*(4), 367–374. https://doi.org/10.1016/S0144-8617(00)00181-8

Gaunt, J. L., & Lehmann, J. (2008). Energy balance and emissions associated with biochar sequestration and pyrolysis bioenergy production. *Environmental Science and Technology*, *42*(11), 4152–4158. https://doi.org/10.1021/es071361i

Gaur, R., Soam, S., Sharma, S., Gupta, R. P., Bansal, V. R., Kumar, R., & Tuli, D. K. (2016). Bench scale dilute acid pretreatment optimization for producing fermentable sugars from cotton stalk and physicochemical characterization. *Industrial Crops and Products*, *83*, 104–112. https://doi.org/10.1016/j.indcrop.2015.11.056

Ghahri, S., & Pizzi, A. (2018). Improving soy-based adhesives for wood particleboard by tannins addition. *Wood Science and Technology*, *52*(1), 261–279. https://doi.org/10.1007/s00226-017-0957-y

Ghysels, S., Ronsse, F., Dickinson, D., & Prins, W. (2019). Production and characterization of slow pyrolysis biochar from lignin-rich digested stillage from lignocellulosic ethanol production. *Biomass and Bioenergy*, *122*(January 2018), 349–360. https://doi.org/10.1016/j.biombioe.2019.01.040

Gisip, J. (2023). Effects of Resin Content on Mechanical and Physical Properties of Treated Kenaf Particleboard. *Scientific Research Journal*, *September 2022*. https://doi.org/10.24191/srj.v19i2.17580

Glushkov, D., Nyashina, G., Shvets, A., Pereira, A., & Ramanathan, A. (2021). Current status of the pyrolysis and gasification mechanism of biomass. *Energies*, *14*(22). https://doi.org/10.3390/en14227541

Gonçalves, F. A., Ruiz, H. A., Silvino dos Santos, E., Teixeira, J. A., & de Macedo, G. R. (2016). Bioethanol production by Saccharomyces cerevisiae, Pichia stipitis and Zymomonas mobilis from delignified coconut fibre mature and lignin extraction according to biorefinery concept. *Renewable Energy*, *94*, 353–365. https://doi.org/10.1016/j.renene.2016.03.045

Grigoriou, A., Passialis, C., & Voulgaridis, E. (2000). Kenaf core and bast fiber chips as raw material in production of one-layer experimental particleboards. *Holz Als Roh - Und Werkstoff*, *58*(4), 290–291. https://doi.org/10.1007/s001070050429

Guillou, J., Lavadiya, D. N., Munro, T., Fronk, T., & Ban, H. (2018). From lignocellulose to biocomposite: Multi-level modelling and experimental investigation of the thermal properties of kenaf fiber reinforced composites based on constituent materials. *Applied Thermal Engineering*, *128*, 1372–1381. https://doi.org/10.1016/j.applthermaleng.2017.09.095

Güleç, F., Şimşek, E. H., & Tanıker Sarı, H. (2022). Prediction of Biomass Pyrolysis Mechanisms and Kinetics: Application of the Kalman Filter. *Chemical Engineering and Technology*, *45*(1), 167–177. https://doi.org/10.1002/ceat.202100229

Guler, C., & Ozen, R. (2004). Some properties of particleboards made from cotton stalks (Gossypium hirsitum L.). *Holz Als Roh - Und Werkstoff*, *62*(1), 40–43. https://doi.org/10.1007/s00107-003-0439-9

Gumowska, A., Robles, E., & Kowaluk, G. (2021). Evaluation of functional features of lignocellulosic particle composites containing biopolymer binders. In *Materials* (Vol. 14, Issue 24). https://doi.org/10.3390/ma14247718

Guo, A., Sun, Z., & Satyavolu, J. (2019a). Impact of chemical treatment on the physiochemical and mechanical properties of kenaf fibers. *Industrial Crops and Products*, *141*. https://doi.org/10.1016/j.indcrop.2019.111726

Guo, A., Sun, Z., & Satyavolu, J. (2019b). Impact of chemical treatment on the physiochemical and mechanical properties of kenaf fibers. *Industrial Crops and Products*, *141*(March), 111726. https://doi.org/10.1016/j.indcrop.2019.111726

Guo, M., & Wang, G. (2016a). Milk protein polymer and its application in environmentally safe adhesives. *Polymers*, *8*(9). https://doi.org/10.3390/polym8090324

Guo, M., & Wang, G. (2016b). Whey protein polymerisation and its applications in environmentally safe adhesives. *International Journal of Dairy Technology*, *69*(4), 481–488. https://doi.org/10.1111/1471-0307.12303

Gupta, A., Thengane, S. K., & Mahajani, S. (2020). Kinetics of pyrolysis and gasification of cotton stalk in the central parts of India. *Fuel*, *263*(December 2019), 116752. https://doi.org/10.1016/j.fuel.2019.116752

Gupta, G. K., & Mondal, M. K. (2019). Bioenergy generation from agricultural wastes and enrichment of end products. In *Refining Biomass Residues for Sustainable Energy and Bioproducts: Technology, Advances, Life Cycle Assessment, and Economics*. Elsevier Inc. https://doi.org/10.1016/B978-0-12-818996-2.00015-6

Hajihassani, R., Gerami, M., Salehi, K., & Ghahri, S. (2022). *The potential of utilizing hemp-core fibers in particleboard industry*. *October*. https://doi.org/10.22069/JWFST.2022.20477.1977

Halip, J. A., Hua, L. S., Md. Tahir, P., Al Edrus, S. S., Md Ishak, S. M., Selimin, M. A., & Ab Hamid, A. A. R. (2019). Kenaf and Kenaf-rubberwood hybrid particleboards. *International Journal of Recent Technology and Engineering*, *8*(2 Special Issue 4), 464–468. https://doi.org/10.35940/ijrte.B1090.0782S419

Halvarsson, S., Edlund, H., & Norgren, M. (2009). Manufacture of non-resin wheat straw fibreboards. *Industrial Crops and Products*, *29*(2–3), 437–445. https://doi.org/10.1016/j.indcrop.2008.08.007

Hamidon, M. H., Sultan, M. T. H., Ariffin, A. H., & Shah, A. U. M. (2019). Effects of fibre treatment on mechanical properties of kenaf fibre reinforced composites: A review. In *Journal of Materials Research and Technology* (Vol. 8, Issue 3, pp. 3327–3337). https://doi.org/10.1016/j.jmrt.2019.04.012

Hamza, S., Saad, H., Charrier, B., Ayed, N., & Charrier-El Bouhtoury, F. (2013). Physico-chemical characterization of Tunisian plant fibers and its utilization as reinforcement for plaster based composites. *Industrial Crops and Products*, *49*, 357–365. https://doi.org/10.1016/j.indcrop.2013.04.052

Harussani, M. M., & Sapuan, S. M. (2022). Development of Kenaf Biochar in Engineering and Agricultural Applications. *Chemistry Africa*, *5*(1). https://doi.org/10.1007/s42250-021-

00293-1

He, Y. (2005). Rapid thermal conductivity measurement with a hot disk sensor: Part 2. Characterization of thermal greases. *Thermochimica Acta*, *436*(1–2), 130–134. https://doi.org/10.1016/j.tca.2005.07.003

He, Y., Chen, S., & Chen, M. (2020). Study on Screw-holding Ability of Three Screw Connections in Medium Density Fiberboard Components. *IOP Conference Series: Materials Science and Engineering*, *782*(2). https://doi.org/10.1088/1757-899X/782/2/022089

Herzog, A., Kerschbaumer, T., Schwarzenbrunner, R., Barbu, M. C., Petutschnigg, A., & Tudor, E. M. (2021). Efficiency of high-frequency pressing of spruce laminated timber bonded with casein adhesives. *Polymers*, *13*(23). https://doi.org/10.3390/polym13234237

Holt, G. A., Chow, P., Wanjura, J. D., Pelletier, M. G., & Wedegaertner, T. C. (2014). Evaluation of thermal treatments to improve physical and mechanical properties of bio-composites made from cotton byproducts and other agricultural fibers. *Industrial Crops and Products*, *52*, 627–632. https://doi.org/10.1016/j.indcrop.2013.11.003

Hou, X., Sun, F., Yan, D., Xu, H., Dong, Z., Li, Q., & Yang, Y. (2014). Preparation of lightweight polypropylene composites reinforced by cotton stalk fibers from combined steam flash-explosion and alkaline treatment. *Journal of Cleaner Production*, *83*, 454–462. https://doi.org/10.1016/j.jclepro.2014.07.018

Hua, L. S., Chen, L. W., Geng, B. J., Kristak, L., Antov, P., Pędzik, M., Rogoziński, T., Taghiyari, H. R., Rahandi Lubis, M. A., Fatriasari, W., Yadav, S. M., Chotikhun, A., & Pizzi, A. (2022). Particleboard from Agricultural Biomass and Recycled Wood Waste: A Review. *Journal of Materials Research and Technology*, 100310. https://doi.org/10.1016/j.jmrt.2022.08.166

Ibrahim, T. (2020). *Assessment of the Sudane Ses ' Sugar Industry Life Cycle and Technical Factors Influencing the Productivity*. *October*.

Ighalo, J. O., & Adeniyi, A. G. (2021). Modelling the Valorisation of Cassava Peel (Manihot esculenta) Waste Via Pyrolysis and in-Line Steam Reforming. *Environmental Processes*, *8*(1), 267–285. https://doi.org/10.1007/s40710-020-00486-9

Iliopoulou, E. F., Antonakou, E. V., Karakoulia, S. A., Vasalos, I. A., Lappas, A. A., & Triantafyllidis, K. S. (2007). Catalytic conversion of biomass pyrolysis products by mesoporous materials: Effect of steam stability and acidity of Al-MCM-41 catalysts. *Chemical Engineering Journal*, *134*(1–3), 51–57. https://doi.org/10.1016/j.cej.2007.03.066

Ingram, L., Mohan, D., Bricka, M., Steele, P., Strobel, D., Crocker, D., Mitchell, B., Mohammad, J., Cantrell, K., & Pittman, C. U. (2008). Pyrolysis of wood and bark in an auger reactor: Physical properties and chemical analysis of the produced bio-oils. *Energy and Fuels*, *22*(1), 614–625. https://doi.org/10.1021/ef700335k

Ishak, M. R., Leman, Z., Sapuan, S. M., Edeerozey, A. M. M., & Othman, I. S. (2010). Mechanical properties of kenaf bast and core fibre reinforced unsaturated polyester composites. *IOP Conference Series: Materials Science and Engineering*, *11*, 012006. https://doi.org/10.1088/1757-899x/11/1/012006

Islam, M. N., Zailani, R., & Ani, F. N. (1999). Pyrolytic oil from fluidised bed pyrolysis of oil

palm shell and itscharacterisation. *Renewable Energy*, *17*(1), 73–84. https://doi.org/10.1016/s0960-1481(98)00112-8

Islam, M. R., Parveen, M., & Haniu, H. (2010). Properties of sugarcane waste-derived bio-oils obtained by fixed-bed fire-tube heating pyrolysis. *Bioresource Technology*, *101*(11), 4162–4168. https://doi.org/10.1016/j.biortech.2009.12.137

Issaoui, H., de Hoyos-Martinez, P. L., Pellerin, V., Dourges, M. A., Deleuze, H., Bourbigo, S., & Bouhtoury, F. C. El. (2021). Effect of catalysts and curing temperature on the properties of biosourced phenolic foams. *ACS Sustainable Chemistry and Engineering*, *9*(18), 6209–6223. https://doi.org/10.1021/acssuschemeng.0c08234

Iswanto, A. H., Tarigan, I. G., Nuryawan, A., & Oktaviani, F. (2021). The properties of particleboards made from corn stalks and bagasse at various compositions. *IOP Conference Series: Earth and Environmental Science*, *713*(1). https://doi.org/10.1088/1755-1315/713/1/012033

Iwuozor, K. O., Chizitere Emenike, E., Ighalo, J. O., Omoarukhe, F. O., Omuku, P. E., & George Adeniyi, A. (2022). A Review on the thermochemical conversion of sugarcane bagasse into biochar. *Cleaner Materials*, *6*(April), 100162. https://doi.org/10.1016/j.clema.2022.100162

Jahanshahi, S., Pizzi, A., Abdulkhani, A., Doosthoseini, K., Shakeri, A., Lagel, M. C., & Delmotte, L. (2016). MALDI-TOF, 13C NMR and FT-MIR analysis and strength characterization of glycidyl ether tannin epoxy resins. *Industrial Crops and Products*, *83*, 177–185. https://doi.org/10.1016/j.indcrop.2015.11.067

Jawaid, M., Paridah, M. T., & Saba, N. (2017). Introduction to biomass and its composites. In *Lignocellulosic Fibre and Biomass-Based Composite Materials: Processing, Properties and Applications*. Elsevier Ltd. https://doi.org/10.1016/B978-0-08-100959-8.00001-9

Jensen, C. U., Rodriguez Guerrero, J. K., Karatzos, S., Olofsson, G., & Iversen, S. B. (2017). Fundamentals of Hydrofaction^{TM}: Renewable crude oil from woody biomass. *Biomass Conversion and Biorefinery*, *7*(4), 495–509. https://doi.org/10.1007/s13399-017-0248-8

Jimenez, J. P., Acda, M. N., Razal, R. A., Abasolo, W. P., Hernandez, H. P., & Elepaño, A. R. (2022). Influence of mixing waste tobacco stalks and paper mulberry wood chips on the physico-mechanical properties, formaldehyde emission, and termite resistance of particleboard. *Industrial Crops and Products*, *187*(February). https://doi.org/10.1016/j.indcrop.2022.115483

K.C. NATARAJA, D. BALAGURAVAIAH, CH. SRINIVASA RAO, T. GIRIDHARA KRISHNA, Y. R. R. and P. L. K. L. K. (2021). Comparative Analysis of Chemical Composition and Spectral Properties of Biochar Produced From Pigeonpea and Cotton Residues. *The Journal of Research ANGRAU*, *49*(2), 43–54. http://jorangrau.org/

Kadja, K., Banna, M., Atcholi, K. E., & Sanda, K. (2011). Utilization of bone adhesive to produce particleboards from stems of cotton plant at the pressing temperature of 140°C. *American Journal of Applied Sciences*, *8*(4), 318–322. https://doi.org/10.3844/ajassp.2011.318.322

Kalaycioglu, H., & Nemli, G. (2006). Producing composite particleboard from kenaf (Hibiscus cannabinus L.) stalks. *Industrial Crops and Products*, *24*(2), 177–180.

https://doi.org/10.1016/j.indcrop.2006.03.011

Kan, T., Strezov, V., & Evans, T. J. (2016). Lignocellulosic biomass pyrolysis: A review of product properties and effects of pyrolysis parameters. *Renewable and Sustainable Energy Reviews*, *57*, 1126–1140. https://doi.org/10.1016/j.rser.2015.12.185

Kanwal, S., Chaudhry, N., Munir, S., & Sana, H. (2019). Effect of torrefaction conditions on the physicochemical characterization of agricultural waste (sugarcane bagasse). *Waste Management*, *88*, 280–290. https://doi.org/10.1016/j.wasman.2019.03.053

Karimi, S., Tahir, P. M., Karimi, A., Dufresne, A., & Abdulkhani, A. (2014). Kenaf bast cellulosic fibers hierarchy: A comprehensive approach from micro to nano. *Carbohydrate Polymers*, *101*(1), 878–885. https://doi.org/10.1016/j.carbpol.2013.09.106

Katyal, S., Thambimuthu, K., & Valix, M. (2003). Carbonisation of bagasse in a fixed bed reactor: Influence of process variables on char yield and characteristics. *Renewable Energy*, *28*(5), 713–725. https://doi.org/10.1016/S0960-1481(02)00112-X

Kaygusuz, K., & Bilgen, S. (2009). Thermodynamic aspects of renewable and sustainable development. *Energy Sources, Part A: Recovery, Utilization and Environmental Effects*, *31*(4), 287–298. https://doi.org/10.1080/15567030701715401

Keshk, S., Suwinarti, W., & Sameshima, K. (2006). Physicochemical characterization of different treatment sequences on kenaf bast fiber. *Carbohydrate Polymers*, *65*(2), 202–206. https://doi.org/10.1016/j.carbpol.2006.01.005

Kharel, G., Sacko, O., Feng, X., Morris, J. R., Phillips, C. L., Trippe, K., Kumar, S., & Lee, J. W. (2019). Biochar Surface Oxygenation by Ozonization for Super High Cation Exchange Capacity [Research-article]. *ACS Sustainable Chemistry and Engineering*, *7*(19), 16410–16418. https://doi.org/10.1021/acssuschemeng.9b03536

Khiari, R., Mhenni, M. F., Belgacem, M. N., & Mauret, E. (2010). Chemical composition and pulping of date palm rachis and Posidonia oceanica - A comparison with other wood and non-wood fibre sources. *Bioresource Technology*, *101*(2), 775–780. https://doi.org/10.1016/j.biortech.2009.08.079

Khristova, P., Kordsachia, O., Patt, R., Khider, T., & Karrar, I. (2002). Alkaline pulping with additives of kenaf from Sudan. *Industrial Crops and Products*, *15*(3), 229–235. https://doi.org/10.1016/S0926-6690(01)00118-2

Kowaluk, G. (2014). Properties of Lignocellulosic Composites Containing Regenerated Cellulose Fibers. *BioResources*, *9*(3), 5339–5348. https://doi.org/10.15376/biores.9.3.5339-5348

Kuba, M., Kraft, S., Kirnbauer, F., Maierhans, F., & Hofbauer, H. (2018). Influence of controlled handling of solid inorganic materials and design changes on the product gas quality in dual fluid bed gasification of woody biomass. *Applied Energy*, *210*(July 2017), 230–240. https://doi.org/10.1016/j.apenergy.2017.11.028

Kumar, A., Jones, D. D., & Hanna, M. A. (2009). Thermochemical biomass gasification: A review of the current status of the technology. *Energies*, *2*(3), 556–581. https://doi.org/10.3390/en20300556

Lacoste, C., Basso, M. C., Pizzi, A., Celzard, A., Ella Ebang, E., Gallon, N., & Charrier, B. (2015). Pine (P. pinaster) and quebracho (S. lorentzii) tannin-based foams as green acoustic absorbers. *Industrial Crops and Products*, *67*, 70–73. https://doi.org/10.1016/j.indcrop.2014.12.018

Lacoste, C., Pizzi, A., Basso, M. C., Laborie, M. P., & Celzard, A. (2014). Pinus pinaster tannin/furanic foams: PART I. Formulation. *Industrial Crops and Products*, *52*, 450–456. https://doi.org/10.1016/j.indcrop.2013.10.044

Lacoste, C., Pizzi, A., Laborie, M. P., & Celzard, A. (2014). Pinus pinaster tannin/furanic foams: Part II. Physical properties. *Industrial Crops and Products*, *61*, 531–536. https://doi.org/10.1016/j.indcrop.2014.04.034

Lam, M. K., Loy, A. C. M., Yusup, S., & Lee, K. T. (2019). Biohydrogen Production From Algae. In *Biomass, Biofuels, Biochemicals: Biohydrogen, Second Edition*. Elsevier B.V. https://doi.org/10.1016/B978-0-444-64203-5.00009-5

Lee, M. K., Tsai, W. T., Tsai, Y. L., & Lin, S. H. (2010). Pyrolysis of napier grass in an induction-heating reactor. *Journal of Analytical and Applied Pyrolysis*, *88*(2), 110–116. https://doi.org/10.1016/j.jaap.2010.03.003

Lee, S. H., Lum, W. C., Boon, J. G., Kristak, L., Antov, P., Pedzik, M., Rogozinski, T., Taghiyari, H. R., Lubis, M. A. R., Fatriasari, W., Yadav, S. M., Chotikhun, A., & Pizzi, A. (2022). Particleboard from agricultural biomass and recycled wood waste: a review. *Journal of Materials Research and Technology*, *20*, 4630–4658. https://doi.org/10.1016/j.jmrt.2022.08.166

Lee, S. Y., Sankaran, R., Chew, K. W., Tan, C. H., Krishnamoorthy, R., Chu, D.-T., & Show, P.-L. (2019). Waste to bioenergy: a review on the recent conversion technologies. *BMC Energy*, *1*(1), 1–22. https://doi.org/10.1186/s42500-019-0004-7

Leng, E., Zhang, Y., Peng, Y., Gong, X., Mao, M., Li, X., & Yu, Y. (2018). In situ structural changes of crystalline and amorphous cellulose during slow pyrolysis at low temperatures. *Fuel*, *216*(January), 313–321. https://doi.org/10.1016/j.fuel.2017.11.083

Li, G., Wang, Y., Yu, D., Zhu, P., Zhao, G., Liu, C., & Zhao, H. (2022). Ligninolytic characteristics of Pleurotus ostreatus cultivated in cotton stalk media. *Frontiers in Microbiology*, *13*(November), 1–12. https://doi.org/10.3389/fmicb.2022.1035040

Li, H., Wang, L., Ji, Y., Xue, S., & Wang, Z. (2019). Study on the Mechanism of Gas Component Release for Biomass Pyrolysis. *E3S Web of Conferences*, *118*. https://doi.org/10.1051/e3sconf/201911803058

Li, H., Xia, S., & Ma, P. (2016). Upgrading fast pyrolysis oil: Solvent-anti-solvent extraction and blending with diesel. *Energy Conversion and Management*, *110*, 378–385. https://doi.org/10.1016/j.enconman.2015.11.043

Li, J., Zhang, S., Gao, B., Yang, A., Wang, Z., Xia, Y., & Liu, H. (2016). Characteristics and deoxy-liquefaction of cellulose extracted from cotton stalk. *Fuel*, *166*, 196–202. https://doi.org/10.1016/j.fuel.2015.10.115

Li, X., Tabil, L. G., & Panigrahi, S. (2007). Chemical treatments of natural fiber for use in natural

fiber-reinforced composites: A review. *Journal of Polymers and the Environment*, *15*(1), 25–33. https://doi.org/10.1007/s10924-006-0042-3

Lin, F., Waters, C. L., Mallinson, R. G., Lobban, L. L., & Bartley, L. E. (2015). Relationships between biomass composition and liquid products formed via pyrolysis. *Frontiers in Energy Research*, *3*(OCT). https://doi.org/10.3389/fenrg.2015.00045

Lin, H., Long, J., Gu, Q., Zhang, W., Ruan, R., Li, Z., & Wang, X. (2012). In situ IR study of surface hydroxyl species of dehydrated TiO 2: Towards understanding pivotal surface processes of TiO 2 photocatalytic oxidation of toluene. *Physical Chemistry Chemical Physics*, *14*(26), 9468–9474. https://doi.org/10.1039/c2cp40893g

Liu, N. A. and Fan, W. C. (1999). Modeling the thermal decompositions of wood and leaves under a nitrogen atmosphere. *Fuel and Energy*, *July*, 274.

Liu, D. T., Xia, K. F., Yang, R. D., Li, J., Chen, K. F., & Nazhad, M. M. (2012). Manufacturing of a biocomposite with both thermal and acoustic properties. *Journal of Composite Materials*, *46*(9), 1011–1020. https://doi.org/10.1177/0021998311414069

Liu, Q., Wang, S., Zheng, Y., Luo, Z., & Cen, K. (2008). Mechanism study of wood lignin pyrolysis by using TG-FTIR analysis. *Journal of Analytical and Applied Pyrolysis*, *82*(1), 170–177. https://doi.org/10.1016/j.jaap.2008.03.007

Lourenço, A., & Gominho, J. (2023). Lignin as Feedstock for Nanoparticles Production. *Lignin - Chemistry, Structure, and Application [Working Title]*, *February*. https://doi.org/10.5772/intechopen.109267

Mahieu, A., & Leblanc, N. (2017). New particleboards based on agricultural byproducts: physicochemical properties with different binders. *Academic Journal of Civil Engineering*, *35*(2), 613–619.

Mahieu, A., Vivet, A., Poilane, C., & Leblanc, N. (2021). Performance of particleboards based on annual plant byproducts bound with bio-adhesives. *International Journal of Adhesion and Adhesives*, *107*(March), 102847. https://doi.org/10.1016/j.ijadhadh.2021.102847

Makavana, J. M., Sarsavadia, P. N., & Chauhan, P. M. (2020). Effect of Pyrolysis Temperature and Residence Time on Bio-char Obtained from Pyrolysis of Shredded Cotton Stalk. *International Research Journal of Pure and Applied Chemistry*, *August*, 10–28. https://doi.org/10.9734/irjpac/2020/v21i1330236

Mathew, S., & Zakaria, Z. A. (2015). Pyroligneous acid—the smoky acidic liquid from plant biomass. *Applied Microbiology and Biotechnology*, *99*(2), 611–622. https://doi.org/10.1007/s00253-014-6242-1

McKendry, P. (2002). Energy production from biomass (part 1): Overview of biomass. *Bioresource Technology*, *83*(1), 37–46. https://doi.org/10.1016/S0960-8524(01)00118-3

Melville, J. (2014). UC Berkeley College of Chemistry Bomb Calorimetry and Heat of Combustion. *Physical Chemistry Laboratory*.

Mesa-Perez, J. M., Cortez, L. A. B., Rocha, J. D., Brossard-Perez, L. E., & Olivares-Gómez, E. (2005). Unidimensional heat transfer analysis of elephant grass and sugar cane bagasse slow

pyrolysis in a fixed bed reactor. *Fuel Processing Technology*, *86*(5), 565–575. https://doi.org/10.1016/j.fuproc.2004.05.014

Meyer, S., Glaser, B., & Quicker, P. (2011). Technical, economical, and climate-related aspects of biochar production technologies: A literature review. *Environmental Science and Technology*, *45*(22), 9473–9483. https://doi.org/10.1021/es201792c

Mierzwa-Hersztek, M., Gondek, K., Jewiarz, M., & Dziedzic, K. (2019). Assessment of energy parameters of biomass and biochars, leachability of heavy metals and phytotoxicity of their ashes. *Journal of Material Cycles and Waste Management*, *21*(4), 786–800. https://doi.org/10.1007/s10163-019-00832-6

Mihiretie, B. M., Cederkrantz, D., Rosén, A., Otterberg, H., Sundin, M., Gustafsson, S. E., & Karlsteen, M. (2017). Finite element modeling of the Hot Disc method. *International Journal of Heat and Mass Transfer*, *115*, 216–223. https://doi.org/10.1016/j.ijheatmasstransfer.2017.08.036

Mishra, R. K., Chistie, S. M., Naik, S. U., & Kumar, P. (2022). Thermocatalytic co-pyrolysis of waste biomass and plastics: Studies of physicochemical properties, kinetics behaviour, and characterization of liquid product. *Journal of the Energy Institute*, *105*(July), 192–202. https://doi.org/10.1016/j.joei.2022.09.003

Mishra, S., & Upadhyay, R. K. (2021). Review on biomass gasification: Gasifiers, gasifying mediums, and operational parameters. *Materials Science for Energy Technologies*, *4*(August 2021), 329–340. https://doi.org/10.1016/j.mset.2021.08.009

Mitchual, S. J., Mensah, P., Frimpong-Mensah, K., & Appiah-Kubi, E. (2020). Characterization of Particleboard Produced from Residues of *Plantain pseudostem*, Cocoa Pod and Stem and *Ceiba*. *Materials Sciences and Applications*, *11*(12), 817–836. https://doi.org/10.4236/msa.2020.1112054

Modak, S., Katiyar, P., Yadav, S., Jain, S., Gole, B., & Talukdar, D. (2023). Generation and characterization of bio-oil obtained from the slow pyrolysis of cooked food waste at various temperatures. *Waste Management*, *158*(September 2022), 23–36. https://doi.org/10.1016/j.wasman.2023.01.002

MOHAMED, A., & FAWZI BANI MFARREJ, M. (2020). SUDANESE EXPERIENCE TOWARDS IMPLEMENTATION OF BIOMASS GASIFICATION AS AN ALTERNATIVE SOURCE OF ENERGY FOR RURAL ELECTRIFICATION. *Global Journal of Science & Engineering*, 9–14. https://doi.org/10.37516/global.j.sci.eng.2020.002

Mohan, D., Pittman, C. U., & Philip, S. (2017). Pyrolysis of Wood/Biomass for Bio-oil: A Critical Review Dinesh. *Progress in Energy and Combustion Science*, *62*(4), 848–889. http://dx.doi.org/10.1016/j.pecs.2017.05.004

Mohan, D., Pittman, C. U., & Steele, P. H. (2006). Pyrolysis of wood/biomass for bio-oil: A critical review. *Energy and Fuels*, *20*(3), 848–889. https://doi.org/10.1021/ef0502397

Monteiro, S. N., Calado, V., Rodriguez, R. J. S., & Margem, F. M. (2012). Thermogravimetric behavior of natural fibers reinforced polymer composites-An overview. *Materials Science and Engineering A*, *557*, 17–28. https://doi.org/10.1016/j.msea.2012.05.109

Moubarik, A., Mansouri, H. R., Pizzi, A., Charrier, F., Allal, A., & Charrier, B. (2013). Corn flour-mimosa tannin-based adhesives without formaldehyde for interior particleboard production. *Wood Science and Technology*, *47*(4), 675–683. https://doi.org/10.1007/s00226-012-0525-4

Moubarik, A., Pizzi, A., Allal, A., Charrier, F., Khoukh, A., & Charrier, B. (2010). Cornstarch-mimosa tannin-urea formaldehyde resins as adhesives in the particleboard production. *Starch/Staerke*, *62*(3–4), 131–138. https://doi.org/10.1002/star.200900228

Moubarik, A., Pizzi, A., Charriera, F., Allala, A., Badia, M., Mansouri, H. R., & Charrier, B. (2013). Mechanical characterization of industrial particleboard panels glued with cornstarch-mimosa tannin-urea formaldehyde resins. *Journal of Adhesion Science and Technology*, *27*(4), 423–429. https://doi.org/10.1080/01694243.2012.711739

Munir, S., Nimmo, W., & Gibbs, B. M. (2010). Shea meal and cotton stalk as potential fuels for co-combustion with coal. *Bioresource Technology*, *101*(19), 7614–7623. https://doi.org/10.1016/j.biortech.2010.04.055

Mustafa, A. H., Rashid, S. S., Rahim, M. H. A., Roslan, R., Musa, W. A. M., Sikder, B. H., & Sasi, A. A. (2022). Enzymatic Pretreatment of Lignocellulosic Biomass: An Overview. *Journal of Chemical Engineering and Industrial Biotechnology*, *8*(1), 1–7. https://doi.org/10.15282/jceib.v8i1.7030

Nadhari, W. N. A. W., Karim, N. A., Boon, J. G., Salleh, K. M., Mustapha, A., Hashim, R., Sulaiman, O., & Azni, M. E. (2020). Sugarcane (Saccharum officinarium L.) bagasse binderless particleboard: Effect of hot pressing time study. *Materials Today: Proceedings*, *31*, 313–317. https://doi.org/10.1016/j.matpr.2020.06.016

Nagai, H., Rossignol, F., Nakata, Y., Tsurue, T., Suzuki, M., & Okutani, T. (2000). Thermal conductivity measurement of liquid materials by a hot-disk method in short-duration microgravity environments. *Materials Science and Engineering A*, *276*(1–2), 117–123. https://doi.org/10.1016/S0921-5093(99)00519-5

Naima, R., Oumam, M., Hannache, H., Sesbou, A., Charrier, B., Pizzi, A., & Charrier - El Bouhtoury, F. (2015). Comparison of the impact of different extraction methods on polyphenols yields and tannins extracted from Moroccan Acacia mollissima barks. *Industrial Crops and Products*, *70*, 245–252. https://doi.org/10.1016/j.indcrop.2015.03.016

Nargotra, P., Sharma, V., Lee, Y. C., Tsai, Y. H., Liu, Y. C., Shieh, C. J., Tsai, M. L., Dong, C. Di, & Kuo, C. H. (2023). Microbial Lignocellulolytic Enzymes for the Effective Valorization of Lignocellulosic Biomass: A Review. *Catalysts*, *13*(1), 1–28. https://doi.org/10.3390/catal13010083

Nasution, M. H., Lelinasari, S., & Kelana, M. G. S. (2022). A review of sugarcane bagasse pretreatment for bioethanol production. *IOP Conference Series: Earth and Environmental Science*, *963*(1). https://doi.org/10.1088/1755-1315/963/1/012014

Navarro, A. F., Cegarra, J., Roig, A., & Garcia, D. (1993). Relationships between organic matter and carbon contents of organic wastes. *Bioresource Technology*, *44*(3), 203–207. https://doi.org/10.1016/0960-8524(93)90153-3

Nazerian, M., Beygi, Z., Mohebbi Gargari, R., & Kool, F. (2018). Application of response surface

methodology for evaluating particleboard properties made from cotton stalk particles. *Wood Material Science and Engineering*, *13*(2), 73–80. https://doi.org/10.1080/17480272.2017.1307280

Ndazi, B., Tesha, J. V., & Bisanda, E. T. N. (2006). Some opportunities and challenges of producing bio-composites from non-wood residues. *Journal of Materials Science*, *41*(21), 6984–6990. https://doi.org/10.1007/s10853-006-0216-3

Ndiwe, B., Pizzi, A., Danwe, R., Tibi, B., Konai, N., & Amirou, S. (2019). Particleboard bonded with bio-hardeners of tannin adhesives. *European Journal of Wood and Wood Products*, *77*(6), 1221–1223. https://doi.org/10.1007/s00107-019-01460-5

Nguyen, D. L., Luedtke, J., Nopens, M., & Krause, A. (2023). Production of wood-based panel from recycled wood resource: a literature review. *European Journal of Wood and Wood Products*, *81*(3), 557–570. https://doi.org/10.1007/s00107-023-01937-4

Nguyen, T. T., Bailleres, H., Redman, A., Leggate, W., Vandi, L. J., & Heiztmann, M. (2020). Homogenous Particleboard Made from Whole Cotton (Gossypium hirsutum L.) Stalk Agricultural Waste: Optimisation of Particle Size and Influence of Cotton Residue on Performance. *BioResources*, *15*(4), 7730–7748. https://doi.org/10.15376/biores.15.4.7730-7748

Nikvash, N., Kharazipour, A., & Euring, M. (2012). Effects of wheat protein as a biological binder in the manufacture of particleboards using a mixture of canola, hemp, bagasse, and commercial wood. *Forest Products Journal*, *62*(1), 49–57. https://doi.org/10.13073/FPJ-D-11-00102.1

Ning, P., Yang, G., Hu, L., Sun, J., Shi, L., Zhou, Y., Wang, Z., & Yang, J. (2021). Recent advances in the valorization of plant biomass. *Biotechnology for Biofuels*, *14*(1), 1–22. https://doi.org/10.1186/s13068-021-01949-3

Nourbakhsh, A. (2010). Mechanical and thickness swelling of particleboard composites made from three-year-old poplar clones. *Journal of Reinforced Plastics and Composites*, *29*(4), 481–489. https://doi.org/10.1177/0731684408097771

Nunes de Oliveira Júnior, J., Perissé Duarte Lopes, F., Tonini Simonassi, N., Souza, D., Neves Monteiro, S., & Fontes Vieira, C. M. (2023). Evaluation of the physical properties of composite panels with eucalyptus sawdust waste and castor oil-based polyurethane. *Journal of Materials Research and Technology*, *23*, 1084–1093. https://doi.org/10.1016/j.jmrt.2023.01.067

Nunes, L. J. R., De Oliveira Matias, J. C., & Da Silva Catalão, J. P. (2018). Introduction. In *Torrefaction of Biomass for Energy Applications*. https://doi.org/10.1016/b978-0-12-809462-4.00001-8

Nyang, M. G., Muumbo, A. M., & Ondieki, C. M. M. (2019). Production of Particle Boards from Sugarcane Bagasse and Euphorbia Sap. *International Journal of Composite Materials*, *9*(1), 1–6. https://doi.org/10.5923/j.cmaterials.20190901.01

Odetoye, T. E., & Adeoye, V. A. (2022). Biocomposite production from waste low-density polyethylene sachets and Prosopis africana pods biomass residue. *FUOYE Journal of*

Engineering and Technology, *7*(2), 229–235. https://doi.org/10.46792/fuoyejet.v7i2.761

Ojo, O. T., & Olugbade, T. O. (2022). Physicomechanical Properties of Bio-based Sawdust-Cow Horn-Coconut Husk Particleboards. *Journal of The Institution of Engineers (India): Series D*, *103*(1), 287–294. https://doi.org/10.1007/s40033-022-00341-1

Oliveira, S. L., Mendes, R. F., Mendes, L. M., & Freire, T. P. (2016). Particleboard panels made from sugarcane bagasse: Characterization for use in the furniture industry. *Materials Research*, *19*(4), 914–922. https://doi.org/10.1590/1980-5373-MR-2015-0211

Olivito, R. S., Cevallos, O. A., & Carrozzini, A. (2014). Development of durable cementitious composites using sisal and flax fabrics for reinforcement of masonry structures. *Materials and Design*, *57*, 258–268. https://doi.org/10.1016/j.matdes.2013.11.023

Omer, A. M., & Fadalla, Y. (2003). Biogas energy technology in Sudan. *Renewable Energy*, *28*(3), 499–507. https://doi.org/10.1016/S0960-1481(02)00053-8

Osman, A. I., Mehta, N., Elgarahy, A. M., Al-Hinai, A., Al-Muhtaseb, A. H., & Rooney, D. W. (2021). Conversion of biomass to biofuels and life cycle assessment: a review. In *Environmental Chemistry Letters* (Vol. 19, Issue 6). Springer International Publishing. https://doi.org/10.1007/s10311-021-01273-0

Osman, Z. (2013). Comparative Thermodynamic Study on the Contribution of the Autocondensation and Copolymerization Reactions for the Tannins of the Subspecies of Acacia nilotica. *Journal of Polymers and the Environment*, *21*(4), 1100–1108. https://doi.org/10.1007/s10924-013-0611-1

Osman, Z., Pizzi, A., & Alamin, I. H. (2009). Comparative properties of agrofiber based particle boards using newly developed bonding materials. *Journal of Biobased Materials and Bioenergy*, *3*(3), 275–281. https://doi.org/10.1166/jbmb.2009.1034

Ouajai, S., & Shanks, R. A. (2005). Composition, structure and thermal degradation of hemp cellulose after chemical treatments. *Polymer Degradation and Stability*, *89*(2), 327–335. https://doi.org/10.1016/j.polymdegradstab.2005.01.016

Owodunni, A. A., Lamaming, J., Hashim, R., Taiwo, O. F. A., Hussin, M. H., Mohamad Kassim, M. H., Bustami, Y., Sulaiman, O., Amini, M. H. M., & Hiziroglu, S. (2020). Adhesive application on particleboard from natural fibers: A review. *Polymer Composites*, *41*(11), 4448–4460. https://doi.org/10.1002/pc.25749

Özbay, N., Pütün, A. E., Uzun, B. B., & Pütün, E. (2001). Biocrude from biomass: Pyrolysis of cottonseed cake. *Renewable Energy*, *24*(3–4), 615–625. https://doi.org/10.1016/S0960-1481(01)00048-9

Pan, H., Zheng, B., Yang, H., Guan, Y., Zhang, L., Xu, X., Wu, A., & Li, H. (2023). Effect of Loblolly Pine (Pinus taeda L.) Hemicellulose Structure on the Properties of Hemicellulose-Polyvinyl Alcohol Composite Film. *Molecules*, *28*(1), 1–16. https://doi.org/10.3390/molecules28010046

Papadopoulou, E., & Chrissafis, K. (2017). Particleboards from agricultural lignocellulosics and biodegradable polymers prepared with raw materials from natural resources. In *Natural Fiber-Reinforced Biodegradable and Bioresorbable Polymer Composites*. Elsevier Ltd.

https://doi.org/10.1016/B978-0-08-100656-6.00002-9

Paridah, M. T., Juliana, A. H., El-Shekeil, Y. A., Jawaid, M., & Alothman, O. Y. (2014). Measurement of mechanical and physical properties of particleboard by hybridization of kenaf with rubberwood particles. *Measurement: Journal of the International Measurement Confederation*, *56*, 70–80. https://doi.org/10.1016/j.measurement.2014.06.019

Paridah, M. T., Juliana, A. H., Zaidon, A., & Abdul Khalil, H. P. S. (2015). Nonwood-based composites. *Current Forestry Reports*, *1*(4), 221–238. https://doi.org/10.1007/s40725-015-0023-7

Park, S., Kim, S. J., Oh, K. C., Cho, L. H., & Kim, D. H. (2023). Developing a Proximate Component Prediction Model of Biomass Based on Element Analysis. *Energies*, *16*(1), 1–14. https://doi.org/10.3390/en16010509

Parr Instrument Company. (2013). *Introduction to Bomb Calorimetry Introduction to Bomb Calorimetry*. 12.

Pecha, M. B., & Garcia-Perez, M. (2020). Pyrolysis of lignocellulosic biomass: oil, char, and gas. In *Bioenergy: Biomass to Biofuels and Waste to Energy* (Second Edi). Elsevier. https://doi.org/10.1016/B978-0-12-815497-7.00029-4

Pędzik, M., Janiszewska, D., & Rogoziński, T. (2021). Alternative lignocellulosic raw materials in particleboard production: A review. *Industrial Crops and Products*, *174*(June). https://doi.org/10.1016/j.indcrop.2021.114162

Peng, F., Peng, P., Xu, F., & Sun, R. C. (2012). Fractional purification and bioconversion of hemicelluloses. *Biotechnology Advances*, *30*(4), 879–903. https://doi.org/10.1016/j.biotechadv.2012.01.018

Pereira, B. L. C., de Angélica de C.O. Carneiro, A., Carvalho, A. M. M. L., Colodette, J. L., Oliveira, A. C., & Fontes, M. P. F. (2013). Influence of Chemical Composition of Eucalyptus Wood on Gravimetric Yield and Charcoal Properties. *BioResources*, *8*(2), 4574–4592. https://doi.org/10.15376/biores.8.3.4574-4592

Petráš, R., Mecko, J., Kukla, J., & Kuklová, M. (2019). Calorific Value of Basic Fractions of Above-Ground Biomass for Scots Pine. *Acta Regionalia et Environmentalica*, *16*(2), 34–37. https://doi.org/10.2478/aree-2019-0007

Pimenta, A. S., Fasciotti, M., Monteiro, T. V. C., & Lima, K. M. G. (2018). Chemical composition of pyroligneous acid obtained from eucalyptus GG100 clone. *Molecules*, *23*(2). https://doi.org/10.3390/molecules23020426

Pinheiro Pires, A. P., Arauzo, J., Fonts, I., Domine, M. E., Fernández Arroyo, A., Garcia-Perez, M. E., Montoya, J., Chejne, F., Pfromm, P., & Garcia-Perez, M. (2019). Challenges and opportunities for bio-oil refining: A review. *Energy and Fuels*, *33*(6), 4683–4720. https://doi.org/10.1021/acs.energyfuels.9b00039

Pizzi, A. (2013). Bioadhesives for wood and fibres: A critical review. *Reviews of Adhesion and Adhesives*, *1*(1), 88–113. https://doi.org/10.7569/RAA.2013.097303

Platače, R., & Adamovičs, A. (2014). The evaluation of ash content in grass biomass used for

energy production. *WIT Transactions on Ecology and the Environment*, *190 VOLUME*, 1057–1065. https://doi.org/10.2495/EQ140992

Policella, M., Wang, Z., Burra, K. G., & Gupta, A. K. (2019). Characteristics of syngas from pyrolysis and CO2-assisted gasification of waste tires. *Applied Energy*, *254*, 1–32. https://doi.org/10.1016/j.apenergy.2019.113678

Popescu, C. M. (2017). Wood as bio-based building material. In *Performance of Bio-based Building Materials*. https://doi.org/10.1016/B978-0-08-100982-6.00002-1

Popp, J., Kovács, S., Oláh, J., Divéki, Z., & Balázs, E. (2021). Bioeconomy: Biomass and biomass-based energy supply and demand. *New Biotechnology*, *60*(October 2020), 76–84. https://doi.org/10.1016/j.nbt.2020.10.004

Popper, Z. A., Michel, G., Hervé, C., Domozych, D. S., Willats, W. G. T., Tuohy, M. G., Kloareg, B., & Stengel, D. B. (2011). Evolution and diversity of plant cell walls: From algae to flowering plants. *Annual Review of Plant Biology*, *62*(May), 567–590. https://doi.org/10.1146/annurev-arplant-042110-103809

Posom, J., & Sirisomboon, P. (2017). Evaluation of the higher heating value, volatile matter, fixed carbon and ash content of ground bamboo using near infrared spectroscopy. *Journal of Near Infrared Spectroscopy*, *25*(5), 301–310. https://doi.org/10.1177/0967033517728733

Pothula, R. R. (2016). Mechanical Properties of Particleboard Composites Made from Sugarcane Bagasse and Spirulina Algae. *ProQuest Dissertations and Theses*, 100. https://ezproxyprod.ucs.louisiana.edu:2443/login?url=https://www.proquest.com/dissertations-theses/mechanical-properties-particleboard-composites/docview/1937880778/se-2%0Ahttps://louis.hosts.atlas-sys.com/illiad/LWA/illiad.dll/OpenURL?ctx_ver=Z39.88-2004

Prajapati, S. B., Gautam, A., Gautam, S., Yao, Z., Tesfaye, F., & Lü, X. (2023). Co-Pyrolysis Behavior, Kinetic and Mechanism of Waste-Printed Circuit Board with Biomass. *Processes*, *11*(1). https://doi.org/10.3390/pr11010229

Prakash Bamboriya, O., Singh Thakur, L., Parmar, H., Kumar Varma, A., & Hinge, V. K. (2019). A review on mechanism and factors affecting pyrolysis of biomass. *International Journal of Research in Advent Technology*, *7*(3), 1014–1024. www.ijrat.org

Priharto, N., Ronsse, F., Yildiz, G., Heeres, H. J., Deuss, P. J., & Prins, W. (2020). Fast pyrolysis with fractional condensation of lignin-rich digested stillage from second-generation bioethanol production. *Journal of Analytical and Applied Pyrolysis*, *145*(November), 104756. https://doi.org/10.1016/j.jaap.2019.104756

Rahbar Shamskar, K., Heidari, H., & Rashidi, A. (2016). Preparation and evaluation of nanocrystalline cellulose aerogels from raw cotton and cotton stalk. *Industrial Crops and Products*, *93*, 203–211. https://doi.org/10.1016/j.indcrop.2016.01.044

Raydan, N. D. V., Leroyer, L., Charrier, B., & Robles, E. (2021). Recent advances on the development of protein-based adhesives for wood composite materials—a review. *Molecules*, *26*(24). https://doi.org/10.3390/molecules26247617

Rezaei, P. S., Shafaghat, H., & Daud, W. M. A. W. (2014). Production of green aromatics and

olefins by catalytic cracking of oxygenate compounds derived from biomass pyrolysis: A review. *Applied Catalysis A: General*, *469*, 490–511. https://doi.org/10.1016/j.apcata.2013.09.036

Righetti, M. C., Cinelli, P., Mallegni, N., Massa, C. A., Bronco, S., Stäbler, A., & Lazzeri, A. (2019). Thermal, mechanical, and rheological properties of biocomposites made of poly(Lactic acid) and potato pulp powder. *International Journal of Molecular Sciences*, *20*(3). https://doi.org/10.3390/ijms20030675

Robles-García, M. Á., Del-Toro-Sánchez, C. L., Márquez-Ríos, E., Barrera-Rodríguez, A., Aguilar, J., Aguilar, J. A., Reynoso-Marín, F. J., Ceja, I., Dórame-Miranda, R., & Rodríguez-Félix, F. (2018). Nanofibers of cellulose bagasse from Agave tequilana Weber var. azul by electrospinning: preparation and characterization. *Carbohydrate Polymers*, *192*, 69–74. https://doi.org/10.1016/j.carbpol.2018.03.058

Robles, E., Urruzola, I., Labidi, J., & Serrano, L. (2015). Surface-modified nano-cellulose as reinforcement in poly(lactic acid) to conform new composites. *Industrial Crops and Products*, *71*, 44–53. https://doi.org/10.1016/j.indcrop.2015.03.075

Rojas, A., & Valués, A. (2003). An isoperibol micro-bomb calorimeter for measurement of the enthalpy of combustion of organic compounds. Application to the study of succinic acid and acetanilide. *Journal of Chemical Thermodynamics*, *35*(8), 1309–1319. https://doi.org/10.1016/S0021-9614(03)00095-8

Ronsse, F., Nachenius, R. W., & Prins, W. (2015). Carbonization of Biomass. In *Recent Advances in Thermochemical Conversion of Biomass*. Elsevier B.V. https://doi.org/10.1016/B978-0-444-63289-0.00011-9

Rowell, R. M., Han, J. S., & Rowell, J. S. (2000). Characterization and Factors Effecting Fiber Properties. *Natural Polymers an Agrofibers Composites*, 115–134.

Rozyanty, A. R., Zhafer, S. F., Shayfull, Z., Nainggolan, I., Musa, L., & Zheing, L. T. (2021). Effect of water and mechanical retting process on mechanical and physical properties of kenaf bast fiber reinforced unsaturated polyester composites. *Composite Structures*, *257*(June 2020), 113384. https://doi.org/10.1016/j.compstruct.2020.113384

Saba, N., Jawaid, M., Hakeem, K. R., Paridah, M. T., Khalina, A., & Alothman, O. Y. (2015). Potential of bioenergy production from industrial kenaf (Hibiscus cannabinus L.) based on Malaysian perspective. *Renewable and Sustainable Energy Reviews*, *42*, 446–459. https://doi.org/10.1016/j.rser.2014.10.029

Saeed, A. A. H., Harun, N. Y., Sufian, S., Afolabi, H. K., Al-Qadami, E. H. H., Roslan, F. A. S., Rahim, S. A., & Ghaleb, A. A. S. (2021). Production and characterization of rice husk biochar and kenaf biochar for value-added biochar replacement for potential materials adsorption. *Ecological Engineering and Environmental Technology*, *22*(1), 1–8. https://doi.org/10.12912/27197050/132099

Saeed, H. A. M., Liu, Y., Lucia, L. A., & Chen, H. (2017). Evaluation of Sudanese sorghum and bagasse as a pulp and paper feedstock. *BioResources*, *12*(3), 5212–5222. https://doi.org/10.15376/biores.12.3.5212-5222

Saha, P., Manna, S., Chowdhury, S. R., Sen, R., Roy, D., & Adhikari, B. (2010). Enhancement of tensile strength of lignocellulosic jute fibers by alkali-steam treatment. *Bioresource Technology*, *101*(9), 3182–3187. https://doi.org/10.1016/j.biortech.2009.12.010

Şahin, H. İ. (2020). The Potential of Using Forest Waste as a Raw Material in Particleboard Manufacturing. *BioResources*, *15*(4), 7780–7795. https://doi.org/10.15376/biores.15.4.7780-7795

Sala, C. M., Robles, E., & Kowaluk, G. (2021). Influence of the Addition of Spruce Fibers to Industrial-Type High-Density Fiberboards Produced with Recycled Fibers. In *Waste and Biomass Valorization* (Vol. 12, Issue 7, pp. 4033–4042). https://doi.org/10.1007/s12649-020-01250-8

Santiago-Medina, F. J., Tenorio-Alfonso, A., Delgado-Sánchez, C., Basso, M. C., Pizzi, A., Celzard, A., Fierro, V., Sánchez, M. C., & Franco, J. M. (2018). Projectable tannin foams by mechanical and chemical expansion. *Industrial Crops and Products*, *120*(March), 90–96. https://doi.org/10.1016/j.indcrop.2018.04.048

Sasmal, S., Goud, V. V., & Mohanty, K. (2012). Characterization of biomasses available in the region of North-East India for production of biofuels. *Biomass and Bioenergy*, *45*, 212–220. https://doi.org/10.1016/j.biombioe.2012.06.008

Schramm, C. (2020). High temperature ATR-FTIR characterization of the interaction of polycarboxylic acids and organotrialkoxysilanes with cellulosic material. *Spectrochimica Acta - Part A: Molecular and Biomolecular Spectroscopy*, *243*, 118815. https://doi.org/10.1016/j.saa.2020.118815

Schwarzenbrunner, R., Barbu, M. C., Petutschnigg, A., & Tudor, E. M. (2020). Water-resistant casein-based adhesives for veneer bonding in biodegradable ski cores. *Polymers*, *12*(8), 1–10. https://doi.org/10.3390/POLYM12081745

Shah, J. B., & Valaki, J. B. (2022). Characterization of Bio-oil, Bio-char, and Pyro-gas derived from cotton stalk slow pyrolysis-as sustainable energy sources. *Indian Journal of Chemical Technology*, *29*(4), 380–389. https://doi.org/10.56042/ijct.v29i4.60904

Sharma, P. R., & Varma, A. J. (2014). Thermal stability of cellulose and their nanoparticles: Effect of incremental increases in carboxyl and aldehyde groups. *Carbohydrate Polymers*, *114*, 339–343. https://doi.org/10.1016/j.carbpol.2014.08.032

Sheng, C., & Azevedo, J. L. T. (2005). Estimating the higher heating value of biomass fuels from basic analysis data. *Biomass and Bioenergy*, *28*(5), 499–507. https://doi.org/10.1016/j.biombioe.2004.11.008

Sidhu, G. K., & Sandhya. (2015). Engineering properties of cotton stalks (Gossypium hirsitum L.). *Indian Journal of Agricultural Research*, *49*(5), 456–459. https://doi.org/10.18805/ijare.v49i5.5811

Singh, M., SINGH, R., & GILL, G. (2020). Estimating The Correlation Between The Calorific Value And Elemental Components Of Biomass Using Regrassion Analysis 18 ESTIMATING THE CORRELATION BETWEEN THE CALORIFIC VALUE AND ELEMENTAL COMPONENTS OF BIOMASS USING. *International Journal of Industrial*

Electronics and Electrical Engineering, *3*(9), 2347–6982. https://doi.org/10.13140/RG.2.2.27308.82565

Singh, S., Varanasi, P., Singh, P., Adams, P. D., Auer, M., & Simmons, B. A. (2013). Understanding the impact of ionic liquid pretreatment on cellulose and lignin via thermochemical analysis. *Biomass and Bioenergy*, *54*, 276–283. https://doi.org/10.1016/j.biombioe.2013.02.035

Sorek, N., Yeats, T. H., Szemenyei, H., Youngs, H., & Somerville, C. R. (2014). The implications of lignocellulosic biomass chemical composition for the production of advanced biofuels. *BioScience*, *64*(3), 192–201. https://doi.org/10.1093/biosci/bit037

Spinacé, M. A. S., Lambert, C. S., Fermoselli, K. K. G., & De Paoli, M. A. (2009). Characterization of lignocellulosic curaua fibres. *Carbohydrate Polymers*, *77*(1), 47–53. https://doi.org/10.1016/j.carbpol.2008.12.005

Srichan, S., & Raongjant, W. (2020). Characteristics of particleboard manufactured from bamboo shoot sheaths. *E3S Web of Conferences*, *187*(January). https://doi.org/10.1051/e3sconf/202018703011

Strezov, V., Evans, T. J., & Hayman, C. (2008). Thermal conversion of elephant grass (Pennisetum Purpureum Schum) to bio-gas, bio-oil and charcoal. *Bioresource Technology*, *99*(17), 8394–8399. https://doi.org/10.1016/j.biortech.2008.02.039

Sun, P., Heng, M., Sun, S. H., & Chen, J. (2011). Analysis of liquid and solid products from liquefaction of paulownia in hot-compressed water. *Energy Conversion and Management*, *52*(2), 924–933. https://doi.org/10.1016/j.enconman.2010.08.020

Szczurek, A., Fierro, V., Pizzi, A., Stauber, M., & Celzard, A. (2014). A new method for preparing tannin-based foams. *Industrial Crops and Products*, *54*, 40–53. https://doi.org/10.1016/j.indcrop.2014.01.012

Tabarsa, T., Ashori, A., & Gholamzadeh, M. (2011). Evaluation of surface roughness and mechanical properties of particleboard panels made from bagasse. *Composites Part B: Engineering*, *42*(5), 1330–1335. https://doi.org/10.1016/j.compositesb.2010.12.018

Tanobe, V. O. A., Sydenstricker, T. H. D., Munaro, M., & Amico, S. C. (2010). Corrigendum to "A comprehensive characterization of chemically treated Brazilian sponge-gourds (Luffa cylindrica)" [Polymer Testing. Volume 24 (2005) p. 474-482] (DOI:10.1016/j.polymertesting.2004.12.004). *Polymer Testing*, *29*(2), 288–289. https://doi.org/10.1016/j.polymertesting.2009.12.009

Tawasil, D. N. B., Aminudin, E., Abdul Shukor Lim, N. H., Nik Soh, N. M. Z., Leng, P. C., Ling, G. H. T., & Ahmad, M. H. (2021). Coconut fibre and sawdust as green building materials: A laboratory assessment on physical and mechanical properties of particleboards. *Buildings*, *11*(6). https://doi.org/10.3390/buildings11060256

Teixeira Cardoso, A. R., Conrado, N. M., Krause, M. C., Bjerk, T. R., Krause, L. C., & Caramão, E. B. (2019). Chemical characterization of the bio-oil obtained by catalytic pyrolysis of sugarcane bagasse (industrial waste) from the species Erianthus Arundinaceus. *Journal of Environmental Chemical Engineering*, *7*(2). https://doi.org/10.1016/j.jece.2019.102970

Tiilikkala, K., Fagernäs, L., & Tiilikkala, J. (2014). History and Use of Wood Pyrolysis Liquids as Biocide and Plant Protection Product. *The Open Agriculture Journal*, *4*(1), 111–118. https://doi.org/10.2174/1874331501004010111

Torri, I. D. V., Paasikallio, V., Faccini, C. S., Huff, R., Caramão, E. B., Sacon, V., Oasmaa, A., & Zini, C. A. (2016). Bio-oil production of softwood and hardwood forest industry residues through fast and intermediate pyrolysis and its chromatographic characterization. *Bioresource Technology*, *200*, 680–690. https://doi.org/10.1016/j.biortech.2015.10.086

Tronc, E., Hernández-Escobar, C. A., Ibarra-Gómez, R., Estrada-Monje, A., Navarrete-Bolaños, J., & Zaragoza-Contreras, E. A. (2007). Blue agave fiber esterification for the reinforcement of thermoplastic composites. *Carbohydrate Polymers*, *67*(2), 245–255. https://doi.org/10.1016/j.carbpol.2006.05.027

Tsai, W. T., Lee, M. K., & Chang, Y. M. (2006). Fast pyrolysis of rice straw, sugarcane bagasse and coconut shell in an induction-heating reactor. *Journal of Analytical and Applied Pyrolysis*, *76*(1–2), 230–237. https://doi.org/10.1016/j.jaap.2005.11.007

Tsubota, Y., & Ichiryu, K. (2005). Development of riding simulator. *Proceedings of the 6th International Conference on Fluid Power Transmission and Control, ICFP 2005*, *6*(Sur 2005), 686–689.

Tuerxun, D., Pulingam, T., Nordin, N. I., Chen, Y. W., Kamaldin, J. Bin, Julkapli, N. B. M., Lee, H. V., Leo, B. F., & Johan, M. R. Bin. (2019). Synthesis, characterization and cytotoxicity studies of nanocrystalline cellulose from the production waste of rubber-wood and kenaf-bast fibers. *European Polymer Journal*, *116*(November 2018), 352–360. https://doi.org/10.1016/j.eurpolymj.2019.04.021

Tutus, A., Ezici, A. C., & Ates, S. (2010). Chemical, morphological and anatomical properties and evaluation of cotton stalks (Gossypium Hirsutum L.) in pulp industry. *Scientific Research and Essays*, *5*(12), 1553–1560.

Uddin, M. N., Daud, W. M. A. W., & Abbas, H. F. (2014). Effects of pyrolysis parameters on hydrogen formations from biomass: A review. *RSC Advances*, *4*(21), 10467–10490. https://doi.org/10.1039/c3ra43972k

Vachon, C., Yu, H. L., Yefsah, R., Alain, R., St-Gelais, D., & Lacroix, M. (2000). Mechanical and structural properties of milk protein edible films cross-linked by heating and γ-irradiation. *Journal of Agricultural and Food Chemistry*, *48*(8), 3202–3209. https://doi.org/10.1021/jf991055r

Varma, A. K., & Mondal, P. (2016). Physicochemical Characterization and Pyrolysis Kinetic Study of Sugarcane Bagasse Using Thermogravimetric Analysis. *Journal of Energy Resources Technology, Transactions of the ASME*, *138*(5), 1–11. https://doi.org/10.1115/1.4032729

Varma, A. K., & Mondal, P. (2017). Pyrolysis of sugarcane bagasse in semi batch reactor: Effects of process parameters on product yields and characterization of products. *Industrial Crops and Products*, *95*, 704–717. https://doi.org/10.1016/j.indcrop.2016.11.039

Vassilev, S. V., Baxter, D., Andersen, L. K., & Vassileva, C. G. (2013). An overview of the

composition and application of biomass ash. Part 1. Phase-mineral and chemical composition and classification. *Fuel*, *105*, 40–76. https://doi.org/10.1016/j.fuel.2012.09.041

Venkatesh, G., & Venkateswarlu, B. (2013). Biochar Production Technology for Conversion of Cotton Stalk Bioresidue into Biochar and its Characterization for Soil Amendment Qualities. *Indian Journal of …*, *28*(1), 48–57. http://www.indianjournals.com/ijor.aspx?target=ijor:ijdard&volume=28&issue=1&article=007%5Cnpapers2://publication/uuid/3DB77DEF-5076-48C3-A53D-AB4ED25AB84F

W. G. Escobar. (2008). Influence of wood species on properties of wood/HDPE composites. In *Biotechnology Department - College of Science - University of Baghdad: Vol. Volume 49*.

Wang, S., Ai, Q., Zou, T. qi, Sun, C., & Xie, M. (2020). Analysis of radiation effect on thermal conductivity measurement of semi-transparent materials based on transient plane source method. *Applied Thermal Engineering*, *177*(April 2019), 115457. https://doi.org/10.1016/j.applthermaleng.2020.115457

Wang, S., Dai, G., Yang, H., & Luo, Z. (2017). Lignocellulosic biomass pyrolysis mechanism: A state-of-the-art review. *Progress in Energy and Combustion Science*, *62*, 33–86. https://doi.org/10.1016/j.pecs.2017.05.004

Wang, X., Yang, S., Shen, B., Yang, J., & Xu, L. (2022). Pyrolysis of Biomass Pineapple Residue and Banana Pseudo-Stem: Kinetics, Mechanism and Valorization of Bio-Char. *Catalysts*, *12*(8). https://doi.org/10.3390/catal12080840

Wielage, B., Lampke, T., Marx, G., Nestler, K., & Starke, D. (1999). Thermogravimetric and differential scanning calorimetric analysis of natural fibres and polypropylene. *Thermochimica Acta*, *337*(1–2), 169–177. https://doi.org/10.1016/s0040-6031(99)00161-6

Wronka, A., & Kowaluk, G. (2022). The Influence of Multiple Mechanical Recycling of Particleboards on Their Selected Mechanical and Physical Properties. *Materials*, *15*(23). https://doi.org/10.3390/ma15238487

Wronka, A., Robles, E., & Kowaluk, G. (2021). Upcycling and recycling potential of selected lignocellulosic waste biomass. In *Materials* (Vol. 14, Issue 24). https://doi.org/10.3390/ma14247772

Wu, H., Liang, X., Huang, L., Xie, Y., Tan, S., & Cai, X. (2016). The utilization of cotton stalk bark to reinforce the mechanical and thermal properties of bio-flour plastic composites. *Construction and Building Materials*, *118*, 337–343. https://doi.org/10.1016/j.conbuildmat.2016.02.095

Xie, Y., Zeng, K., Flamant, G., Yang, H., Liu, N., He, X., Yang, X., Nzihou, A., & Chen, H. (2019). Solar pyrolysis of cotton stalk in molten salt for bio-fuel production. *Energy*, *179*, 1124–1132. https://doi.org/10.1016/j.energy.2019.05.055

Xu, J., Han, G., Wong, E. D., & Kawai, S. (2003). Development of binderless particleboard from kenaf core using steam-injection pressing. *Journal of Wood Science*, *49*(4), 327–332. https://doi.org/10.1007/s10086-002-0485-7

Yaghoobi, H., & Fereidoon, A. (2019). Preparation and characterization of short kenaf fiber-based biocomposites reinforced with multi-walled carbon nanotubes. *Composites Part B:*

Engineering, *162*, 314–322. https://doi.org/10.1016/j.compositesb.2018.11.015

Yang, H., Yan, R., Chen, H., Lee, D. H., & Zheng, C. (2007). Characteristics of hemicellulose, cellulose and lignin pyrolysis. *Fuel*, *86*(12–13), 1781–1788. https://doi.org/10.1016/j.fuel.2006.12.013

Yang, X., Wang, H., Strong, P. J., Xu, S., Liu, S., Lu, K., Sheng, K., Guo, J., Che, L., He, L., Ok, Y. S., Yuan, G., Shen, Y., & Chen, X. (2017). Thermal properties of biochars derived from Waste biomass generated by agricultural and forestry sectors. *Energies*, *10*(4). https://doi.org/10.3390/en10040469

Yorgun, S., & Yildiz, D. (2015). Slow pyrolysis of paulownia wood: Effects of pyrolysis parameters on product yields and bio-oil characterization. *Journal of Analytical and Applied Pyrolysis*, *114*, 68–78. https://doi.org/10.1016/j.jaap.2015.05.003

Yu, Q., Wang, Y., Van Le, Q., Yang, H., Hosseinzadeh-Bandbafha, H., Yang, Y., Sonne, C., Tabatabaei, M., Lam, S. S., & Peng, W. (2021). An Overview on the Conversion of Forest Biomass into Bioenergy. *Frontiers in Energy Research*, *9*(July), 1–10. https://doi.org/10.3389/fenrg.2021.684234

Yu, Z. T., Xu, X., Hu, Y. C., Fan, L. W., & Cen, K. F. (2011). Unsteady natural convection heat transfer from a heated horizontal circular cylinder to its air-filled coaxial triangular enclosure. *Fuel*, *90*(3), 1128–1132. https://doi.org/10.1016/j.fuel.2010.11.031

Yub Harun, N., Jin Han, T., Vijayakumar, T., Saeed, A., & Afzal, M. T. (2019). Ash Deposition Characteristics of Industrial Biomass Waste and Agricultural Residues. *Materials Today: Proceedings*, *19*, 1712–1721. https://doi.org/10.1016/j.matpr.2019.11.201

Yunusa, S. U., Abdulsalam, M., Yunusa, S. U., Shehu, H. H., & Abdulsalam, M. (2022). Synthesızıng bio-particleboards from sugarcane bagasse and expanded polystyrene foam: an assessment of physical and mechanical properties. *Researchgate.Net*, *September*.

Zhang, Q., Chang, J., Wang, T., & Xu, Y. (2007). Review of biomass pyrolysis oil properties and upgrading research. *Energy Conversion and Management*, *48*(1), 87–92. https://doi.org/10.1016/j.enconman.2006.05.010

Zhao, Z., & Umemura, K. (2014). Investigation of a new natural particleboard adhesive composed of tannin and sucrose. *Journal of Wood Science*, *60*(4), 269–277. https://doi.org/10.1007/s10086-014-1405-3

Zheng, Q., Kaur, S., Dames, C., & Prasher, R. S. (2020). Analysis and improvement of the hot disk transient plane source method for low thermal conductivity materials. *International Journal of Heat and Mass Transfer*, *151*. https://doi.org/10.1016/j.ijheatmasstransfer.2020.119331

Zhou, B., Wang, L., Ma, G., Zhao, X., & Zhao, X. (2020). Preparation and properties of bio-geopolymer composites with waste cotton stalk materials. *Journal of Cleaner Production*, *245*. https://doi.org/10.1016/j.jclepro.2019.118842

Zhou, X., Li, W., Mabon, R., & Broadbelt, L. J. (2017). A critical review on hemicellulose pyrolysis. *Energy Technology*, *5*(1), 52–79. https://doi.org/10.1002/ente.201600327

Zimeri, J. E., & Kokini, J. L. (2002). The effect of moisture content on the crystallinity and glass transition temperature of inulin. *Carbohydrate Polymers*, *48*(3), 299–304. https://doi.org/10.1016/S0144-8617(01)00260-0

Zuber, S. H., Hashikin, N. A. A., Yusof, M. F. M., & Hashim, R. (2020). Physical and mechanical properties of soy-lignin bonded Rhizophora spp. particleboard as a tissue-equivalent phantom material. *BioResources*, *15*(3), 5558–5576. https://doi.org/10.15376/biores.15.3.5558-5576